

MECHANISMS OF DOWNHILL CREEP  
IN EXPANSIVE SOILS

A Dissertation

by

Lawrence Dana Dyke

Submitted to the Graduate College of  
Texas A&M University  
in partial fulfillment of the requirement for the degree of  
DOCTOR OF PHILOSOPHY

December 1979

Major Subject: Geology

MECHANISMS OF DOWNHILL CREEP  
IN EXPANSIVE SOILS

A Dissertation

by

Lawrence Dana Dyke

Approved as to style and content by:

CC Mathewson  
(Chairman of Committee)

Phonms T. Tiel  
(Member)

Grann Johnson  
(Member)

Joe B. Dixon  
(Member)

Byron L. Dyllo  
(Member)

Robert J. Stimpert  
(Head of Department)

December 1979

1497741

## ABSTRACT

## MECHANISMS OF DOWNHILL CREEP

IN EXPANSIVE SOILS (December, 1979)

Lawrence Dana Dyke, B.S., University of British Columbia

M.S., Texas A&amp;M University

Chairman of Advisory Committee: Dr. C. C. Mathewson

A detailed survey of two tracts of houses on sloping terrain underlain by expansible clay-rich soils indicates that expansive soils are especially susceptible to downhill creep. This poses an additional threat on top of the already well recognized problem of expansive soil damage to light structures. The sites are located in Waco on the South Bosque shale and in San Antonio on the Houston Black clay. Increases in the plasticity index, slope and age all favour increasing damage in Waco and the creep motions preferentially induce cracking on the sides of the houses parallel to the slope. Little dependence on age or slope at the San Antonio site indicates downhill creep is not an important factor there.

A study of volume changes vs. soil water potential verifies that a difference exists in mechanical behavior between the soils of the two sites. Both soils exhibit a sudden increase in water content at a low soil water potential as the potential is decreased from -15 bars. However, only the Waco soil exhibits a corresponding rapid increase in volume. Creep tests were performed on undisturbed samples of the natural soils over a range of soil water potentials and on a suite of artificial soils of increasing montmorillonite content. The Waco soil shows a rapid increase in creep rate over the range of potential that produces the sudden volume increase whereas the San Antonio soil retains a relatively high stiffness to a very low potential. For the artificial soils a rapid increase in creep rate does not begin until a montmorillonite content of about 50% is reached. The weakening influence of montmorillonite is thought to be due to its pronounced ability to

acquire adsorbed water and to the existence of this water in the spaces between stacks of clay plates. This water is capable of accommodating all of the shear deformation in one of these stacks and so represents a weak component of the soil fabric. As the proportion of montmorillonite and thus adsorbed water bonds increases, so does the creep rate for a given stress and soil water potential. Rate process theory can be adopted to predict a creep rate response similar to that seen for the creep tests. The activation energy of bond rupture can be divided into a component offered by mineral to mineral contacts and a component due to the activation energy for bonds formed by the adsorbed water between montmorillonite plates. This agreement offers a verification that the creep response of expansive soils is caused by the water-adsorbing properties of montmorillonite.

The volume change capability of an expansible clay soil is related to its geologic history. The South Bosque shale is heavily overconsolidated, producing an intimate contact between montmorillonite particles and the rest of the soil. Accordingly, volume changes are readily transmitted to the bulk soil. The Houston Black clay has formed as a residue from the leaching of the carbonate component of a marl and so has never been deeply buried. An isotropic fabric and the presence of relatively large pores which can accommodate some of the montmorillonite expansion may explain the stiffness and lack of large bulk volume increase of this soil.

## ACKNOWLEDGMENTS

Little can be gleaned from the following pages to reveal the integral part my chairman, Dr. C.C. Mathewson, took in every phase of the study. From late night sessions spent outfitting field laboratories to keeping the ultimate goal in sight, I am indebted to his concern. I am fortunate to have had the patience and brilliance of Dr. R.L. Lytton to confront with my ideas on mechanics. Dr. J.B. Dixon kept an eye on the scientific continuity of the whole dissertation while Dr. T.T. Tieh steered me away from the pitfalls of technical writing and Dr. C.B. Johnson drew attention to many points which improved the overall clarity. I must thank Dr. J. Neff for his service as Graduate Council Representative.

This study would not have been possible without the cooperation of the homeowners, city officials and consulting engineers in the four cities surveyed. It also would not have been possible without capable and good natured help of Mark Dobson, Joe Watson and Brian Powers during the field work. Jack Magouirk and Jack Calhoun of the Department of Geology and Dr. W.A. Dunlap and Ron Bogess of Civil Engineering provided materials and technical assistance for the construction of soil testing apparatus. Chester Michalak of Civil Engineering made sure the computer analysis of the home survey data worked properly. Dr. K. Brown and Ken Launius of Agronomy introduced me to the principles of soil physics and provided space and apparatus for part of the experimental program.

I must add a note for my office partner, Mary Bishop, who concerned herself with my welfare, as did my long-suffering roommate Jim Morse.

Parents always seem to be delegated to the end of the acknowledgments page but perhaps this is appropriate as mine are ultimately responsible for having the foresight and forbearance to let me follow the course I choose.

This study was made possible by funding supplied through the National Science Foundation Grant No. ENG75-09348 for which I am grateful.

## TABLE OF CONTENTS

	Page
ABSTRACT . . . . .	iii
ACKNOWLEDGEMENTS . . . . .	v
LIST OF TABLES . . . . .	viii
LIST OF FIGURES . . . . .	ix
INTRODUCTION . . . . .	1
Statement of the Problem . . . . .	1
Objectives . . . . .	1
IS SITU CREEP OF SOIL . . . . .	4
THE HOME SURVEY . . . . .	12
Previous work . . . . .	12
Conclusions pertinent to the present study . . . . .	14
The present house survey . . . . .	14
San Antonio . . . . .	16
Waco . . . . .	17
Modifications . . . . .	25
ANALYSIS OF THE HOME SURVEY DATA . . . . .	32
Sensitivity analysis . . . . .	32
Crack distribution study . . . . .	37
THE RESISTANCE OF EXPANSIVE SOILS TO SHEAR . . . . .	47
VOLUME CHANGE STUDY . . . . .	55
General Principles . . . . .	55
Water change experiments . . . . .	56
general approach . . . . .	56
procedure . . . . .	57
experimental results - moisture content versus potential . . . . .	59
experimental results - linear extensibility versus potential . . . . .	59
DEFORMATION STUDY . . . . .	67
Experimental design . . . . .	67
Apparatus . . . . .	70
Conduct of experiments . . . . .	70
Tests of artificial soils . . . . .	71
materials . . . . .	71
conduct of experiments . . . . .	71
Results for creep tests conducted under pre-determined soil water potentials on natural soils . . . . .	82
Results for creep tests conducted on artificial soils . . . . .	85

	Page
ANALYSIS OF EXPERIMENTAL RESULTS . . . . .	89
Preliminary analysis . . . . .	89
Mechanism of expansive soil hysteresis . . . . .	90
Clay soil fabric . . . . .	91
Shearing resistance . . . . .	93
Expansive soil deformation mechanism . . . . .	94
Behavior of expansive soils on natural slopes . . . . .	97
CONCLUSIONS . . . . .	106
Home survey . . . . .	106
Volume change tests . . . . .	107
Creep tests . . . . .	108
General Conclusions . . . . .	108
REFERENCES . . . . .	110
APPENDIX . . . . .	117
MECHANISM OF VOLUME CHANGE IN EXPANSIVE SOILS . . . . .	118
Clay as a charged particle and clay-water inter- action . . . . .	119
Mechanisms of volume change . . . . .	124
VITA . . . . .	140

## LIST OF TABLES

Table		Page
1	Rainfall, geologic, soil, and topographic conditions at the study sites . . . . .	15
2	Grain size analysis for the Houston Black clay and South Bosque shale . . . . .	27
3	Average maximum width and standard deviation for cracks according to type and position on house relative to slope . . . . .	40
4	Analysis of Figure 16 showing average values of variables and standard deviations for given intervals of the interaction values . . . . .	45
5	Grain size analysis and Atterbert Limit data for artificial soils . . . . .	81
6	Home Survey Data: San Antonio . . . . .	128
7	Home Survey Data: Waco . . . . .	130
8	Creep Test Data . . . . .	133



## LIST OF FIGURES

Figure		Page
1	Representative creep profiles for soil slopes . . . .	7
2	Typical boring log in the Houston Black clay . . . .	18
3	Typical boring log in the weathered Anacacho Limestone . . . . .	19
4	Boring log showing the abrupt contrast in soil properties at the contact of the Houston Black clay and the Anacacho limestone . . . . .	20
5	Topographic map of the San Antonio study site showing bore hole locations. Contour Interval equals 10 feet. . . . .	21
6	Isopach map of Houston Black clay . . . . .	22
7	Geologic and topographic map of the Waco study site . . . . .	23
8	Distribution of the near-surface geologic formations in the Waco study area . . . . .	24
9	Typical soil boring in the upper South Bosqu shale .	26
10	Typical soil boring n the lower South Bosque shale .	28
11	Home resting on an excavated platform showing creep profiles as they existed before the excavation. Homes tend to be constructed on cut rather than fill as evidenced by large trees immediately downslope . . . . .	29
12	Sensitivity analysis showing the influence of topography on damage in San Antonio . . . . .	34
13	Sensitivity analysis showing the influence of topography on damage in Waco . . . . .	35
14	Sensitivity analysis showing the influence of topography on damage in College Station . . . . .	36
15	Sensitivity analysis showing the influence of age on damage for San Antonio . . . . .	38
16	Sensitivity analysis showing the influence of age on damage in Waco . . . . .	39
17	The width of the largest crack on the sides parallel to or facing down the slope plotted against the corresponding value of the selected interaction for each house in Waco . . . . .	42

Figure		Page
18	The width of the largest crack on the side facing up the slope plotted against the selected interaction for each house in Waco . . . . .	42
19	The width of the largest crack on the sides parallel to or facing down the slope plotted against the corresponding value of the selected interaction for each house in San Antonio . . . . .	44
20	a. Schematic diagram of pressure vessel used for desorption tests. b. Schematic diagram of set-up used for adsorption tests . . . . .	58
21	Soil water characteristic for South Bosque shale desorbed to -15 bars . . . . .	60
22	Soil water characteristic for Houston Black clay desorbed to -15 bars . . . . .	61
23	Volume change hysteresis loop for South Bosque shale desorbed to -15 bars . . . . .	63
24	Volume change data for Houston Black clay desorbed to -15 bars . . . . .	64
25	Schematic diagram of creep test apparatus . . . . .	69
26	Creep curves for South Bosque shale, unconfined, samples CSBS3, CSBS4 . . . . .	72
27	Creep curves for South Bosque shale, unconfined, samples CSBS5, CSBS6 . . . . .	73
28	Creep curve for South Bosque shale, unconfined, sample CSB9 . . . . .	74
29	Creep curve for South Bosque shale, saturated, unconfined . . . . .	75
30	Creep curves for Houston Black clay, unconfined . . . . .	76
31	Creep curve for artificial soil, saturated, confined at 2 psi, sampled CK1, CKM2 . . . . .	77
32	Creep curves for artificial soil, saturated, confined at 2 psi, samples CKM3, CKM7 . . . . .	78
33	Creep curve for artificial soil, saturated, confined at 2 psi, sample CKM4 . . . . .	79
34	Creep curve for artificial soil, saturated, confined at 2 psi, sample CKM8 . . . . .	80
35	Synthesis of creep test data for South Bosque shale (solid lines) and Houston Black clay (dashed lines). Each curve shows the total axial shortening according to soil water potential at the end of each two hour stress increment (labelled) . . . . .	83

Figure		Page
36	Synthesis of creep test data for South Bosque shale (solid lines) and Houston Black clay (dashed lines). Each curve shows the axial shortening rate according to soil water potential at the end of each two hour stress increment (labelled) .	84
37	Synthesis of creep test data for artificial soils. Each curve shows the total axial shortening according to composition at the end of each 2 hour creep stress increment (labelled) . . . . .	86
38	Synthesis of creep test data for artificial soils. Each curve shows the axial shortening rate according to composition at the end of each 2 hour creep stress increment (labelled) . . . . .	87
39	Two-dimensional inferred nature of clay fabric for a flocculated expansive soil . . . . .	95
40	The relation between $\Delta F$ , the change in free energy and $n$ , the number of grams of water transferred from a source of free water to 1 gram of air-dried Na-montmorillonite . . . . .	101
41	Prediction of relative strain rate based on rate process theory according to soil water potential and proportion ( $n_2$ ) of mineral to mineral bonding .	104
42	A 1:1 clay mineral, kaolinite . . . . .	120
43	A 2:1 clay mineral, muscovite . . . . .	122
44	Montmorillonite, one of the smectite groups of clay minerals . . . . .	123

## INTRODUCTION

### Statement of the Problem

The ability of certain soils to shrink and swell (ie. change bulk volume), depending on mineralogy and availability of moisture, may provide a mechanism for enhancing downhill creep. The widespread occurrence of soil creep suggests a potential hazard to structures on slopes, especially light structures relying on shallow foundations for support. Damage to homes, in the form of foundation and wall cracks is an all too well recognized problem (Jones and Holtz, 1973; Gromko, 1974) on expansive soils and the possibility that expansive soils may be promoting creep poses an additional threat to homes on slopes. To evaluate this possibility evidence that expansive soils are especially susceptible to creep must be found.

The rate of creep in a soil will be controlled by geologic, mineralogy, climatic and other environmental factors that determine how easily the soil is deformed. If creep is to be attributed to the shrink-swell ability it must be shown that the creep rate is controlled by the soil and environmental factors that cause the shrink-swell phenomenon. This knowledge is required if the risk of damage due to soil creep is to be evaluated.

### Objectives

The primary objectives of this research are to determine if expansive soils are especially susceptible to downhill creep and to determine what soil, geologic and climatic factors control the creep rate.

### Approach to the problem

The potential for expansive soil damage to homes has generally been studied from the viewpoint of the single structure case history. A major departure from this approach was made by Castleberry (1974) and Mathewson et al. (1975) by evaluating possible causes of damage to a

---

The style and format used in this thesis is taken from the American Association of Petroleum Geologists.

large tract of single story, brick veneer, slab-on-grade foundation, homes. It was hypothesized that damage was related to a number of independent environmental factors and a mathematical model was computed which related these possible causes to the degree of damage. The advantage of this method is that factors controlling volume change, which are important in varying degree to all structures, tend to be emphasized whereas the significance attached to unusual conditions that may influence the performance of a particular structure is reduced. This approach is followed, employing the home as a deformation gauge that has been in place for a time period of interest in engineering considerations. A house having a slab foundation and brick exterior may be used as a reliable and sensitive indicator of differential ground movement because of the rigidity of the brick walls. Concrete, which is subject to creep (Neville, 1970) may show no failure, while walls crack as a result of the relatively weak mortar-brick contact. Lateral separations in walls then provide an indication of creep movements.

The hypothesis that expansive soils are especially susceptible to creep requires that the characteristics of the soil making it expansive control the amount of strain. The ability of expansible clays to adsorb water and swell provides a mechanism for controlling this strain. Most clays have the ability to attract water due to a matric or capillary potential developed between dipolar water molecules and the negatively charged surfaces of the clay plates. In addition, expansible clays develop an osmotic potential which tends to draw water in to the spaces between expansible clay layers. An increase in the matric potential generally results in a significant peak shear strength increase for clay-rich soils (Croney and Coleman, 1960; Williams and Shaykewich, 1970). An increase in the osmotic potential in an expansible clay results in an increase in the ability to adsorb water for a given swelling pressure (Warkentin et al., 1957; El Swaify and Henderson, 1967). Based on the water-adsorbing property of expansible clays, peak shear strength should be controlled by the expansible clay content and the amount of water adsorbed. As water is allowed access to an expansive soil, not only is matric potential reduced, but also clay particle interaction

and so shear strength should decrease. With increasing expansible clay content this phenomenon should become more apparent.

For this study, soil strength must be interpreted in terms of creep rate because the shearing stress exerted on soil at any depth will be constant and generally well below that required for a shear failure. The particle interaction mentioned above has been thought of as a process of breaking and reforming electrochemical bonds (Mitchell et al., 1968). This being the case, the creep rate should increase with particle separation because the electrochemical bonds will be weaker. Rheologically, creep will appear as a viscous process because the creep rate will also be controlled by the energy (ie. shear stress and shear strain) available for breaking or straining bonds.

The shape of an expansive soil creep profile will depend on several factors, the most important of which will probably be 1) the amount of expansible clay and 2) the amount of moisture adsorbed by the expansible clay component. If the nature of the creep profile is to be determined, the creep response of an expansive soil must be tested according to variations in these two parameters. The results of deformation experiments combined with a study of published research on clay deformation, physical chemistry, and fabric of clays are used to propose an explanation for the correlation of damage intensity with topography, soil properties and climate. Knowing the response of homes to these factors and having laboratory data on the control of expansive soil creep, it should then be possible to predict the risk of creep-induced damage at other sites based on their environmental conditions and corresponding laboratory data.

## IN SITU CREEP OF SOIL

The downhill creep of soil was first recognized as a geomorphic process contributing to the development of topography (Davis, 1892; Gilbert, 1909). Gilbert called upon a supposed increase in creep rate with increase in slope to move more material on steeper slopes and so produce convex hilltops. He also suggested that a cyclic change in the physical nature of a soil due to climatic influences was responsible for the changes in the ability of the soil to flow. Davison (1899) had already observed that a net downhill displacement resulted from the action of freeze-thaw cycles but he did not include a downhill component due to gravity-induced deformation in his mechanism. These observations have subsequently been expanded by field measurements to develop mechanisms for downhill soil creep.

Terzaghi (1950) proposed two types of soil creep: continuous creep and seasonal creep. Continuous creep involves an almost constant displacement of material to a depth below that influenced by yearly or more frequent changes in soil physical conditions. Seasonal creep displays a periodic movement in the zone of these seasonal changes. Continuous creep has been observed in the movement of large soil masses where shearing deformations are restricted to a narrow zone of failure. Depending on the geologic history of the soil, the deformations may result in a decrease from the peak strength offered toward a residual strength (Haefeli, 1950; Skempton, 1964). According to Terzaghi (1950), this process results in progressive failure of slopes whereby a failure surface is gradually formed as the weight of a soil body is progressively transferred to a developing sliding surface which resists sliding only with the residual strength (Bjerrum, 1967). Seasonal creep is characterized by penetrative deformation and may never produce a discrete zone of failure.

An increase in the induration of a soil or the bonding between soil particles causes the difference between peak and residual strengths to increase. It is also observed that clay fabric (ie., the orientation of soil particles) influences this difference. Morgenstern and Tchalenko (1967) have illustrated the development of particle alignment in

an artificial kaolinite soil as the residual strength is approached and have shown that parallel alignment of the kaolinite particles is necessary before the residual strength can be reached. An artificially produced flocculent fabric in kaolinite has been shown by Mitchell and McConell (1965) to result in a large decrease from the peak strength, whereas an initially parallel fabric produces only a gradual increase to the residual strength in the same material. This is probably due to the differences in stiffness of these fabrics in that an interlocking arrangement of particles is present in the flocculated fabric producing a maximum of high angle and thus high friction particle contacts. The common observation that overconsolidated clays show a comparatively large peak value despite a preferred particle orientation is probably due to the stiffness of the clay resulting from diagenesis and energy required to produce volume increases as particle rotations take place. Whatever the initial fabric, all deformations should tend toward producing a preferred orientation because interparticle friction is minimized.

Structural features within the soil such as bedding planes, fractures and discontinuities between soil structure units are likely to aid the formation of a failure zone. Skempton and Petley (1967) have shown that the strength along structural discontinuities is usually at the residual value and so a coalescence of these features to form a single failure zone can be imagined. Whether ultimate failure takes place by this mechanism or by the formation of a failure surface from intact material, a creep phenomenon can occur. Infiltration of water from the surface may influence the creep rate indirectly through variation in the water table and hence the effective stress in the soil mass. Bjerrum (1967) has also pointed out that deep-seated creep may be promoted by the release of stored elastic strain on weathering of over-consolidated soils. Lateral stresses would increase to assist existing gravitational stresses in producing movements.

Several in situ measurements of creep have been made within the zone of seasonal influence in an effort to determine rates of movement and distribution of movement with depth. As a generalization, it has



been observed that these movements decrease with depth and movements are either restricted to unindurated or weathered material above bedrock or to the zone of seasonal change in physical characteristics. Profiles of movement according to depth may show a linear, concave-downhill or concave-uphill shape, depending on the mechanism of creep.

The field measurements by Davison (1889) in soils undergoing freeze-thaw cycles show that freezing is accompanied by an expansion almost normal to the soil surface followed by a contraction in a downward direction intermediate between the normal to the soil surface and the vertical. The resultant of such motions leads to a net downhill motion (frost creep) similar to Fig. 1a, but gravity only makes a partial contribution to the deformation. Washburn (1967) has suggested that capillary tension causes the contraction where evaporation and drainage is great enough to maintain an overall negative pore water pressure.

Solifluction is a process first recognized by Anderson (1906) where enough weakening due to excess moisture is present to allow gravity to take effect and cause a downhill flow of soil in a manner approximating a state of simple shear (Fig. 1b). A polar climate is not necessary for solifluction but it does favor the buildup of massive ice in the finer grained soils which in turn provides an excessive supply of water on thawing. Therefore the spring would normally be the time of greatest movement, especially in the polar regions where rainfall is low. The actual creep profile that is produced by freeze-thaw will depend on the availability of water. The maximum amount of shear may take place below the surface in the case of solifluction because of evaporation losses and drainage. The result is a graphical addition of profiles a and b in Fig. 1 (Fig. 1c) which would probably be representative of many freeze-thaw situations. Rates vary widely but seem to not exceed 30 cm per year (Embleton and King, 1975) and the depth to which creep occurs will be mostly controlled by the thaw or active layer in polar climates.

The study of rock glaciers has revealed a type of creep that may, on a macroscopic or continuum scale, approach the idealized behavior

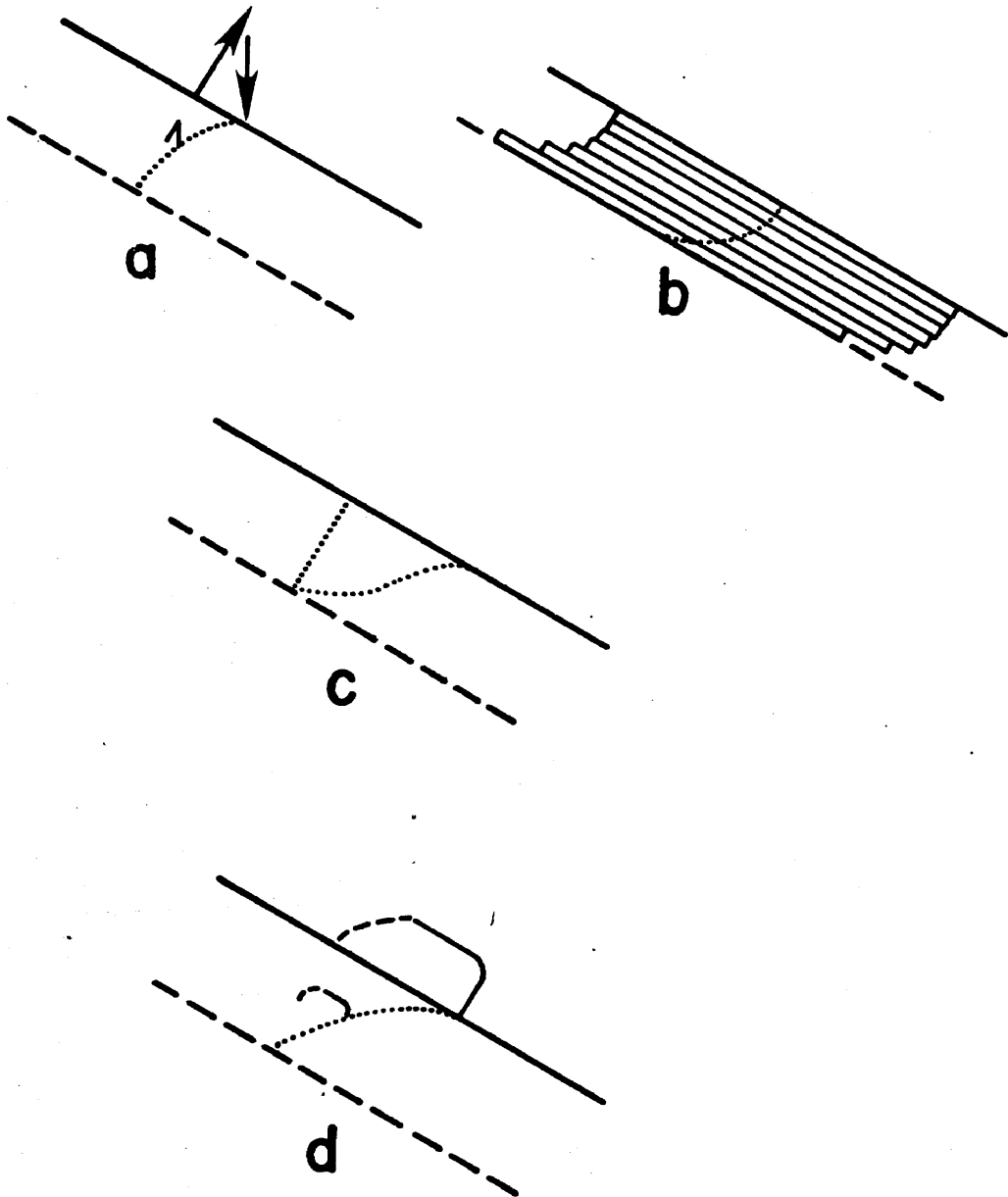


Figure 1. Representative creep profiles for soil slopes. a. Frost creep profile. b. Viscous laminar flow profile for a normal stress-independent material. c. Sum of profiles a and b. d. Profile for a soil experiencing expansion and weakening with wetting, followed by drying.

of the laminar viscous flow of an inclined sheet. Rock glaciers examined by Wahrhafting and Cox (1959) consist of coarse, blocky rock debris cemented by ice a few feet below the surface. Movement takes place as a result of the flow of the interstitial ice. The ice may be thought of as an easily deformable bond and in bulk enables the mass to behave as a fluid.

The concept of Newtonian viscous flow provides a description of the flow of a viscous layer down an inclined plane.

$$\frac{d\epsilon}{dt} = \frac{dv}{dz} = \frac{\tau}{\eta}$$

where  $\frac{d\epsilon}{dt}$  is the strain rate,  $\frac{dv}{dz}$  is the velocity gradient,  $\tau$  is the shear stress, and  $\eta$  is the viscosity. The shear stress acting parallel to the inclined plane can be described as

$$\tau = \rho g (H - z) \sin\alpha$$

where  $\rho$  is the density of the material,  $g$  is the acceleration of gravity,  $H$  is the thickness of material,  $z$  is the height above the inclined plane and  $\alpha$  is the slope angle. A description for the velocity gradient can be derived by substituting the expression for the shear stress gradient in the Newtonian flow equation and integrating with respect to  $z$ :

$$V_z - V = \frac{\rho g (2zH - z^2) \sin\alpha}{2\eta}$$

where  $V_z$  is the velocity at height  $z$  and  $V$  is the velocity at the base of the flow. This mathematical description gives a velocity profile that is concave upward, i.e. deformation is strictly dependent on shear stress and not influenced by confining pressure. While this description may be appropriate for materials having an ice component, in soils changes in water content, confining pressure, and induration with depth are going to alter the velocity profile so as to change it to a convex upward slope.

Several measurements have been made on slopes in temperate regions where freeze-thaw is not as important a factor (Carson and Kirkby, 1972; Swanson and Swanson, 1976). Most measurements show that the movements generally do not exceed a few centimeters per year and tend to involve only the upper one to two meters of the soil profile when bedrock is at a greater depth. These observations probably all fall into Terzaghi's

seasonal type of creep because of the relatively shallow depths involved.

Kirkby (1967) made extensive creep measurements in southwest Scotland at a site where freezing below 10 cm is rare. The displacement of both segmented columns and rigid rods buried vertically in the soil served to detect movements. His measurements over two years showed a relatively slow rate of a few millimeters per year. He proposed short and long term mechanisms for creep based respectively on the response to individual rainfall events and the average result of these accumulated events. Most of the movement is attributed to moisture content increases but the small creep rate values may be due to the fairly constant amount of soil moisture due to the continuously moist nature of the climate. On the other hand, Fleming and Johnson (1975) monitored soil moisture content during their study in California, where freezing is also rare, and observed that the creep rate increased during wetting but decreased once the maximum water content had been reached. Their overall rates were much higher despite far less rainfall. Despite its low annual rainfall, the California site has a distinct wet and dry season which would permit large changes in moisture content. It is apparent that the process of wetting from a relatively dry state rather than simply a high moisture content may be most conducive to creep. The California soil is montmorillonitic and so a shrink-swell type of creep mechanism perhaps very similar to the frost creep mechanism probably contributes to the observed motions.

The ability of certain soils to exhibit considerable vertical shrink-swell movements is well documented (Ward, 1953; Yaalon and Kalmor, 1972). Such soils are characterized by the presence of montmorillonite and react mainly to changes in moisture content caused by infiltration, evapotranspiration and evaporation. Unlike soil expanding due to freezing, the attendant water content increase may weaken the soil enough to allow creep by simple shear. Fleming and Johnson (1975) also have observed a creep "hardening" whereby the creep rate decreases after initial wetting even though the moisture content may be still increasing. They propose a movement path combining an expansion-contraction motion with

movement parallel to the ground surface to give an inverted "U" shaped path (Fig. 1d). The departure of this hypothesized U-shaped path from the ideal V shape involved in frost creep will depend on the attendant increase in shearing strain as wetting takes place.

An expansive soil can often be identified in the field by the presence of gilgai, a ridge and hollow topographic pattern having a relief of up to half a meter (Gustavson, 1975). Several processes for formation have been offered although horizontal compression due to swelling of the expansive soils seems to be common to all these processes. The presence of slickensided fractures in the soil beneath gilgai (Ritchie et al., 1972; Bartelli, 1976) supports this observation, suggesting that the soil has, locally at least, reached the condition of passive failure. The lateral compression accompanying this processes could augment creep movements, which in any event take place as evidenced by the elongated shape of the gilgai in the downhill direction on slopes as low as 1-2%.

The studies by Kirkby (1967) and Fleming and Johnson (1975) both showed a concave-downhill shape to the measured creep profiles but this net movement in both cases included some uphill and lateral motions where contractions in blocks bounded by dessication cracks were caused by drying. This illustrates a prime difficulty in measuring creep in situ. Measuring net downslope movement as a function of depth requires inserting some sort of deformable probe in the slope. Movements in directions other than downhill are possible due to the forces of attraction between water and soil particles. To be reliable, such measurements must be taken after the probe has seated itself in firm contact with the soil and after creep has exceeded seasonal and/or yearly motions. It may take more than one year to meet these conditions and then at least two more years of observation to obtain a reproducible annual rate.

This study employs houses with slab-on-grade foundations as slope movement indicators. The movement of the slab is based on measurements of cracks in the slab and walls. This method has the advantage that a house that has existed long enough to offer meaningful observations may

be located. Also, the movements detected are a response to soil movement averaged over a relatively large area.

## THE HOME SURVEY

### Previous Work

The widespread occurrence of expansive soil damage is almost certainly linked with a wide range of soil index properties and external environmental factors that respectively estimate and control soil volume change. With this observation in mind, Castleberry (1974) and Mathewson et al. (1975) conducted a detailed survey of a tract of 136 homes in College Station, Texas, an area known to have a history of expansive soil damage. The purpose was to detect any correspondence between a qualitative estimate of the damage and the range of values assigned to all the parameters assumed to be significant in estimating or controlling soil volume change. Their study used single story, brick veneer homes with slab-on-grade foundations, located in an area underlain by interbedded silty and bentonitic clays of the Eocene Yegua Formation. The rigidity of the brick walls provides a very sensitive indicator of slab movement in that very little deformation of the slab is necessary to produce a crack in the brick veneer. Damage was estimated in five categories of increasing severity ranging from none through the appearance of cracks in the walls and then the slab to major damage requiring repair.

The primary recognition that a volume change in an expansive soil requires a moisture content change lead to the selection of factors thought to govern soil moisture content. These are: 1) rainfall over a two month period immediately prior to construction, 2) lot drainage and 3) vegetation as a percentage of foliage cover before and after construction. The plasticity index of the soil weighted in favor of the shallowest soil horizon was determined using soil samples from hand-augered bore holes throughout each tract. This, together with the depth to which yearly soil moisture content changes take place (depth of the active zone) were included as estimates of the potential for volume change. A foundation shape measure was included to test the hypothesis that a more irregular floor plan was prone to greater damage, and age and slope of the lot near the house were included to evaluate the time-dependent and slope movement contributions to damage.

The home survey data was subjected to a multivariate regression analysis using the estimate of damage as the dependent variable and quantifications of the hypothesized damage controls as independent variables. The analysis uses the Hocking-Lomatte-Leslie select regression analysis developed by the Institute of Statistics at Texas A&M University. It produces the statistically optimum regressions on subsets of the independent variables of size 1 through n and for each subset any number of best regressions may be called for because the full range of variables is allowed unlimited access to all regressions. The final result is an equation of the form,

$$Y = a_0 + a_1 X_1 + a_2 X_2 \dots + a_n X_n$$

for a linear regression and

$$Y = a_0 X_1^{b_1} X_2^{b_2} \dots X_n^{b_n}$$

for a logarithmic regression where

Y = dependent variable

a = constant

b = regression coefficient

X = independent variable

n = number of independent variables in subset.

Because it is likely that the value of certain variables is influenced by the values of others, interactions or combinations of variables were submitted as new variables (interaction variables) to the analysis. These interactions were selected both on the basis of experience and the variable associations that were chosen by the preliminary analysis. This second step improved the statistical significance of the regression. The final result is an equation of the form

$$Y = a_0 + a_1 Y_1^{b_1} + a_2 Y_2^{b_2} + \dots + a_n Y_n^{b_n}$$

where  $Y_1$  through  $Y_n$  are now interaction variables.

Castleberry (1974) and Mathewson et al. (1975) were able to subdivide their damage observations according to two deformation mechanisms noted in their study. Homes having wall cracks widest at the top were designated center lift and those with the cracks widest at the bottom, end lift. This subdivision produced the most significant equations and suggested that different variables are responsible for different styles



of damage. Furthermore, it suggested that a home can be used as a deformation gauge sensitive enough to detect movements due to different causes.

#### Conclusions pertinent to the present study

Castleberry (1974) and Mathewson et al. (1975) included the slope of the lot as an independent variable because it was believed that downhill slope movements might contribute to damage, a suggestion already made by Lytton (1973). In fact, it turned out that the severity of damage decreased with increasing slope. However, the maximum lot slope observed was 8 percent and the relief over the whole study site was only 30 feet. Consequently, this correlation may have been sensing a tendency of a low slope to allow the collection of runoff near the house while the greater slopes aided drainage, reducing the time for infiltration of water to the soil. With steeper and longer slopes, damage due to downhill movements may well have been observed.

#### The present house survey

The foregoing analysis produced correlations that were used to make recommendations regarding landscaping and construction methods to reduce the risk of expansive soil-related damage. Different house deformation mechanisms were also inferred from the analysis. These results suggest that the method can successfully be applied to other areas having different geology, climate and ranges of the independent variables. Most importantly, the method may be used to determine if slope does have a positive relation to damage, and therefore reveal a contribution of downhill movement to damage sustained and its dependence on the expansive quality of the soil.

Four cities in Texas were chosen in accordance with the proposal to extend the applicability of the house survey method and examine the influence of slope movements (see Table 1). Two of them, San Antonio and Waco, were chosen for this study because they have considerable topographic relief. Beaumont and Amarillo, areas having virtually no relief, were included and the system interactions for all four have been analyzed in detail by Dobson (1978).

Table 1. Rainfall, geologic, soil, and topographic conditions at the study sites.

City	Avg Annual Rainfall	Formation	Soil	Relief and Max. Slope	No. Houses	No. Soil Borings
San Antonio	28"	Anacacho Ls.	Houston Black clay	80'/10%	102	24
Waco	36"	South Bosque Sh.	Austin-Eddy clay	150'/30%	100	21
Beaumont	54"	Beaumont Clay	Byars-Acadia-Klej silt-clay complex	5'/1%	113	14
Amarillo	19"	Ogallala Ss.	Pullman clay	10'/1%	142	10
College Station	38"	Easterwood Sh.	Lufkin silty loam	30'/8%	136	46

The following criteria were used to determine the actual tract of houses to be studied in each city:

1. The site was shown on the appropriate U.S.D.A. county Soil Survey Report to be situated on soil having a high shrink-swell potential.
2. In order to retain as much consistency as possible in the assignment of the dependent variable (damage severity), the style and quality of construction of the houses was chosen to be as similar as possible to those of the parent site (College Station). Thus homes of brick veneer construction with slab-on-grade foundations and ranging in age from new to 15 years were chosen.
3. Some damage, in the form of cracking in the brick or separations in the wood-brick contacts, was apparent in a cursory inspection.
4. Approximately 100 houses per site were available in a single compact tract.

### San Antonio

San Antonio is located within the Balcones Fault Zone, a wide belt of normal faults forming the transition from the Texas Gulf Coastal Plain to the Edwards Plateau. Blocks bounded by these faults are generally downdropped towards the Gulf Coast and at San Antonio expose limestone and shale of Cretaceous age. The San Antonio study area is situated on the Anacacho Limestone, a pale yellowish brown-weathering marly chalk. The outcrop forms part of a physiographic division known as the Taylor-Navarro Plain (Sellards, 1919). The plain is characterized by the relatively non-resistant strata of the late Cretaceous including the Anacacho, Taylor and Navarro Formations. The rolling topography formed during a period of late Tertiary and Pleistocene erosion when a thin layer of gravelly clays were deposited. These clays are the predecessor of the Houston Black clay (U.S.D.A., 1966), the expansive soil in the study area.

The Houston Black clay is typically a dark brown, dark grey or black, slightly silty clay with occasional chert pebbles and cobbles. In the study area there is a sharp break between it and the underlying Anacacho. When dry the clay is very blocky and appears otherwise

structureless except for occasional slickensides. Typical borehole logs for the San Antonio site are shown in Fig. 2, 3 and 4.

Where observed under the Houston Black clay, the Anacacho was usually as easy to sample as the clay, suggesting that weathering of the normally indurated formation has taken place. The Houston Black clay may have in part been formed by partial leaching of the carbonate component. The plasticity index determined for the clay fraction of a sample of Anacacho Limestone exceeds the average for the Houston Black clay (E. Miller, pers. com., 1976). The clay is rich in montmorillonite, as Kunze and Templin (1956) have recorded from 60 to 85% in the less than 2.0 micron fraction from five profiles in south central Texas. This fraction comprises about 55% of the soil.

Figure 5 shows the topography of the San Antonio site and Fig. 6 is an isopach map of the Houston Black clay. The clay is up to six feet thick at the site and thins to zero where exposures of the Anacacho occur.

## Waco

Waco is located along the Bosque Escarpment, a cuesta and fault line scarp also within the Balcones Fault Zone. The escarpment is held up by the Upper Cretaceous Austin Chalk. Further south along the escarpment the much softer beds of the South Bosque Shale are exposed but a distinct topographic break is maintained by a capping of the Austin Chalk. It is across these two formations that the Waco study area is located.

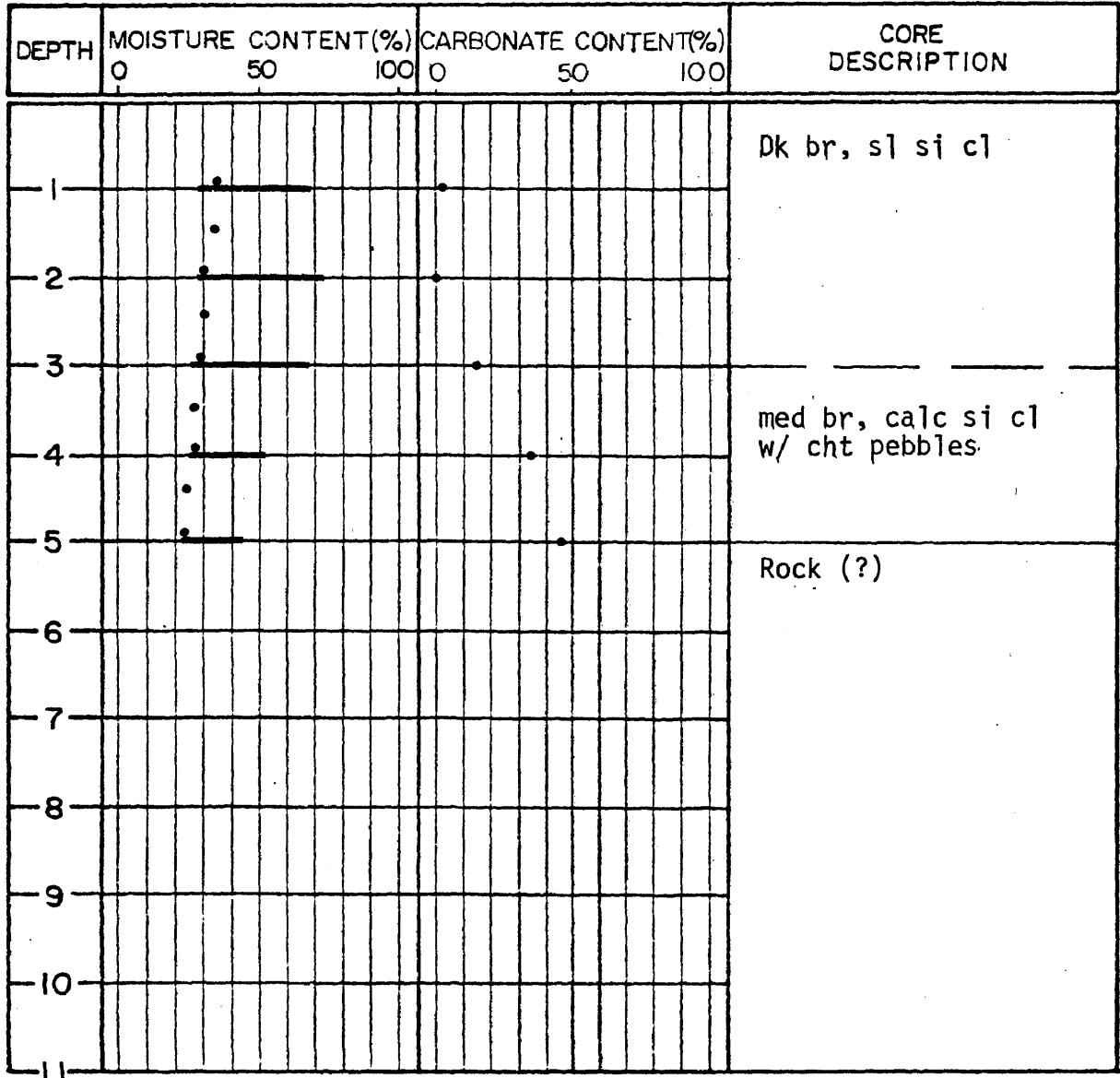
The Austin Chalk consists of alternating beds of chalk and marl and in the study area a greyish brown, highly calcareous soil generally less than two feet thick has developed. Although this soil does have an expansive potential it is usually shallow enough to be removed prior to any construction, resulting in few foundation problems (Burket, 1965). Where foundation problems have occurred, they are usually caused by the nearness to the underlying South Bosque Shale (Font and Williamson, 1970).

Most of the study area lies on the South Bosque Shale, (Fig. 7, Fig. 8), a dark grey to black, blocky to fissile shale. The shale is

SHEET NO. \_\_\_\_\_  
 DATE May, 1976  
 SHEET \_\_\_\_\_ OF \_\_\_\_\_

## ENGINEERING GEOLOGY SOIL PROPERTIES SHEET

BORING NO. 3 SA SAMPLE INTERVAL 0.5' DEPTH 5'  
 LOCATION San Antonio  
 DESCRIBED BY LDD



REMARKS Could not penetrate below 5'.

Figure 2. Typical boring log in the Houston Black clay. Left and right of bars indicate plastic and liquid limits respectively.

SHEET NO. \_\_\_\_\_  
 DATE May, 1976  
 SHEET \_\_\_\_\_ OF \_\_\_\_\_

## ENGINEERING GEOLOGY SOIL PROPERTIES SHEET

BORING NO. 11 SA SAMPLE INTERVAL 0.5' or 1' DEPTH 7'  
 LOCATION San Antonio  
 DESCRIBED BY LDD

DEPTH	MOISTURE CONTENT (%)			CARBONATE CONTENT (%)			CORE DESCRIPTION
	0	50	100	0	50	100	
1	•	•	•	•	•	•	Dk br cl w/ pebbles Lt rd tan si cl
2	•	•	•	•	•	•	Tan, calc si cl
3	•	•	•	•	•	•	
4	•	•	•	•	•	•	
5	•	•	•	•	•	•	
6	•	•	•	•	•	•	Lt br, sl si cl
7	•	•	•	•	•	•	
8							
9							
10							
11							

REMARKS Low moisture content prevented penetration below 7'

Figure 3. Typical boring log in the weathered Anacacho Limestone.

SHEET NO. \_\_\_\_\_  
 DATE May, 1976  
 SHEET \_\_\_\_\_ OF \_\_\_\_\_

## ENGINEERING GEOLOGY SOIL PROPERTIES SHEET

BORING NO. 7 SA SAMPLE INTERVAL 0.5' or 1' DEPTH 9'  
 LOCATION San Antonio  
 DESCRIBED BY LDD

DEPTH	MOISTURE CONTENT (%)			CORE DESCRIPTION
	0	50	100	
1	•			Dk br si cl w/ calc nods and cht pebbles
2	•			
3	•			Med br si cl
4	•			Tan si cl, calc
5	•			
6	•			
7	•			
8	•			
9	•			
10				
11				

REMARKS \_\_\_\_\_  
 Figure 4. Boring log showing the abrupt contrast in soil properties at the contact of the Houston Black clay and the Anacacho limestone.

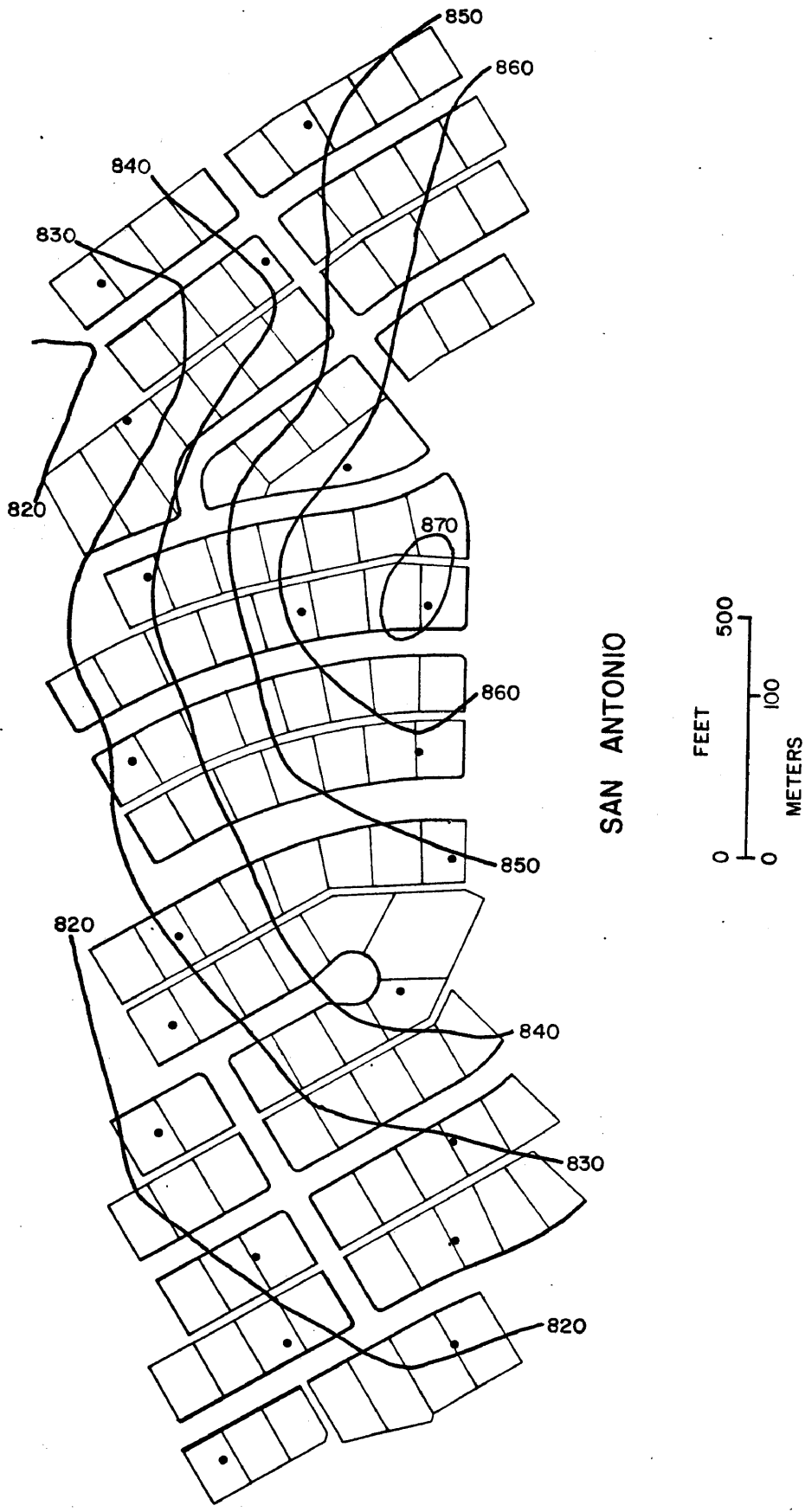


Figure 5. Topographic map of the San Antonio study site showing bore hole locations. Contour Interval equals 10 feet.



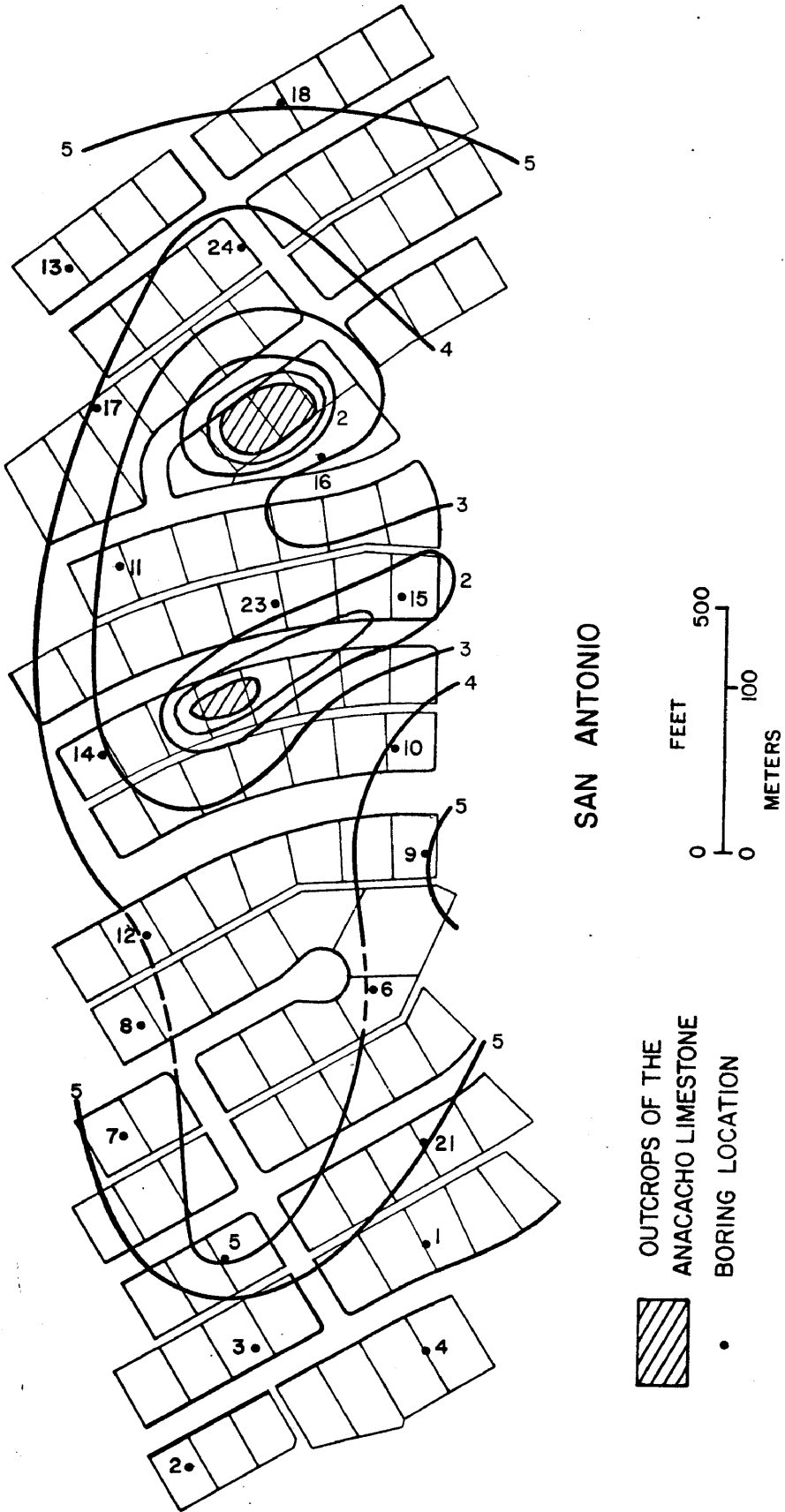


Figure 6. Isopach map of the Houston Black Clay. Isopach interval equals one foot.

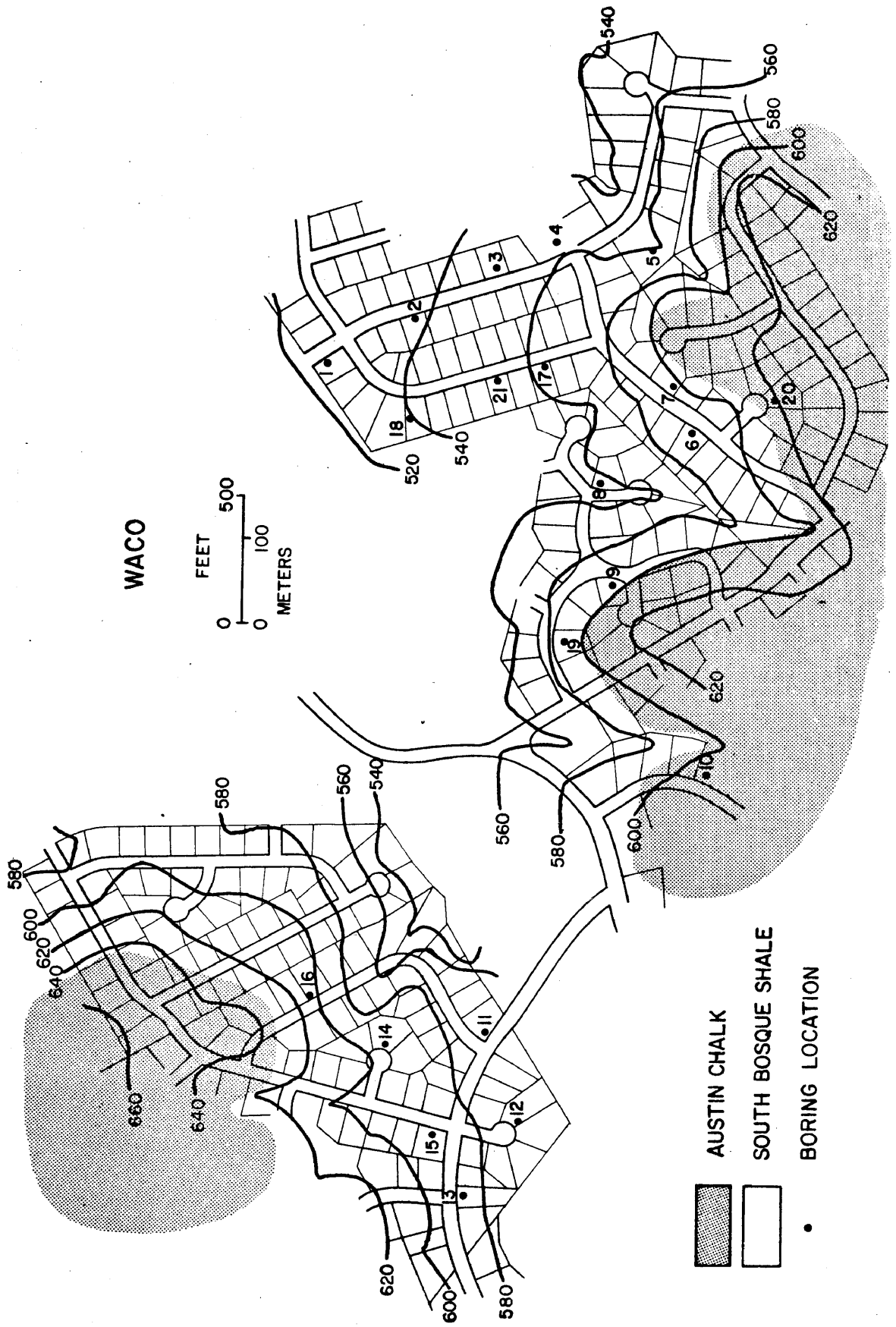


Figure 7. Geologic and topographic map of the Waco study site. Contour interval equals 20 feet.

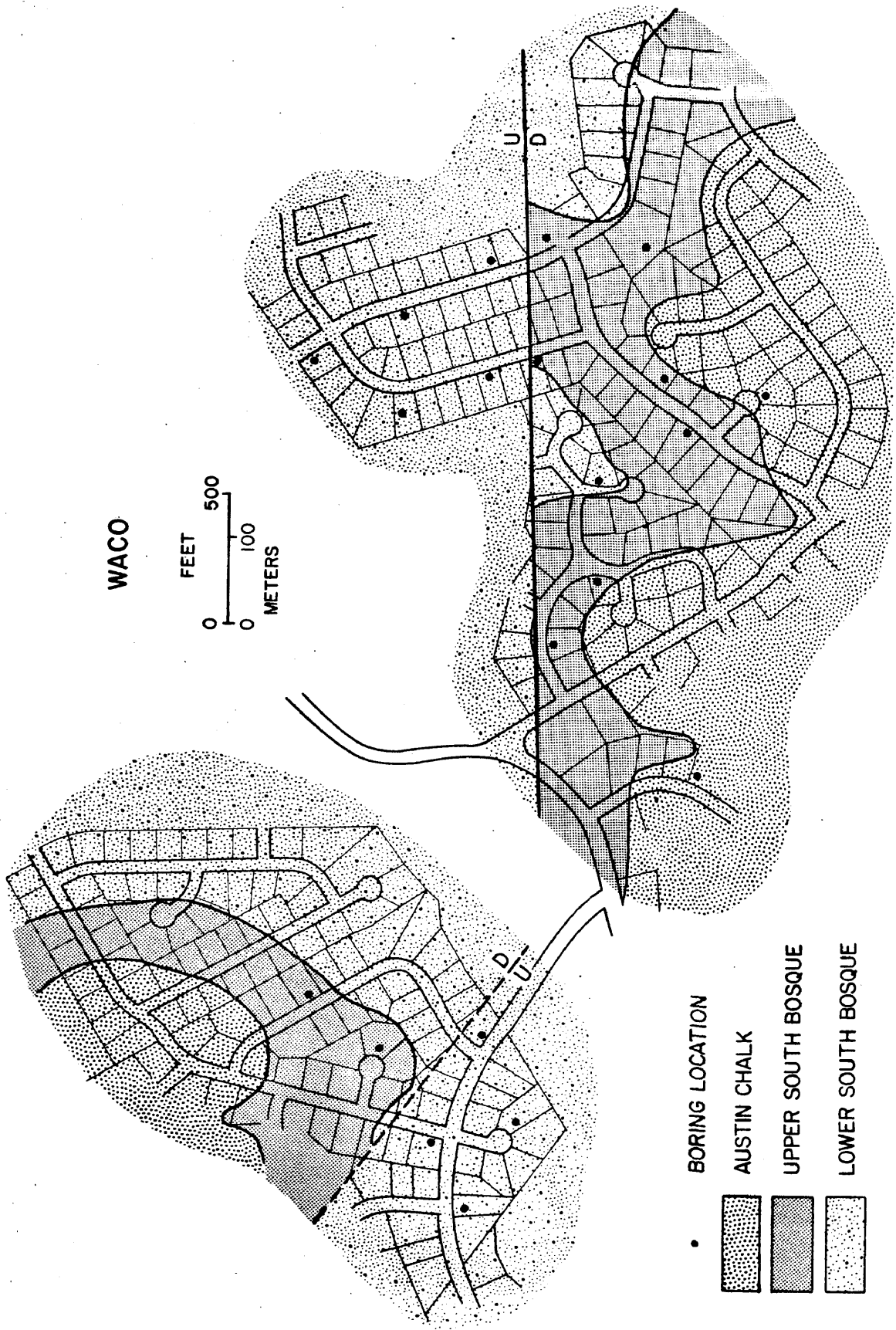


Figure 8. Distribution of the near-surface geologic formations in the Waco study area.

deeply weathered but retains a laminated fissile structure to within a foot or so of the surface. The upper 50 feet of the South Bosque Shale are associated with the worst foundation problems (Font, 1973). A typical borehole log in the upper division (Fig. 9) shows an olive brown-weathering, highly plastic clay having less than 20% carbonate content. A montmorillonite content of 35% was determined for the bulk shale by a combination of X-ray diffraction and chemical analysis. A grain size analysis indicates that 75% is less than 2.0 microns and probably all the montmorillonite is concentrated in this size fraction. The grain size analysis for the two soils is presented in Table 2.

The lower 100 feet of the South Bosque Shale is more stable and is composed of calcareous shales interbedded with thin limestone flags and bentonite seams. This has weathered to a highly calcareous yellowish brown or dark brown clay. Figure 10 shows a typical borehole log in this lower division.

#### Modifications to the house survey

The confidence to be placed in any statistical analysis can be increased by enhancing the continuity of the data. To attempt this for the present study and provide the necessary sensitivity for the detection of downhill movements, a detailed and quantitative measure of damage was made. Wall cracks in homes on level ground were found to be usually oriented in a vertical or stair-step fashion and often wider at one end or another, allowing an estimate of differential vertical movement to be made. For houses located on slopes, creep can be anticipated depending on soil and climatic conditions. As a generalization, field measurements of creep show that rates decrease with depth. Consequently, the foundation of a home resting on a level platform excavated from a slope will be in contact with soil levels that, originally at least, were experiencing different rates of movement (Fig. 11). In theory the downhill side of a house should experience the most movement since this part of the slab will be resting on soil having the highest creep rate. The result should be removal of support from the downhill side of the slab, bending of the slab with eventual failure, followed by increasing lateral separation as creep continues. It is further

SHEET NO. \_\_\_\_\_  
 DATE July, 1976  
 SHEET \_\_\_\_\_ OF \_\_\_\_\_

## ENGINEERING GEOLOGY SOIL PROPERTIES SHEET

BORING NO. 19 WA SAMPLE INTERVAL 0.5' or 1' DEPTH 9'  
 LOCATION Waco  
 DESCRIBED BY LDD

DEPTH	MOISTURE CONTENT (%)			CARBONATE CONTENT (%)			CORE DESCRIPTION
	0	50	100	0	50	100	
1	•	—	—	•			Yel ol, calc sl si cl
2	•	—	—	•			Yel br, sl si cl
3	•	—	—	•			Yel ol to rusty or si cl
4	•	—	—	•			Ol to or ol si cl
5	•	—	—	•			
6	•	—	—	•			
7	•	—	—	•			
8	•	—	—	•			
9	•	—	—	•			
10							
11							

REMARKS Could not penetrate below 9'

Figure 9. Typical soil boring in the upper South Bosque shale.

Table 2. Grain size analysis for the Houston Black clay and South Bosque Shale.

	Clay <2 micron	Fine Silt 2 - 5	Med. Silt 5 - 20	Course Silt 20 - 60	Sand >60
Houston Black clay	56.8%	5.0	15.1	18.5	4.7
South Bosque Shale	75.0	8.2	11.4	5.7	0.4

SHEET NO. \_\_\_\_\_  
 DATE July, 1976  
 SHEET \_\_\_\_\_ OF \_\_\_\_\_

## ENGINEERING GEOLOGY SOIL PROPERTIES SHEET

BORING NO. 2 WA SAMPLE INTERVAL 0.5' or 1' DEPTH 15'  
 LOCATION Waco  
 DESCRIBED BY JQW

DEPTH	MOISTURE CONTENT (%)			CARBONATE CONTENT (%)			CORE DESCRIPTION
	0	50	100	0	50	100	
1	[Graphical data points]			[Graphical data points]			Dk br to blk si cl, calc, w/ calc nods
2	[Graphical data points]			[Graphical data points]			
3	[Graphical data points]			[Graphical data points]			Dk br si cl
4	[Graphical data points]			[Graphical data points]			
5	[Graphical data points]			[Graphical data points]			Dk br to yel br si cl
6	[Graphical data points]			[Graphical data points]			
7	[Graphical data points]			[Graphical data points]			Med tan, calc si cl to 15'
8	[Graphical data points]			[Graphical data points]			
9	[Graphical data points]			[Graphical data points]			
10	[Graphical data points]			[Graphical data points]			
11	[Graphical data points]			[Graphical data points]			

REMARKS \_\_\_\_\_

Figure 10. Typical soil boring in the lower South Bosque shale.

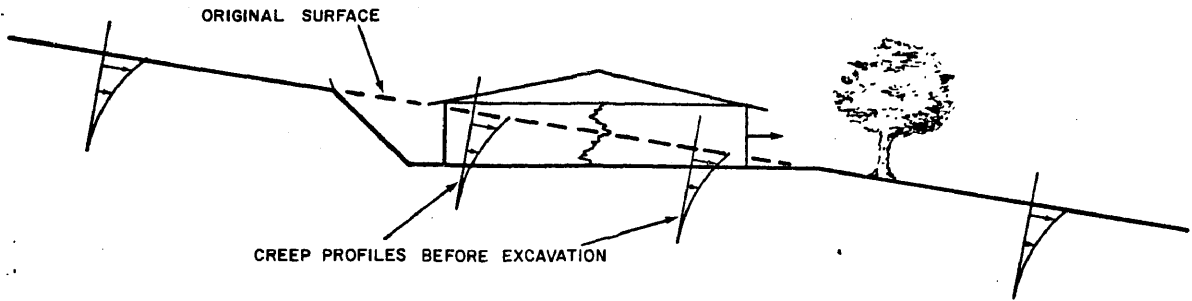


Figure 11. Home resting on an excavated platform showing creep profiles as they existed before the excavation. Homes tend to be constructed on cut rather than fill as evidenced by large trees immediately downslope.



anticipated that cracks on the walls parallel to the slope direction would be widest at the top because of a tendency for the downhill half of the slab to rotate downhill.

For each home, the position, length and width of each crack was recorded. Concave or convex bending of the slab was inferred by noting whether wall cracks were widest at the top or bottom. This detail allowed the following measures of damage to be used as dependent variables:

1. Total area of cracking (number of  $\text{mm}^2$  opened by crack)
2. Area of vertical cracks
3. Maximum width of cracks
4. Number of top tension cracks
5. Number of bottom tension cracks
6. Total area of top tension cracks

Regressions could then be performed using a variety of dependent variables, depending on what deformation mechanism was anticipated. Dependent variables giving damage as an area of cracking provide the most continuous measure of deformation.

An attempt to measure the perception of the damage by the homeowner was made. This was entirely subjective and tended to indicate that only for severe cases of house damage were the owners particularly enraged. In terms of human perception then, the critical degree of damage would be relatively high, ie. that requiring repair.

New independent variables were added and others modified. A qualitative measure of yard maintenance based mainly on the visual appearance of the yard was included. The number of trees on a lot, their average distance from the house and average diameter provided additional measures of vegetation. For houses on slopes, a further attempt to explain downhill movement was added by determining the proportion of the house resting on fill verses intact soil.

Collecting the data in the field included sketching wall elevations and a perimeter and yard plan for each house with cracking superimposed. Two summary sheets for each house were prepared, one containing a quantification of each of the independent variables described in this chapter, the other containing a matrix in which was entered numbers, widths

and areas of cracks according to style and position on the house. Input for the computer analysis was taken directly from these.

## ANALYSIS OF THE HOME SURVEY DATA

Performing the regression analysis on the home survey data provides an almost limitless array of equations, those containing all the independent variables being very cumbersome and difficult to interpret. As would be expected if interactions were important, the variation in the data is better accounted for as the number of independent variables increases. However, this rate of increase falls off rapidly once equations having greater than about five variables are considered. In all cases the correlation coefficient for equations generated by the interaction analysis were at least as good and often better than that given by the individual variable analysis. Although all the listed forms of the dependent variable were run, two in particular, total area of cracking and total area of top tension cracking, were hypothesized to be most indicative of slope movements. In fact, these variables produced the highest correlation coefficients for the two cities exhibiting significant topographic relief. Dobson (1978) conducted a detailed systems interaction analysis of the results and found total area of cracking to be the most significant dependent variable. This is the best overall measure of deformation because it will be sensitive to movements on both sloping and level sites. This dependent variable also gives the best correlation with topography.

### Sensitivity analysis

To observe more quantitatively the influence of topography, a given regression equation can be selected and the additional variables assigned their mean values, reducing the equation to an expression in terms of topography alone. This is called a sensitivity analysis and allows the contribution of a given variable to be evaluated.

For San Antonio, Dobson (1978) used the following equation as the system interaction model:

$$\text{TOTAR} = -2.34 (Y^{-1.6}R^{0.2}DA^{2.5}) + 3.54 (Y^{-1.7}DA^{2.5}) + \\ 0.53 (R^{0.21}T^{0.62}Y^{-1.7}DA^{3.0}) - 0.72 (T^{0.6}Y^{-1.8}DA^{2.9}) + 1.87$$

where TOTAR = total area of cracking

Y = yard maintenance

R = antecedent rainfall ratio

DA = depth of the active zone

T = topography

Conducting the sensitivity analysis in terms of topography gives the relation plotted in Figure 12. It is apparent that damage is not very sensitive to topography, showing only a slight increase over the range of relief available. Dobson interprets this to mean that soil creep is subdued by the reduction in depth of the active zone on the higher, steeper slopes.

The equation determined for Waco is:

$$\begin{aligned} \text{TOTAR} = & 8.86 (\text{NTREE}^{0.22}) + 1.05 (\text{CANOPY}^{0.25} \text{SVI}^{1.9}) + \\ & 0.12 (\text{SVI}^{1.3} \text{T}^{1.5}) + 0.0018 (\text{AVDIST}^{1.4} \text{SVI}^{1.4} \text{AGE}^{0.64} \text{T}^{1.2}) - \\ & 0.17 \text{AVDIST}^{0.42} \text{SVI}^{1.4} \text{T}^{1.2}) - 5.49 \end{aligned}$$

where NTREE = number of trees on the lot

CANOPY = post-construction vegetation

SVI = average plasticity index

AGE = age of the slab

AVDIST = average distance of the trees from the house

The correlation coefficient ( $R^2$ ) for the San Antonio model is 0.31 and for the Waco model is 0.76. Figures 13 and 14 compare the sensitivity analysis for Waco with that produced by Castleberry for College Station. These results compliment each other in that the inverse relation between topography and damage for College Station is included in the plot for Waco. The importance of lot drainage that Castleberry found in the College Station study appears to apply to the Waco site. A contribution to damage from downhill creep appears to be significant for a relief greater than about 15 feet, but creep probably continues to exert a decreasing influence below a relief of 15 feet. For the case of no relief the graphs for San Antonio and Waco show considerably different degrees of cracking. This points to a considerably greater volume change ability on the part of the Waco soil if it is assumed that all other controlling factors are equal.

If deformation is due to creep it should also be time-dependent.

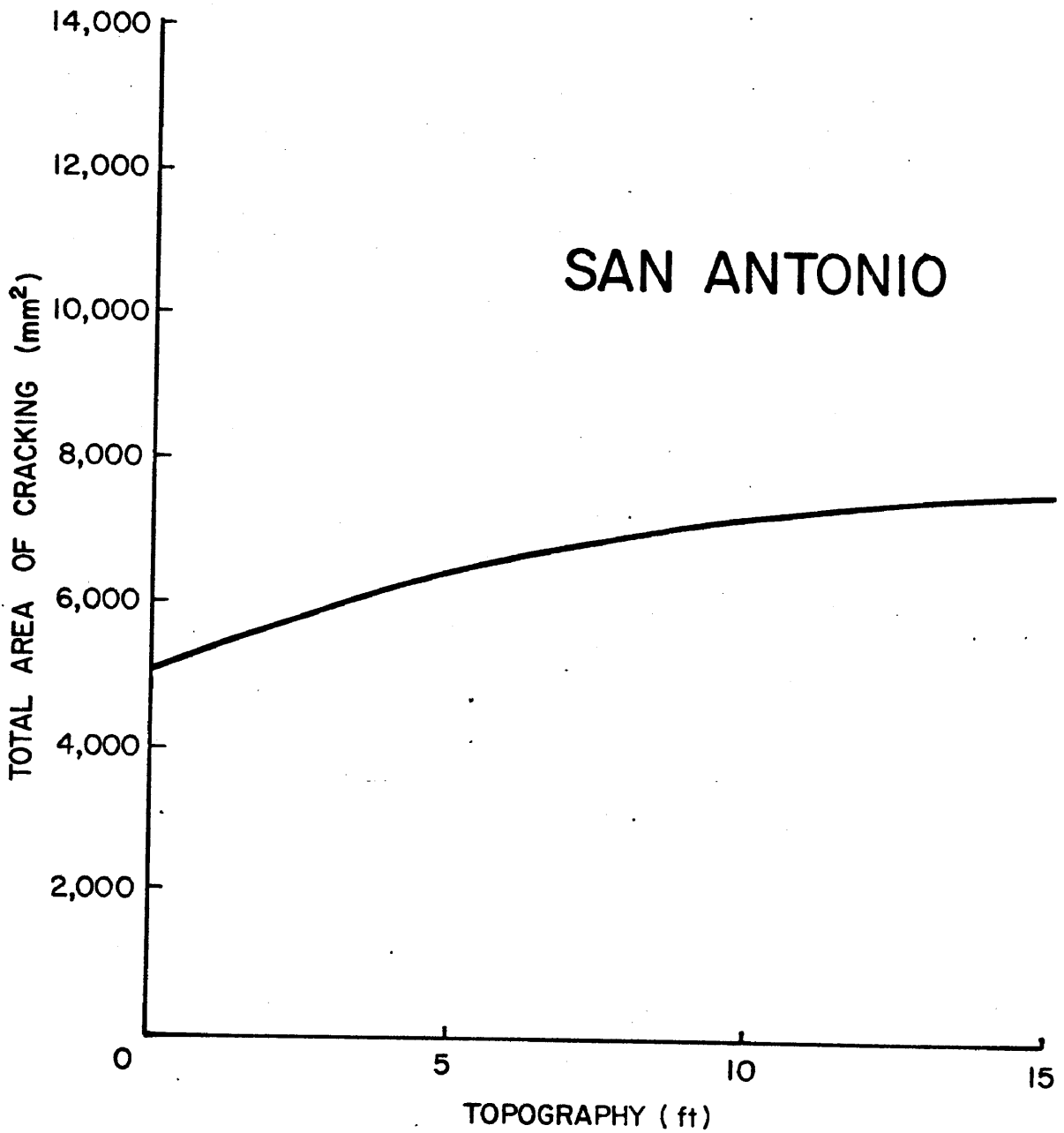


Figure 12. Sensitivity analysis showing the influence of topography (over the average lot dimension of 100') on damage in San Antonio.

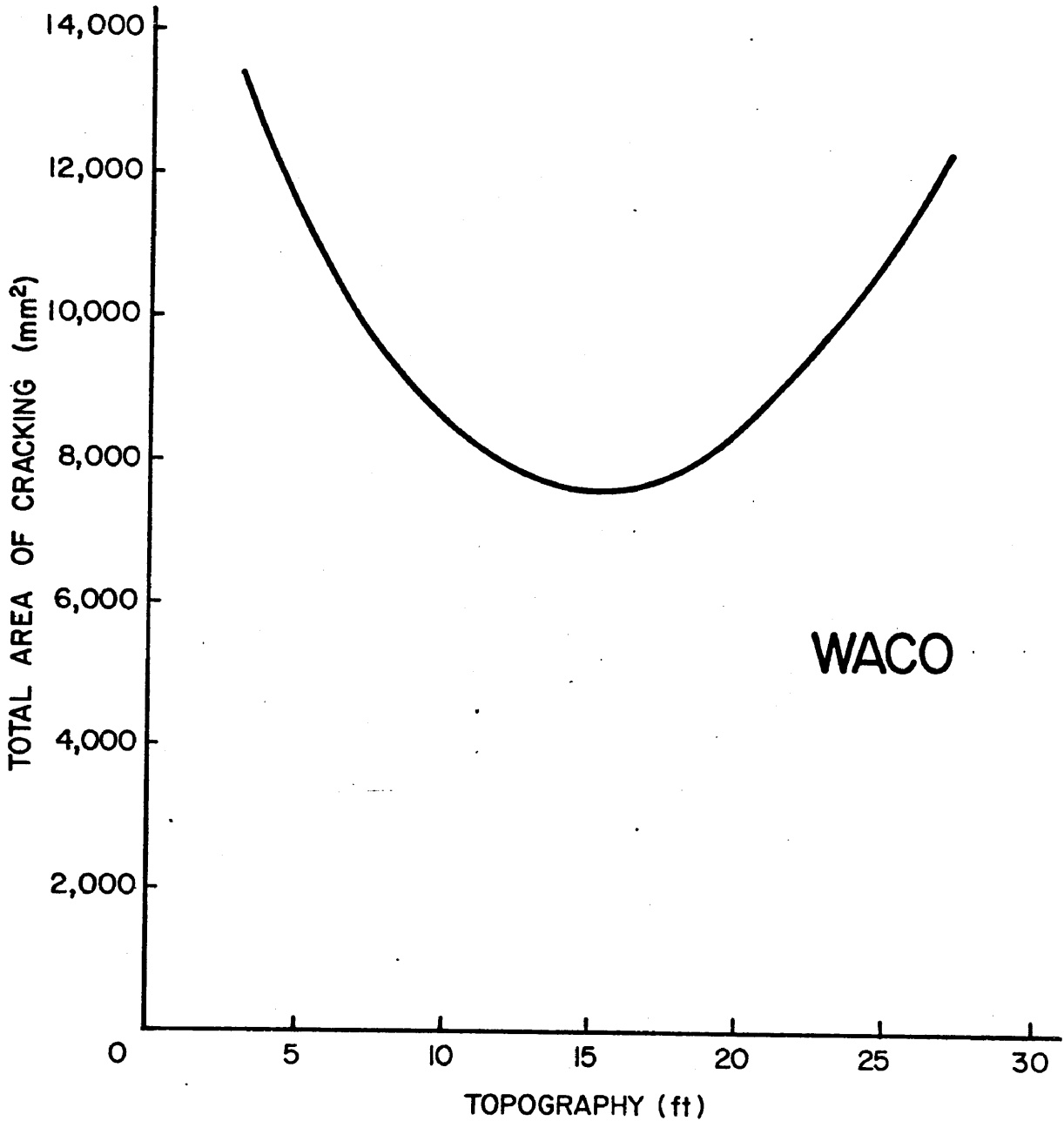


Figure 13. Sensitivity analysis showing the influence of topography (over the average lot dimension of 100') on damage in Waco.

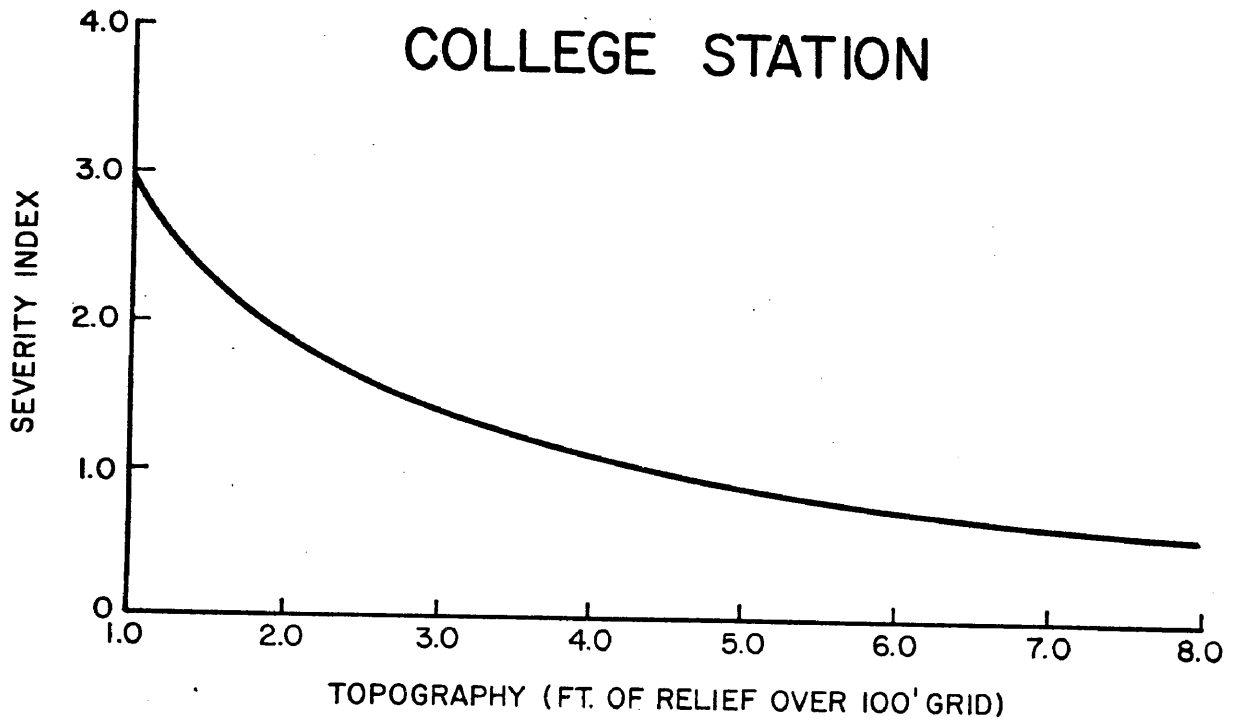


Figure 14. Sensitivity analysis showing the influence of topography on damage in College Station.

This implication can be checked by examining the sensitivity of damage to the age of the house for the two cities. Figures 15 and 16 again suggest that the respective soils are mechanically different. Age appears to exert no influence on the amount of cracking seen in houses on the Houston Black clay while there is a strong positive dependence with the South Bosque shale. The fact that the interaction equation for San Antonio does not contain AGE is indicative that this parameter is insignificant and an equation containing AGE had to be chosen so that an AGE sensitivity curve could be plotted.

#### Crack distribution study

While the regression analysis indicates that damage is associated with the steepness of the slope on which a home rests, a verification of this is available by looking at the distribution of cracks about a house with respect to the slope direction. The home survey data was detailed enough to allow the maximum width of cracks of a given type (ie. top tension, center tension, or bottom tension) to be determined for three categories of wall: wall facing downhill, walls facing uphill, and wall parallel to the slope. Table 3 lists this breakdown for San Antonio and Waco.

In general the houses of the Waco site show the severest deformation. Top tension cracks are common on the walls parallel to the slope as might be expected if creep was tending to carry the downhill portion of a house away from the uphill portion. However, center tension cracks are also prominent. On the downhill side top tension dominates, suggesting that a mechanism peculiar to the downhill side is active. This style of cracking indicates a divergent motion on the part of the downhill side of the house. The tendency for a downhill movement is probably greatest on the downhill side and motions other than directly downhill may be possible. Another observation is the presence of top tension cracks in the uphill walls. This may be due to rebound in response to the unloading caused by construction of the cut. The relative ease of access of water to originally deeper soil levels may also contribute. This feature is not seen in the San Antonio data, perhaps due to the relatively shallow depths of the cuts. The remainder of the San Antonio



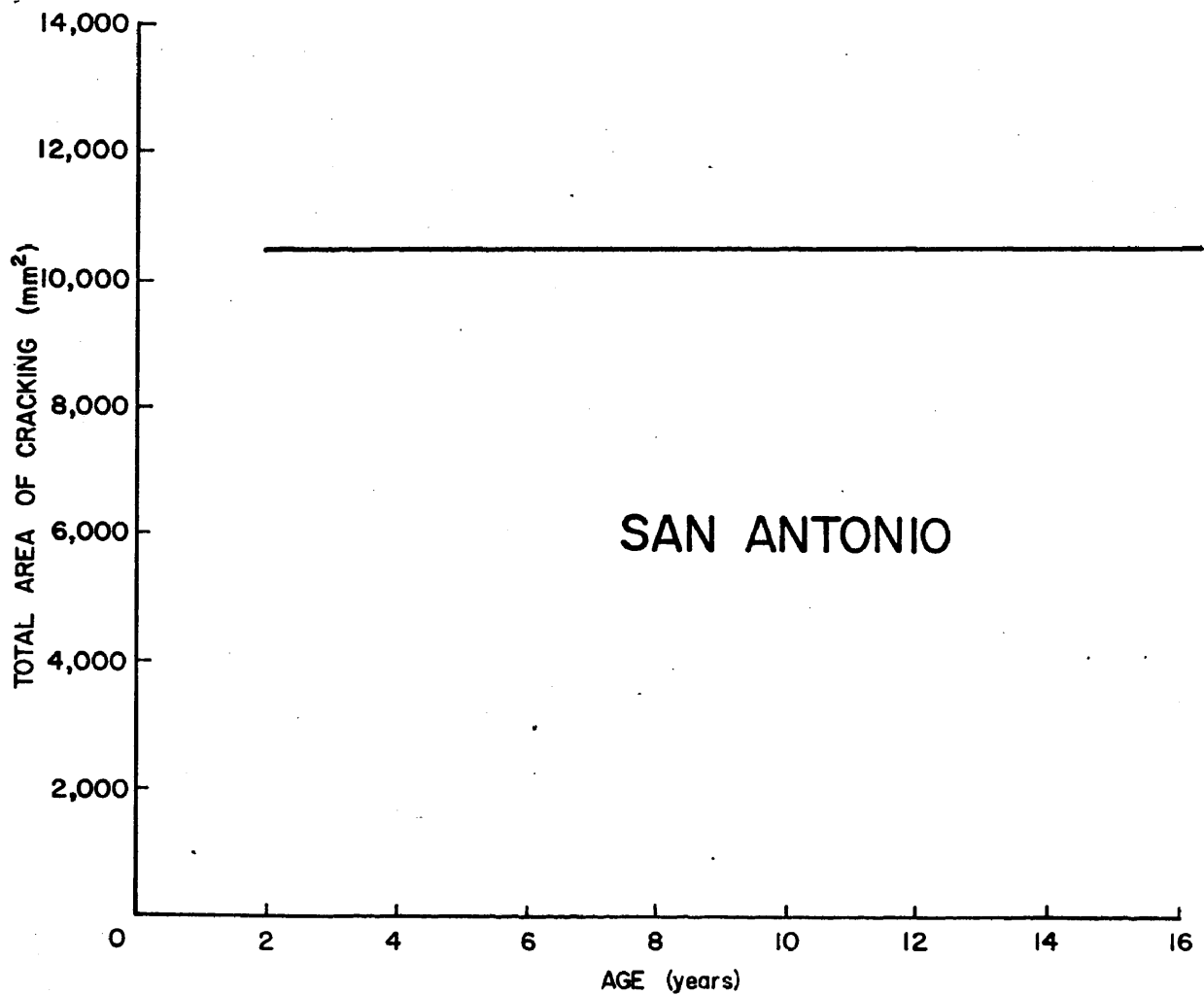


Figure 15. Sensitivity analysis showing the influence of age on damage for San Antonio.

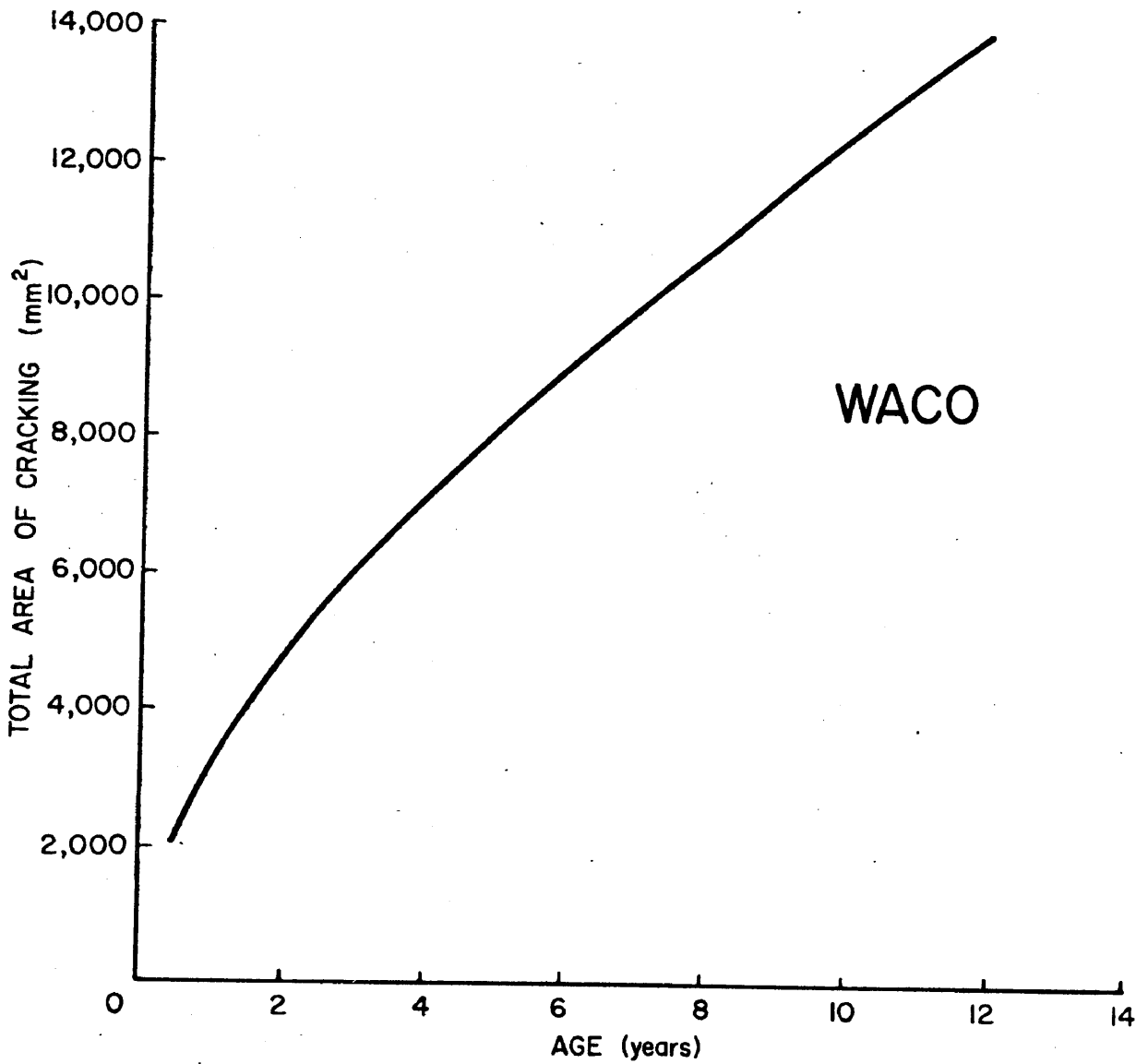


Figure 16. Sensitivity analysis showing the influence of age on damage in Waco.

Table 3. Table showing the average maximum width and standard deviation for cracks according to type and position on house relative to slope.

	SAN. ANTONIO		WACO		
	Ave. Max. Width (mm)	% of Houses Having Cracks of Type	Ave. Max. Width (mm)	% of Houses Having Cracks of Type	
Sides Parallel to Slope	Top Tension	3.7 ± 2.5	29	4.1 ± 4.3	43
	Center Tension	2.3 ± 1.0	23	4.6 ± 5.6	21
	Bottom Tension	1.9 ± 1.0	9	3.2 ± 1.8	12
Side Facing Downhill	Top Tension	3.1 ± 1.9	18	5.3 ± 5.2	40
	Center Tension	2.4 ± 2.	18	2.7 ± 2.6	10
	Bottom Tension	1.9 ± 1.4	9	2.7 ± 2.1	7
Side Facing Uphill	Top Tension	2.3 ± 1.4	27	6.4 ± 5.7	31
	Center Tension	2.1 ± 1.6	24	2.6 ± 2.6	15
	Bottom Tension	2.0 ± 1.6	9	2.3 ± 1.5	4

data show a subdued tendency of top or center tension cracking to occur on the walls paralleling the slope.

As a final indication of the influence of topography on the distribution of cracking, the ability of a regression equation to predict cracking relative to the slope direction was tested. A simple two-variable interaction was chosen which included topography. Average plasticity index, with its use as an index of expansive potential, was chosen as the other variable to verify its positive interaction with topography. Graphs were made by finding the width of the largest crack on side or downhill walls for each house in Waco and plotting this value against an arbitrarily scaled value of the total area of cracking as predicted for each house by the interaction equation (Fig. 17). Side and downhill wall positions were grouped because of the indication that slope movements are contributing to the damage of both. Another graph was plotted for uphill walls (Fig. 18.).

The correlation coefficient for this equation given by the regression analysis for the total area of cracking is 0.45. By plotting the scaled value calculated by the equation for each house against the value for the greatest width of cracking on the side or downhill walls, a correlation of 0.60 is obtained. The correlation for the uphill side is very poor (Fig. 18). A graph was also plotted for San Antonio using a similar equation (Fig. 19). A variable incorporating the plasticity index could not be used because of the constancy of this measure for the San Antonio site. Depth of the active zone was used instead, being the only soil property measure having considerable variation over the site. The scaled values of this equation were plotted against the value of the widest downhill or side wall crack. The results are much less definitive than those for Waco but do show a vague positive correlation.

The degree of interaction between topography and plasticity index can be seen in the Waco case by determining the mean value for these two variables within given intervals of the scaled values for the interaction equation. Table 4 shows that these averages both increase with increasing numerical value of the equation, suggesting that an expansive soil (i.e. one with a high plasticity index) augments the topographic influence on damage.

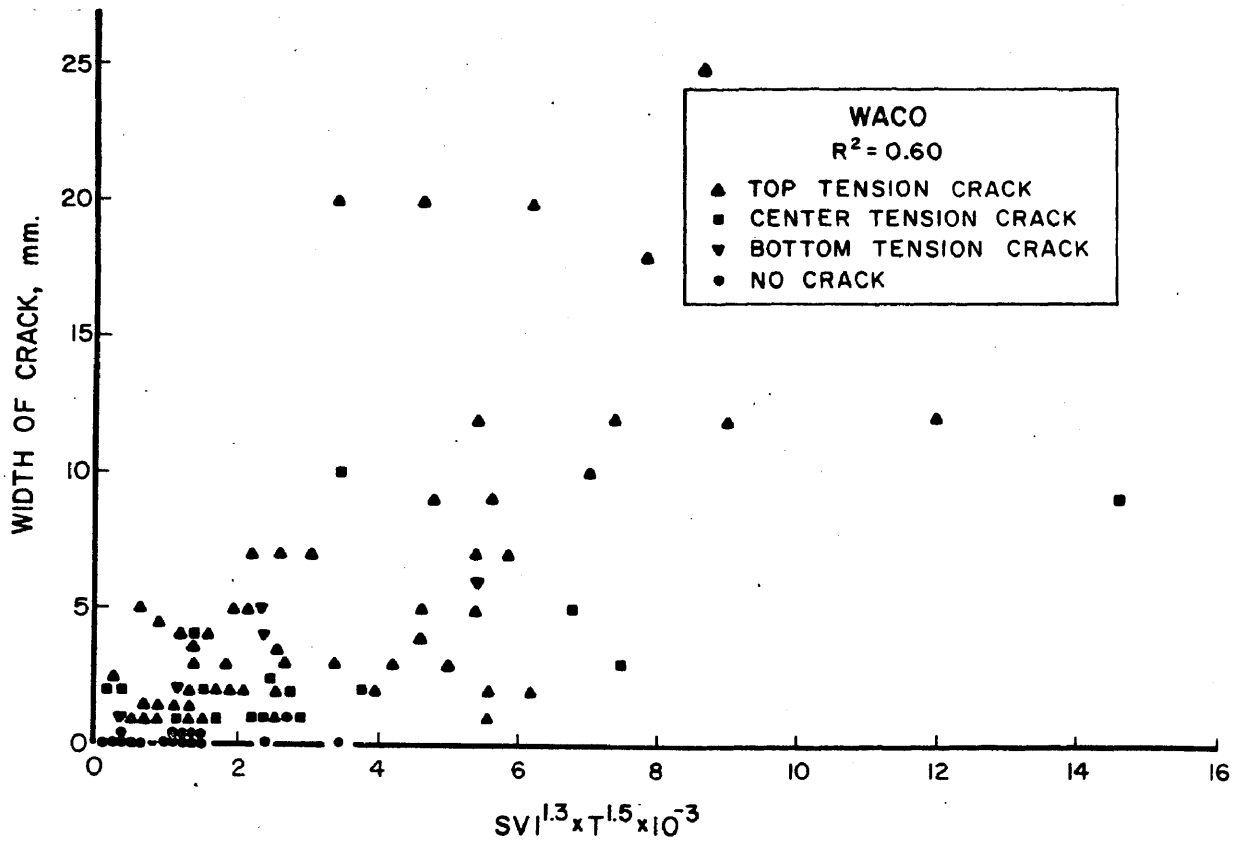


Figure 17. The width of the largest crack on the sides parallel to or facing down the slope plotted against the corresponding value of the selected interaction for each house in Waco.

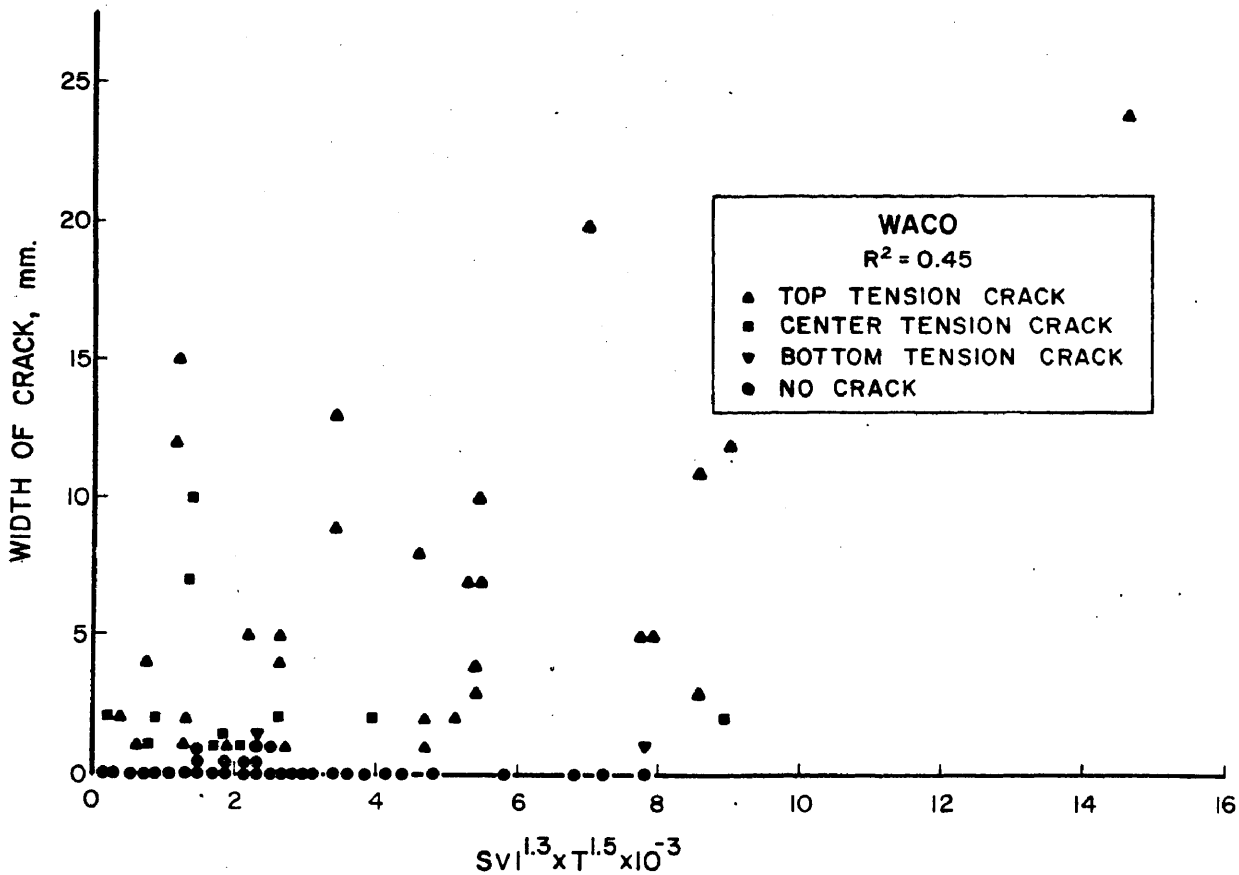


Figure 18. The width of the largest crack on the side facing up the slope plotted against the selected interaction for each house in Waco.

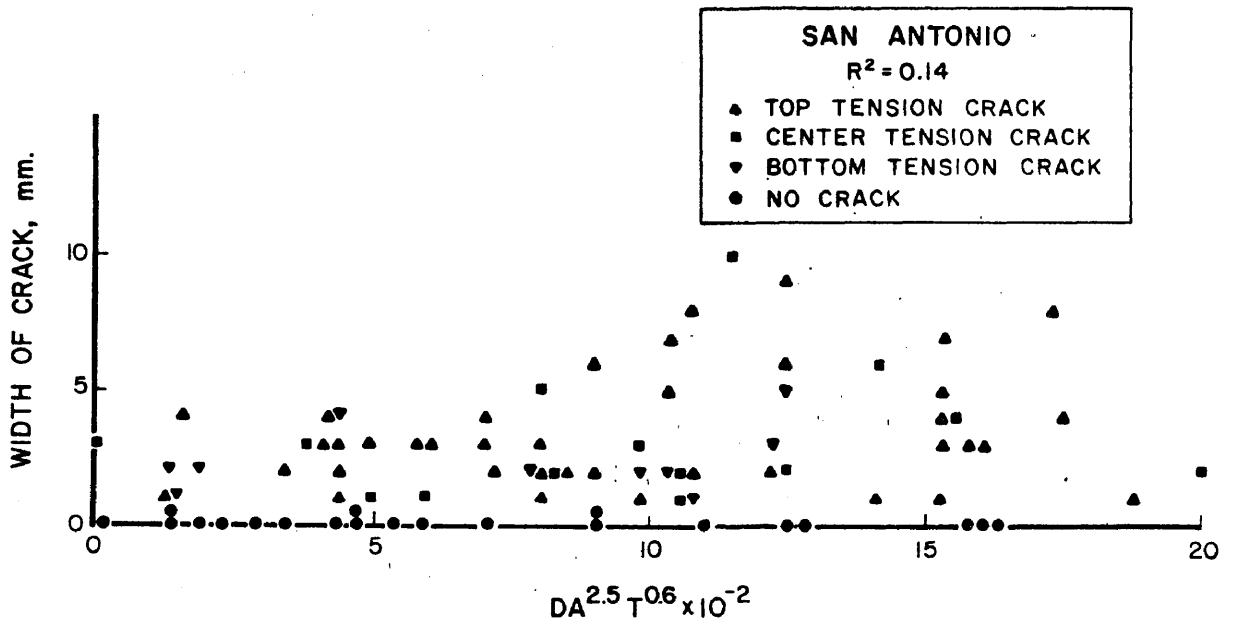


Figure 19. The width of the largest crack on the sides parallel to or facing down the slope plotted against the corresponding value of the selected interaction for each house in San Antonio.

Table 4. Analysis of Fig. 16 showing average values of variables and standard deviations for given intervals of the interaction values.

Interval of scaled interaction value	0 - 2	2 - 4	4 - 6	>6
Average value of T (topography)	5.8±2.5	8.9±2.9	12.3±2.0	16.8±4.0
Average value of SVI (average PI)	29.3±9.0	38.3±9.9	42.0±4.7	43.5±4.6



The results of this field survey provide evidence that damage to houses caused by expansive soil volume changes may have an additional component caused by downhill creep when houses are located on slopes. This observation implies a particular attribute of the soil whereby a pronounced weakening takes place during the volume change phenomenon, allowing downhill deformation to take place. Accordingly it is appropriate to investigate the response of expansive soils to deformation that would occur on a hillslope.

## THE RESISTANCE OF EXPANSIVE SOILS TO SHEAR

### General Scheme

It is typical in the advancement of scientific thinking that many of the most significant contributions have been made early in the history of any field. One of the greatest single advances in the understanding of the shear strength of earth materials was made by C.A. Coulomb in 1776. The simplest form of prediction of failure in soil masses uses the theory of C.A. Coulomb and the Mohr circle construction for the state of stress. The ability of this criterion to predict the shear stress at failure depends on the material having a known response to confining pressure. In its simplest form this is normally assumed to be linear (Lambe and Whitman, 1969), implying that the shear stress required for failure is directly proportional to the confining stress holding the mass together. The application of the Coulomb criterion is most appropriate for uncemented sands because of the frictional nature of the grain to grain contacts. The shear strength-normal stress relation remains linear until the deformation mode of the grains becomes non-elastic but for most engineering purposes non-elastic deformation in sands is not experienced.

The presence of clay minerals introduces a new realm of particle interaction. The negatively charged surface of clay particles combined with their size and shape allows for a particle interaction that may not be fully frictional. Water, attracted to any charged particle, becomes an extension of that particle as an adsorbed layer. The highly ductile character of moist clays results from the relatively large size and tenacity of the water layer compared with the size of a particle. Resistance to shear is offered both by interparticle bonds and the viscosity of the water. A soil is able to deform in a ductile fashion because although bonds may be broken, the water component is capable of being deformed without losing its bonding capacity. The freedom of movement of a particle will be controlled by the water content, the arrangement (fabric) of the mineral particles and the nature of the particles themselves. This view of soil deformation, which is being considered on the scale of the individual particle, is most aptly described as viscous on

the macroscopic scale.

The reason for using the term "viscous" lies in the concept of deformation on the particle scale. The rate of deformation will be controlled by the amount of energy available for moving one particle past another. The ease with which this is done will vary from bond to bond and so not all bonds along a potential failure zone will be breaking simultaneously under a stress less than that determined from a conventional shear strength test. The rate of bond rupture should depend on how much energy is available and how much bond rupture has already taken place. An elastic component is represented by the deformation of the soil particles themselves and by recovery due to strained bonds. However this becomes of small importance when large deformations take place such as would be encountered in the long term creep.

Creep in many materials has been mathematically treated both as continuum process (theory of viscoelasticity) and as an energy of activation process (rate process theory; Glasstone et al., 1941) where bonds are considered to be broken according to a statistical description of the energy available. The latter concept allows an idealized particle interaction to be described and may be most useful for expansive soils because the nature of the particle interaction will be strongly influenced by the presence of montmorillonite. On a long term basis a rheologic description of soil movement would be appropriate but the resultant-downhill motion is divisible on a year to year or shorter basis into volume change motions normal to the slope. The behavior of the soil will depend on the change in soil strength as a shrink-swell cycle is completed. The rheology of an expansive soil is then directly related to its volume changing capability.

If the shrink-swell ability of an expansive soil is to be used as a basis for describing soil strength, a more precise understanding of strength and controls of strength is necessary. Because soil beneath a home foundation on a slope rarely fails but may always deform at some small if still measurable rate, deformation rate is a more appropriate term to describe the load-bearing capability of a soil. The factors that control this rate must be known before home damage due to downhill

movement can be reduced.

Any naturally occurring clay soil will normally be made up of three physically discernible components: solid clay mineral particles, interparticle soil water, and soil air. While soil air can act as a component of the soil pore pressure, its influence on deformability will be taken as negligible here. This is justified by the relatively shallow depths and slow displacement rates under investigation and the small fraction of the total soil volume likely to be taken up by air. The resistance of the soil to deformation should then be dominated by the behavior of the clay-water fraction. Where montmorillonite is present its relatively great capacity for water adsorption would be expected to influence the corresponding soil's mechanical properties according to the amount present and water content.

The reason for expecting this mineralogical influence lies with the nature of clay soil deformation. Unlike the shear failure of rock, failure in clay soils involves extensive interparticle movements before the development of a peak strength. In a soil, clay mineral particles are not held rigidly by an interlocking crystalline structure or cementing agent. Rather, they are held in place by forces of electrical attraction manifest by unsatisfied bonds within the clay minerals or by bonds between clay particles and dipolar-acting water. Deformation must proceed mainly by shearing and rotational motions between grains. While frictional restraint may be operative the degree to which it takes place will depend on the distribution and tenacity of the soil water. Clay minerals capable of preferentially adsorbing water will exert a significant control on strength because of their ability to alter the frictional nature of particle contacts.

That failure will not occur simultaneously throughout a body is commonly suggested by the lack of a sharp knee in force-displacement plots for strength tests on soil specimens. However, on the scale of the individual particle, the use of the Coulomb criterion for describing the stress necessary for initial interparticle movement is useful as a start to considering soil deformation.

Schertman and Hall (1961) analyzed the development of the strength

terms in the Coulomb equation for a clay soil in triaxial compression. Hvorslev (1960) first studied the nature of these terms by conducting strength tests on samples subjected to different consolidation histories but having the same void ratio (ie. water content). However, because the tests are conducted undrained to maintain a constant water content, the strength depends on the rate at which the pore pressure increases. This strength increase is likely to be a function of the fabric developed during consolidation. While the cohesion shows a dependence on water content, the internal friction does not, a condition that does not seem physically probable.

Schmertwann and Hall (1961) in effect deformed a single sample under two simultaneous loads by alternatively loading it at one confining pressure and then another. This allowed them to determine the corresponding cohesion and frictional contributions to the strength mobilized for each pair of applied stress changes. In general the full cohesion is developed very quickly but the friction component continues to increase from zero throughout the test until the ultimate strength is reached.

Mitchell (1964) has attributed resistance to shear as being offered by two types of bond on the atomic scale: electrical bonds between atoms and stress dependent bonds. In order to be broken an "activation energy" must be developed to overcome these bonds. This energy is derived from thermal agitation and an applied shearing stress. An expression is developed that predicts the strain rate a soil will undergo depending on the energy available to overcome bonds. Mitchell also relates his strain rate equation to the Coulomb equation by correlating the activation energy for electrical bonds with cohesion and the energy required to physically translate one atom past another with internal friction.

The study of Schmertwann and Hall (1961) indicates that the way the strength is mobilized changes during the deformation of a test specimen. The increase in internal friction suggests that the number of particle barriers to be physically surmounted is either increasing or the existing barriers are becoming harder to surmount. The latter is probably correct because of consolidation taking place as a test

progresses.

Mitchell's (1964) prediction of a constant or steady state strain rate is based on a constant load being maintained and applies to the steady state region of a creep curve. It is also based on the assumption that the number of bonds remains constant. This must in turn be interpreted to mean that the fabric remains the same in the sense that new particle bonds are made as fast as existing ones are broken. This could be categorized as a type of failure where the load is remaining constant as deformation continues. Eventually steady state creep usually accelerates, indicating that a change in fabric must be taking place.

A clay that has reached a steady state creep condition can be considered to be exhibiting a given value of internal friction. An increase in load may act to increase the internal friction depending on the compressibility. The actual response of the clay in terms of its creep behavior will depend on how sensitive the internal friction is to load. A clay will display an initial rapid deformation response to any load increment but the accompanying compaction may increase the internal friction such that the post-initial response behavior remains essentially the same from one load to the next. The point at which the creep rate begins to accelerate will depend on the capacity of a clay to resist compaction. Interlocking of clay particles is a reasonable explanation for development of internal friction and when this approaches a limit, so should internal friction. Changes in the mode of clay deformation will depend on fabric changes and on changes in the nature of interparticle friction.

There is as yet no direct proof that clay particles make direct crystal structure to crystal structure contact. The doubt arises because of the existence of adsorbed water on clay particles and the probable occurrence of epitaxy, ie. the ability of a species to become an extension of a pre-existing crystal structure. Goldschmidt (1926) first suggested that the plastic behavior of clays may be due to the adherence of water to the clay particles. Before this it had been theorized by Gouy (1910) and Chapman (1913) and later modified by Stern (1924) that a particle exhibiting a charge imbalance would attract

about itself an atmosphere of oppositely charged ions. The dipolar nature of the water molecule lends itself to this phenomena, but also complicates it because of the tendency of the water to form an ordered structure. The exact nature of adsorbed water has been disputed (Low, 1961; Martin, 1962) although there is a considerable volume of evidence for an ordered structure being present (Low and White, 1970).

Rosenquist (1955) investigated the heat of wetting of a clay and found that for the first few molecular layers about a clay particle the values were much higher than for the formation of ice in free water. This was early evidence that the water immediately next to clay particles was tightly bonded in an orderly structure. Derjaguin (1936) had already established that the water next to glass surfaces had a definite rigidity. Comparing Rosenquist's data for heats of wetting with the activation energy for the flow of water in montmorillonites (Low, 1960), it can be seen that at the second or third molecular layer (as calculated from surface area and water content data) the values (approx. 4 kcal./mole) are similar. This suggests that a few molecular layers of water are bound tightly enough to resist the friction set up by moving water. Low's data for montmorillonites may actually represent a relatively high activation energy because of the small pore sizes that are encountered in montmorillonite clays. It is even possible that most of the water in a montmorillonite clay is structured. This follows from the work of Ravina and Low (1972) which has suggested that epitaxy takes place between water and montmorillonite. Structured water will continue to build outward from the surface of a montmorillonite crystal as long as the b-dimension can change. Once the limit is reached, swelling ceases. The exact nature of this water is unclear but considerable evidence has been found for its existence (Low, 1961; Low and White, 1970). The thickness of adsorbed water can reach several 10's or even 100's of angstroms. It is with this phenomenon that changes in the rheologic properties of expansive soils may be associated.

According to Ravina and Low (1972) a significant change in free energy takes place up to a moisture content of approximately 100% in Na-montmorillonite. Consequently this water must exist in a more or less structured form (or at least in a form different from that of free

water) separating the mineral layers. At the greatest distances from the layers the bonding would be weakest and were a shearing couplet to be applied on two montmorillonite layers, the deformation would probably be concentrated along the plane of weakest bonds. To shear these bonds would require relatively little stress because their strength would be approaching that of free water.

The development of the adsorbed water layers will be restricted by the state of pure shear set up between the clay mineral layers if the clay is compressed. An equilibrium clay layer spacing will then be established, governed by the tenacity of the adsorbed water compared to the magnitude of pure shear. Bolt (1956) and Warkentin et al. (1957) have shown that considerable spacings are maintained between montmorillonite particles up to pressures of 10 bars. Furthermore, Rosenquist (1955) has shown that the energy involved in forming adsorbed water becomes relatively small beyond the first few percent increase in water content. These observations suggest that the adsorbed water may remain highly susceptible to shear even where the clays are relatively highly confined.

The possibility also exists that dislocations within the adsorbed water structure would introduce further weakening. Dislocations enable two bonded molecular layers to move past each other by disrupting only one bond at a time. The process can be described as a rate process (Mott, 1956). In this case a clay particle would be equivalent to a single bond or as many bonds as there were dislocations in the structured water of that particle.

The concept of the adsorbed water in a montmorillonite particle acting as a zone of preferred shear may offer an explanation for the deviation of many soils from strict adherence to the Coulomb law. Several observations of low internal friction values for montmorillonite clays have been made (Kenney, 1967; Mesri and Olson, 1970; Chattopudhyay, 1972) suggesting that the presence of adsorbed water layers is acting to reduce the internal friction. The fact that the internal friction values also decrease with increasing normal stress indicates that the adsorbed water layers become the main contribution to shear



resistance. More importantly to this study, a relatively weak bond compared to the frictional bond between interfering clay particles may be afforded which would reduce the activation energy required for creep.

## VOLUME CHANGE STUDY

### General principles

Expansive soils have as a unique property the ability to show relatively large volume changes within certain ranges of moisture content change (a description of volume change mechanisms is provided in the appendix). This phenomenon can be observed on all scales down to that of the individual clay particle. An increase in particle separation accompanies moisture increase and so the number of particle contacts and their tenacity decreases. This change is considered to be responsible for a change in the resistance to shear offered by an expansive soil. The excessive volume changes associated with expansive soils may result in an excessive decrease in shear resistance as the maximum volume is approached.

Determining the shear resistance of an expansive soil will necessarily require testing according to moisture content (defined on a weight basis). The relation will be an inverse one but beyond that the nature of the exact correspondence should have little physical meaning. The moisture content supplies no direct indication of the particle to particle stress state.

Water is attracted to the surfaces of mineral particles and can actually have a structure imparted to it by these hydrogen-bonding forces. For a given soil composition and texture the amount of water present will determine the tenacity with which the farthest water molecules are held. However, the same amount of water in a soil of another texture and density may exist at a different level of attraction. The surface area of the soil particles will determine the maximum distance a water molecule can be from a particle surface.

The energy with which water is held is referred to as the soil water suction or, more appropriately, soil water potential. An attempt to formalize this concept was made during a symposium entitled "Moisture Changes in Soils Beneath Covered Areas" (Aitchison, 1965). The definition arrived at concerns the amount of work required to transport an infinitesimal amount of water from a pool of free water (water at zero potential) to the point in the soil under consideration. The potential

can be expressed in terms of the pressure required to remove the water from this point.

In practice this point likely takes the form of a pore. If the soil is not fully saturated the water-air boundary will be a curved surface, the radius of which is inversely related to the soil water potential. As the moisture content decreases, the remaining water retreats into smaller and smaller openings and comes more and more under the influence of the attraction to particle surfaces. The pressure of water vapor in equilibrium with the soil water also decreases as water content decreases. The soil water has less freedom to change to a vapor form as it comes increasingly under the influence of the particle surfaces. Put another way, the relative humidity varies inversely with the soil water potential. The exact relation is given by the Kelvin equation stating suction as a logarithmic function of the relative humidity.

The foregoing discussion suggests that the soil water potential provides the most physically significant indication of the expansive state of a soil. For a given value of the potential, the energy available for expansion when a source of free water is provided can easily be determined. The potential may be thought of as an internal confining pressure (although strictly equal to the same value of external confining pressure only as long as the soil remains saturated) and as such should directly influence shear resistance. Therefore, to decide on what moisture contents should be used for deformation testing it is appropriate to evaluate the volume change response of the soil to changes in the soil water potential.

#### Water change experiments

General approach. The application of known soil water potentials to soil samples is a well recognized procedure for determining the moisture content response to potential change. Corresponding changes in bulk density and thus volume are also easily obtained. However, the effect of hysteresis, whereby different water contents will be obtained for the same potential depending on whether moisture is being desorbed or adsorbed, requires that both the wetting and drying of the soil be

considered. Knowing the wetting and drying response, a hysteresis loop or soil water characteristic can be plotted relating water content to potential. Knowing the corresponding changes in bulk density the loop can be transformed to relate volume change to potential.

Procedure. Undisturbed samples of South Bosque shale and Houston Black clay were secured by driving two-inch inside diameter PVC plastic tubes (seven inches long) vertically into the soil. Each tube was bevelled on the outside at one end to form a sharp cutting edge and lightly greased on the inside to reduce friction with the soil. The ends of the tubes were sealed with wax in the field to prevent the soil from drying.

For the determination of the desorption half of the loop, a one-half inch thick wafer of saturated soil is placed on a saturated porous ceramic plate which in turn is housed in a pressure vessel (Figure 20a). The wafer is obtained by slicing the PVC tube at the desired thickness and a close contact with the plate is insured by smoothing one side of the wafer on a wet paper towel. An air pressure corresponding to the desired soil water potential is then applied to the pressure vessel. One side of the porous plate is vented to the atmosphere so that water is expelled from the plate. Providing the contact between the soil and the plate is intact, the water forced out of the plate also tends to draw water from the sample until the potential matches the air pressure. The following pressures: 0.1, 0.33, 0.67, 1.0, 2.0, 5.0, 10.0, and 15.0 bars were applied and the samples left in the vessels for at least three days. Half of each sample was then used for moisture content determination and half for dry bulk density determination.

The adsorption curve was determined by in effect reversing the preceding process. Clay samples desorbed to -15 bars were placed in contact with remolded samples of Norwood silty loam (U.S.D.A., 1958) for which the desorption curve had already been produced. The tests were run by filling high wall petrie dishes with saturated Norwood soil, smoothing the top surface and allowing these to dry for various lengths of time but not to a potential greater than -15 bars. For a given Norwood soil preparation the clay sample was placed on the soil and the

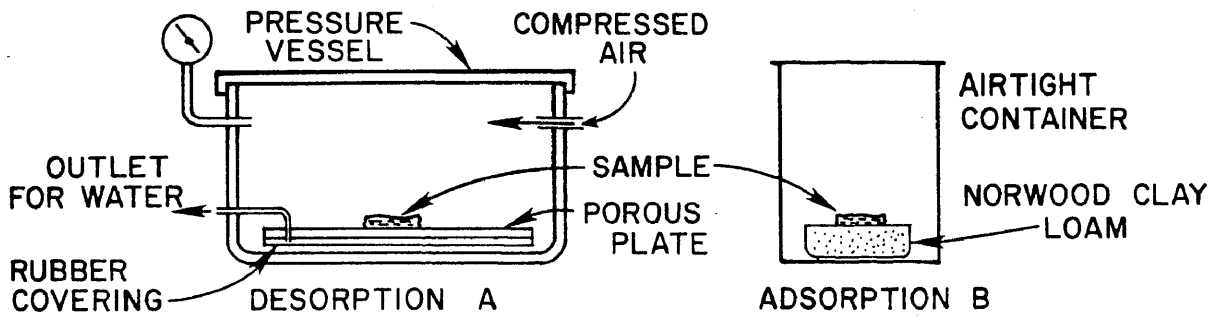


Figure 20. a. Schematic diagram of pressure vessel used for desorption tests. b. Schematic diagram of set-up used for adsorption tests.

two placed in a sealed container (Figure 20b). The clay sample would then adsorb water from the Norwood soil. At equilibrium a moisture content determination of the Norwood soil referred to the desorption curve would give the potential of the clay. Equilibration was monitored by determining successive moisture contents until a constant value was reached. This would require approximately one week.

Experimental results - moisture content versus potential. Soil water characteristics plotted for the two clays show a large degree of hysteresis (Figures 21 and 22). The shape of the loop for the Houston Black clay requires some comment due to the fact that the adsorption curve drops considerably below the minimum moisture content for the desorption curve. The two should show the same value of water content at -15 bars. The only apparent explanation for this falls back on a continuing indication that the two soils differ in their mechanical response to external influences. In the case of this discrepancy either or both of the curves could be incorrect. It is suspected that both are slightly in error due to the inability for the water in the clay samples to be efficiently drawn out. This may be due to the soil having a ped-like structure whereby communication between peds is hindered by relatively large surrounding pores. The result would be incomplete desorption on the porous plate and incomplete adsorption from the Norwood soil. Thus the true loop probably exists within the area bounded by the two observed curves.

Experimental results - linear extensibility versus potential. The coefficient of linear extensibility or COLE (Franzmeier and Ross, 1968) is a measure of the displacement in one direction accompanying the volume change in a soil. It is calculated by the following formula,

$$\sqrt[3]{\frac{D_a}{D_s} - 1}$$

where  $D_a$  is the dry bulk density of the soil at some arbitrary potential, in this case air dry, and  $D_s$  is the dry bulk density at the potential in question.

Total bulk densities were determined by weighing a sample in air, weighing it again with a paraffin coating of known density and then

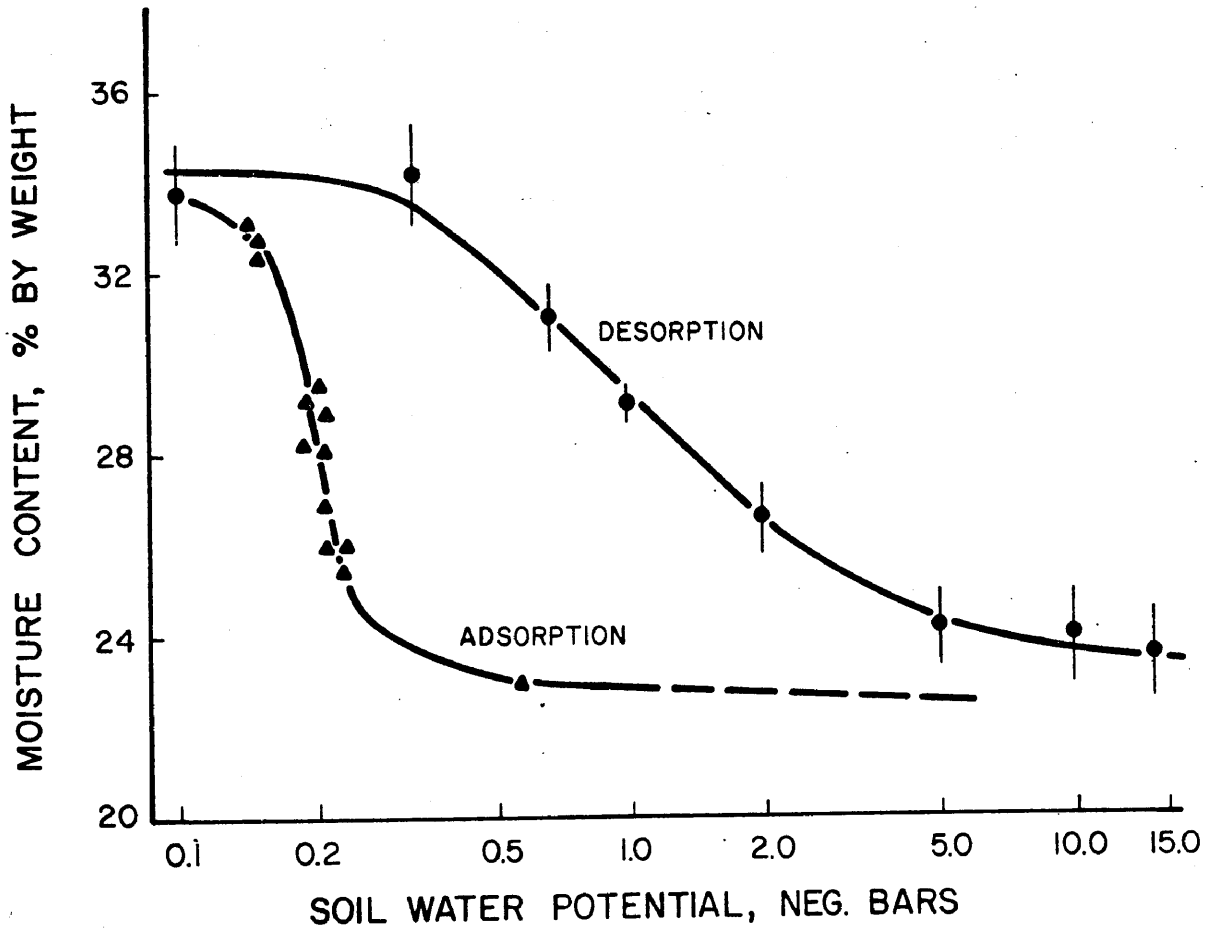


Figure 21. Soil water characteristic for South Bosque shale desorbed to -15 bars. Bars on desorption data points show standard deviation for four determinations on this and the following three graphs.

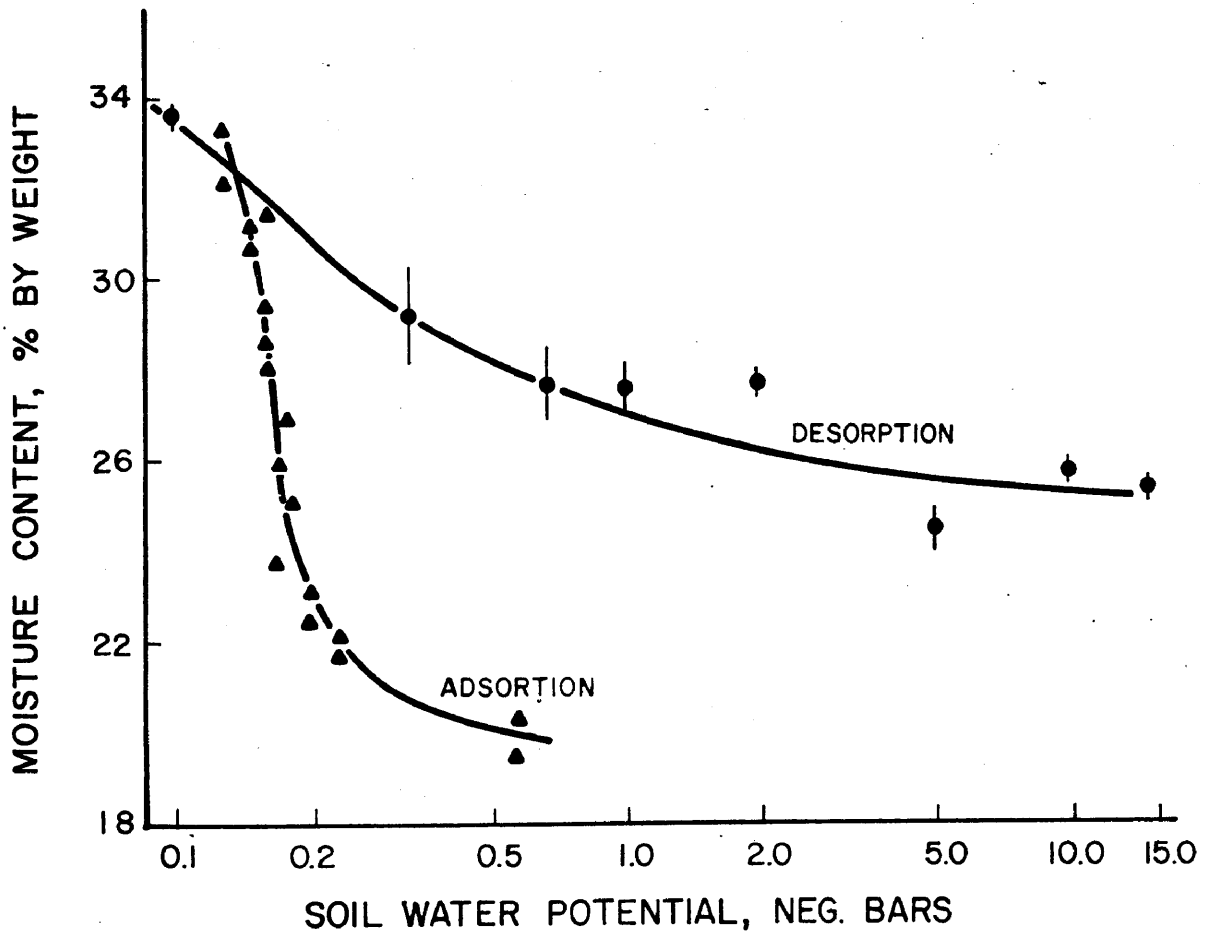


Figure 22. Soil water characteristic for Houston Black clay desorbed to -15 bars.



weighing once more in water. With the total bulk density and the water content known, the dry bulk density may be determined according to the formula,

$$\frac{\gamma_t}{1 + w}$$

where  $\gamma_t$  is the total or wet bulk density and  $w$  is the water content.

Plots similar to the soil water characteristics were made using the resulting data (Fig. 23 and 24). The loop for the South Bosque shale is similar in appearance to the soil water characteristic. The remarkable attribute of both loops for this soil is the sudden increase in water content and COLE with very little decrease in potential at about 0.2 bars. This feature is not seen on the plot exhibiting COLE for the Houston Black clay. The nature of this difference between the two soils is treated in the chapter on analysis of experimental results.

To allow for differential loading conditions in the design of a foundation some estimate of the soil volume change potential is necessary. Several empirical methods, based on soil index properties, have been proposed (Lambe, 1960; Sullivan and McClelland, 1969; McDowell, 1974). All of these methods arrive at predications based on the air-dry soil reaching a fully saturated condition with water available at zero soil water potential. In fact, this is rarely if ever, the case in climates where shrink-swell is a problem. In any locality where the water table is below the surface the soil water potential will trend toward an equilibrium controlled by conditions of evaporation and transpiration, capillary forces which exist above the water table, and overburden pressure (Jennings, 1953). At any point above the water table a negative potential exists at least at equilibrium. Only at the surface will the soil be air dry. If evaporation and transpiration are eliminated (as beneath a home foundation) the potential will decrease to some equilibrium value determined by the water if it is shallow or by climate if it is deep (Aitchinson and Richards, 1965). For this long term case at least, the difference between the covered and uncovered potentials seems most applicable to predicting volume change. For the short term case, where water is introduced at the surface by rainfall, the generally low permeability of expansive soil peds and clods will prevent the full

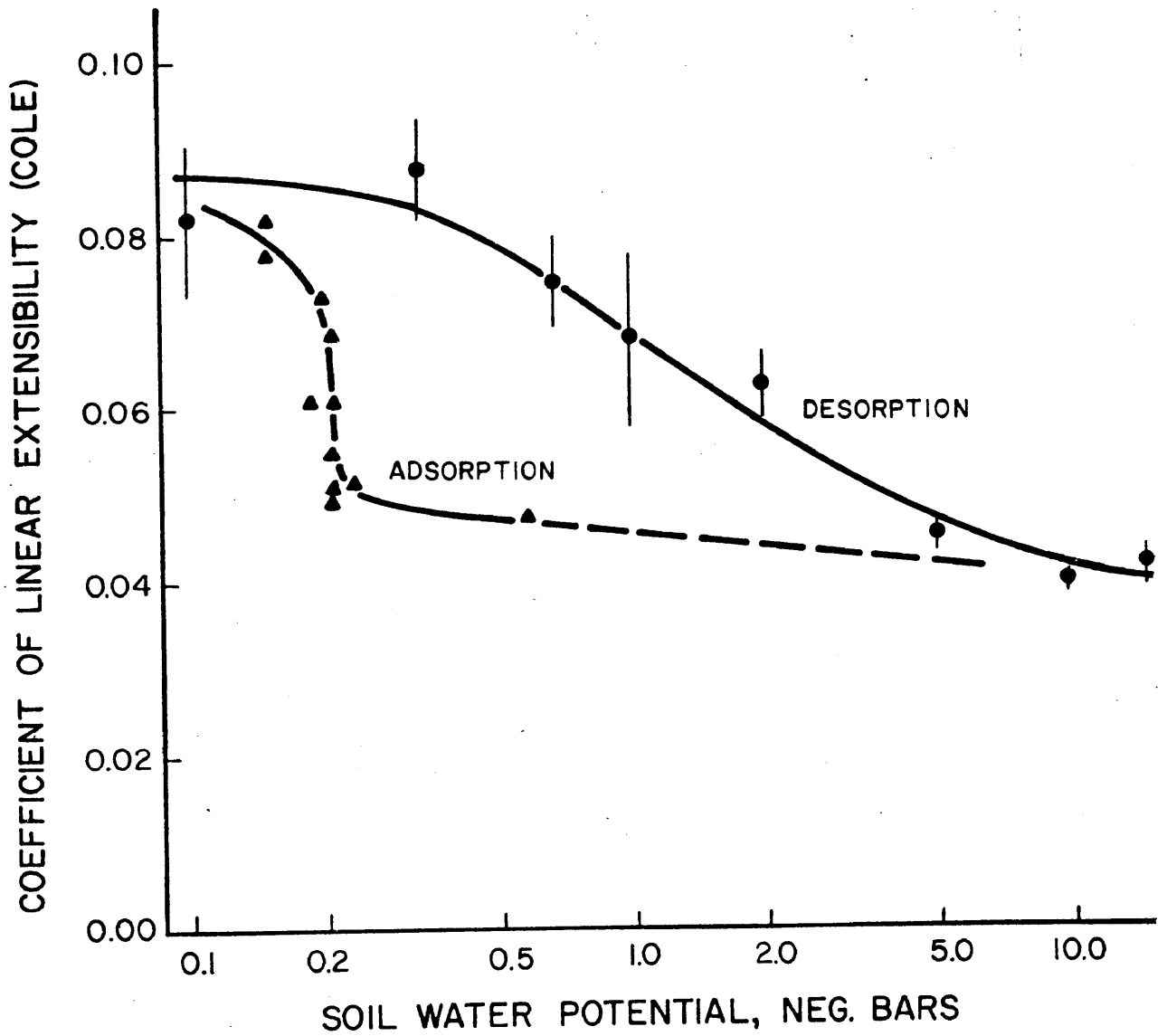


Figure 23. Volume change hysteresis loop for South Bosque shale desorbed to -15 bars.

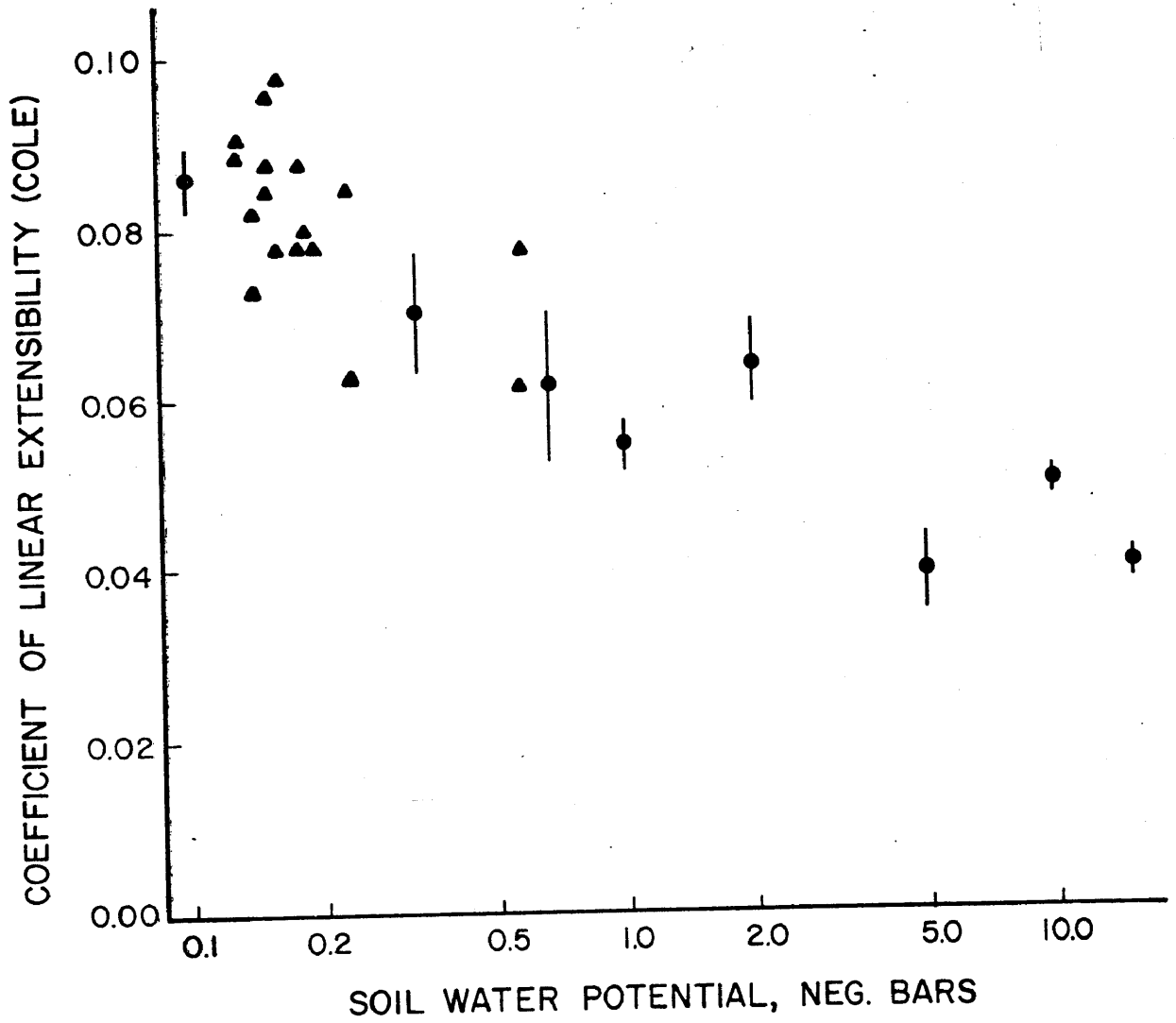


Figure 24. Volume change data for Houston Black clay desorbed to -15 bars.

expansive potential being reached over the period that free water might normally be available.

Assuming a soil to be 100 percent saturated and employing the principle of effective stress, the effect of overburden pressure should be equivalent to a potential of the same value acting on an unconfined sample of soil. This should at least be true for clay soils at potentials up to the agronomist's field capacity, a value of approximately one-third bar and a range of potential over which most of the volume increase takes place. This hypothesis may be tested with the Casagrande consolidometer (Lambe, 1951). It may be adapted for use as a swell meter, allowing vertical expansion for different overburden pressures to be determined. Rather than starting with an air-dry sample, a sample at a representative field moisture content is given free access to water. The value of expansion may then be compared with that predicted from the hysteresis loop.

Samples of South Bosque shale allowed to consolidate under artificial overburden loads of 1.3, 2.7 and 8.1 psi showed swelling of 0.94% for the 1.3 psi pressure, 0.66% for the 2.7 psi pressure and 0.20% for the 8.1 psi pressure. These samples were collected in summer and had a relatively dry moisture content (22-23%) indicating that they were at the high end of the potential range studied. The preparation technique for insertion in the consolidometer resulted in adsorption taking place with moisture contents increasing to 26-27%. It was estimated from the adsorption curve that the potential for these samples decreased to approximately -0.22 bars. One other sample that was prepared without water content increase maintained a potential of approximately -15 bars and swelled 2.0% under a pressure of 2.7 psi. When the COLE for these values of potential are subtracted from the COLE for the values of potential equivalent to the overburden pressures, a linear extensibility for the resulting potential decrease is obtained. These estimates of swell vary in direct proportion to the estimates obtained from the consolidometer but are about three times larger. The amount of swell measured in the consolidometer is not equivalent to linear extensibility probably because the sample is prevented from expanding laterally by the consolidometer ring as well as experiencing a frictional

restraint.

To interpret the sorption curves in terms of the actual amount of shrink-swell to be experienced, the influence of climate must be included. Water contents reach a constant value from about six feet down to a maximum depth of observation of 15 feet in the Waco study area, suggesting the water table to be at too great a depth to significantly influence soil water potential. Given the relationship between equilibrium potential and Thornthwaite Index for a heavy clay developed by Russam and Coleman (1961) it is seen that a potential of about -2 bars should be maintained under covered areas at the Waco site. It is apparent from the adsorption curve that if the potential can be maintained below about -0.3 bars, a significant amount of the shrink-swell capability of the soil will be avoided. Some combination of surcharge with inert overburden and drainage improvement could be helpful in minimizing shrink-swell.

Samples of Houston Black clay were also subjected to this testing procedure. The behavior of this material was markedly different in that samples initially at a potential of -15 bars and loaded at 1.3, 2.7, and 5.4 psi all showed a slight collapse with no expansion even when a sample was redried and rewetted. The difference means that soil fabric and geologic history are important in assessing the volume change behavior and methods for determining expansion potential which do not take these into account may be grossly inaccurate.

The plot of linear extensibility versus soil water potential for the South Bosque shale (Fig. 23) was useful in deciding at what potentials deformation tests should be conducted. It will be noticed that the desorption curve shows a relatively constant shrinkage with increasing potential. It is anticipated that a correspondingly constant decrease in deformation under a constant stress would take place. The adsorption curve appears to be far more distinctive and suggests that a great change in deformational properties should be seen with only a slight change in potential over a small range around -0.2 bars. This criterion is used for the tests described in the next section.

## DEFORMATION STUDY

It has been shown by the home survey that part of the damage sustained by those homes situated on slopes appears to be due to downhill creep. Creep is intended to mean the deformation produced by the constant load imposed on the soil by gravity. The deformation is considered to be penetrative and accomplished in a state of simple shear with the overall movement taking place parallel to the soil surface. Shearing parallel to the ground surface must occur because at some depth, downhill movement will cease.

A shear stress parallel to the surface of a slope can be estimated for a depth that is small compared with the relief formed by the slope. For depths likely to experience a yearly or more frequent change in water content this shear stress would amount to no more than a few pounds per square inch. This concept affords a crude guideline for determining an appropriate stress to be used in deformation tests. As suggested by numerous field studies (see chapter: *In situ Creep of Soil*, p. 4), penetrative creep is normally restricted to the upper few feet of the soil profile where yearly or more frequent changes in soil physical conditions control resistance to shear.

The objective of the deformation testing is to determine the response of the expansive soils from Waco and San Antonio to a loading condition similar to what they might experience in the field. The conditions in the field that will cause the most significant variations in creep behavior are moisture content and depth of burial. While this is an association that applies to any soil, the results of the volume change experiments suggest that these expansive soils may be very sensitive to relatively small changes in water content at or near saturation. The rapid increase in volume below one-third bar may be associated with a dilatant tendency of the clay fabric so as to reduce the shearing resistance.

### Experimental design

Triaxial creep tests were used to determine the response of the expansive soils to shearing. The central portion of a cylindrical

specimen is likely to initially be in a state of pure shear. With continued deformation however, specimens were usually observed to have an inclined shear zone. From an early stage the deformation in a specimen must be trending toward the final development of this zone. Thus a state of simple shear may be assumed to be the dominant mode of deformation in the specimens, at least in the central part.

The history of deformation rate during a creep test will take one of three forms depending on the ratio of the creep stress to some measure of the ultimate strength of the material. If the load is great enough the rate will accelerate until it is fast enough to be termed failure. For a relatively small load the rate will initially be high as the elastic component of strain is mobilized (Mitchell and McConnell, 1965) but will then decelerate indefinitely. Thus a small load will produce a viscoelastic behavior whereby stiffness increases as fabric changes take place and perhaps as an initially increased pore pressure dissipates. The term viscoelasticity is used as an idealization of the creep process. It probably is an important part of the natural creep process on expansive soil slopes and so tests that display it are likely to be the most appropriate for estimating natural behavior. At some intermediate load an interval of constant rate may occur, followed by an acceleration to failure.

Neither rapidly accelerating creep nor constant rate creep are expected on expansive soil slopes. In nature, the displacements probably take place by an accumulation of creep events, each event started by a wetting of the soil. Failure has obviously never taken place at any of the homes and so a creep stress that only produces decelerating displacement after an initial high rate is most appropriate.

To plan the experimental program, the soil water characteristics are used. The possibility of the hysteresis loop being suitable for predicting the creep behavior can most easily be evaluated by testing at potentials in the vicinity of the rapid water content increase portion of the hysteresis loop. The loop seems to be a reliable indicator of expansive potential and so it may be useful as an indicator of creep potential. Specimens may be wetted to some desired potential from the

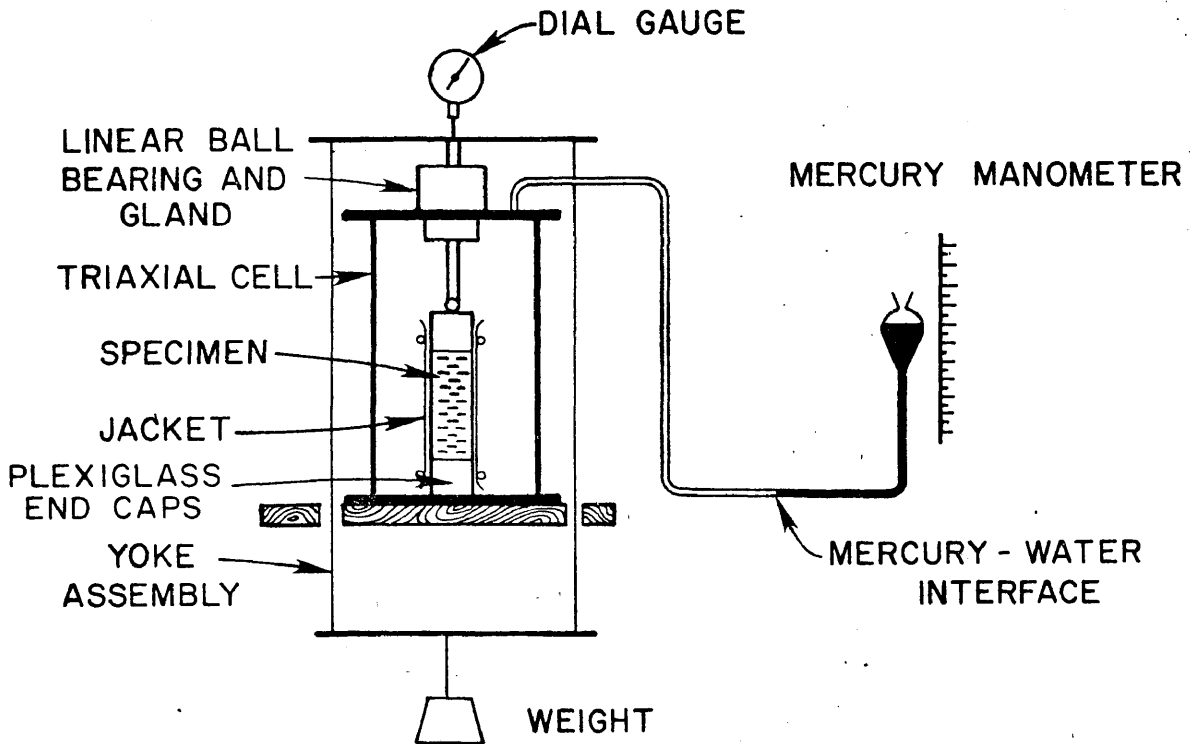


Figure 25. Schematic diagram of creep test apparatus.



arbitrary dry state of -15 bars and then subjected to a creep test. It may then be possible to relate the creep behavior to the expansion.

### Apparatus

A conventional triaxial cell (9 in. high, 6 in. in diameter manufactured by Wickham Farrance, England) was used to contain specimens for the creep tests (Fig. 25). A yoke system was constructed to apply the creep load. It consisted simply of two metal bars connected by two wires, one bar resting on the top of the piston and the other having a hook on which weights were hung. The load was transmitted through a piston sliding on lightly oiled linear ball bearings to two-inch diameter plexiglass end caps, the top cap contacting the piston via a ball bearing. Confining pressure was applied by a column of mercury and interfaced with deionized water as the confining medium.

### Conduct of experiments

Two-inch diameter cores of the expansive soils were collected in the manner described in the chapter on volume change experiments. Samples approximately four inches long were cut from these cores and the PVC coring tube split lengthwise for removal. The ends of the samples were smoothed and two latex rubber jackets placed over each one preparatory to testing.

Two types of creep test were conducted according to moisture content: 1) Samples were saturated by allowing free access of deionized water to a jacketed sample in place in the triaxial cell. Creep tests were then run unconfined and at confining pressures of 2 and 5 psi. 2) To achieve a desired soil water potential within a sample, the moisture content was adjusted to the appropriate value as indicated by the soil water characteristic. The water content of a sample could be monitored non-destructively by monitoring its weight and having an average value for the saturated water content of the soil being studied. Samples were dried over several days to a water content corresponding to a potential of -15 bars and then rewetted to a water content corresponding to the desired potential. All tests performed on these controlled water content specimens were conducted unconfined.

A creep stress was selected that would produce ultimately decelerating creep but with easily discernible displacement. Loads producing deviator stresses of 2, 3.5 and 5 psi were used and all tests were conducted by hanging weights at intervals of two hours to successively produce these stresses. Displacements were read on a dial indicator in contact with the top of the piston and converted to axial shortening (defined as change in length of a specimen divided by the original length). Results for tests at predetermined soil water potentials are plotted in Fig 26-30.

### Tests on artificial soils

The hypothesis that expansive soils are especially susceptible to downhill creep can gain a more general acceptance if the presence of the characteristic clay mineral montmorillonite can be shown to be important in reducing resistance to shear. To enable the composition of a soil to be known, an artificial soil consisting of montmorillonite and kaolinite in varying proportions was used. Creep tests were run in a manner identical to that for the expansive soils.

Materials. The montmorillonite was actually a bentonite collected from thin seams occurring in the lowermost beds of the Tertiary Jackson Group of south-central Texas (Smith, 1962). This material was crushed and the part passing a no. 40 sieve air dried. An X-ray diffractogram was made of a sample of the sieved material after retention in a glycerol atmosphere for two days. It showed a very strong  $16 \text{ \AA}$  peak and a much weaker  $4 \text{ \AA}$  peak. No other diffraction peaks were present, suggesting the material to be relatively pure montmorillonite.

The kaolinite used is produced commercially by the Georgia Kaolin Company, Theile, Georgia. An X-ray diffractogram of an untreated sample indicates the predominance of kaolinite with perhaps 5-10 percent muscovite. Grain size and atterberg limits are given in Table 5 for both materials.

Conduct of experiments. Creep tests were carried out on pure Georgia kaolinite saturated with deionized water or on mixture containing 10, 30, 45, 60 and 80 percent bentonite. The resulting artificial soils were molded in a two-inch inner diameter length of PVC tubing and

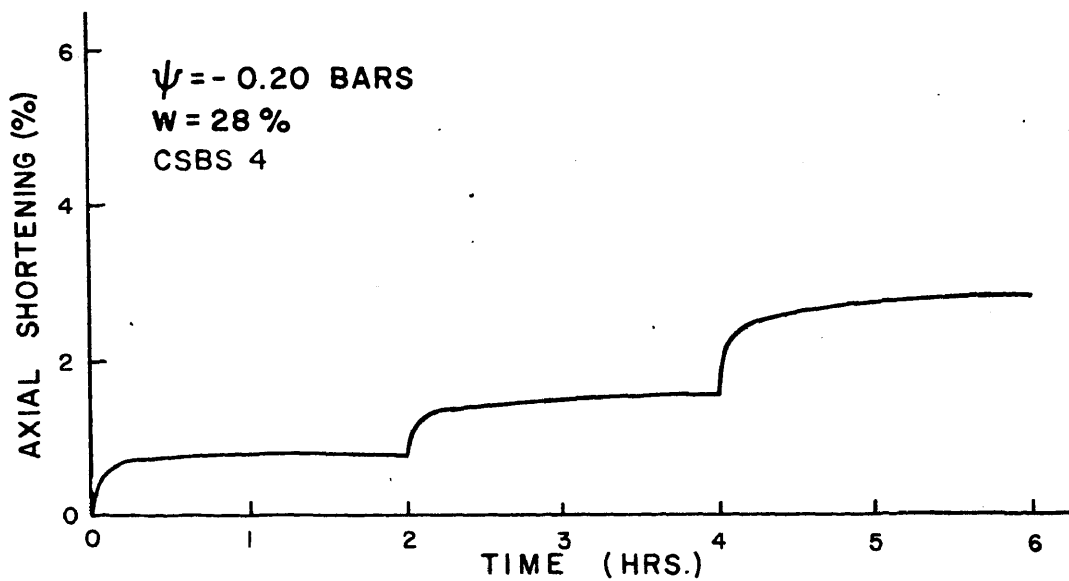
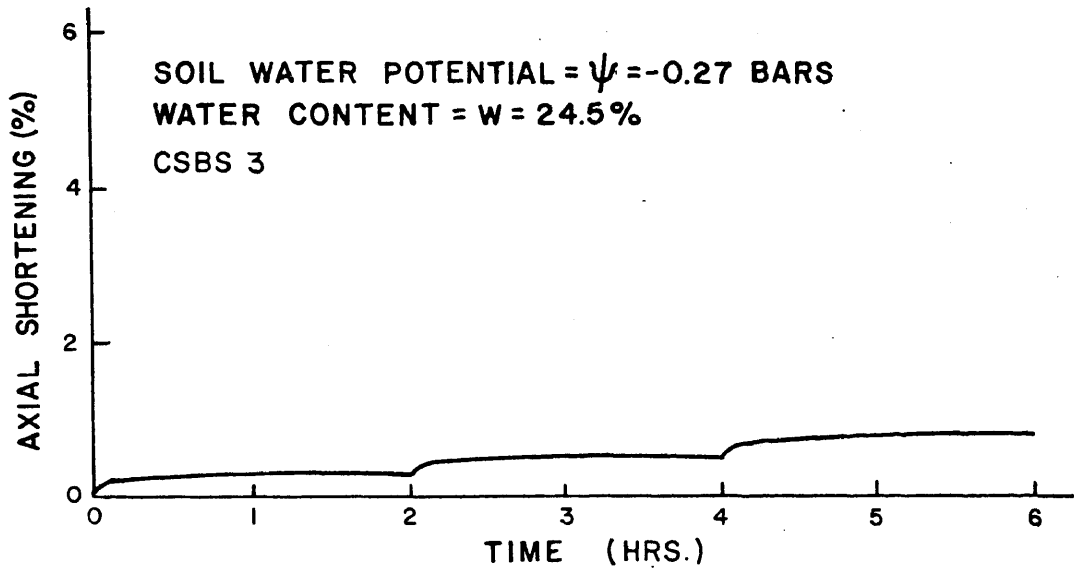


Figure 26. Creep curves for South Bosque shale, unconfined. For all creep plots:  
 deviator stress for 1st two hour segment = 2 psi,  
 deviator stress for 2nd two hour segment = 3.5 psi,  
 deviator stress for 3rd two hour segment = 5 psi.

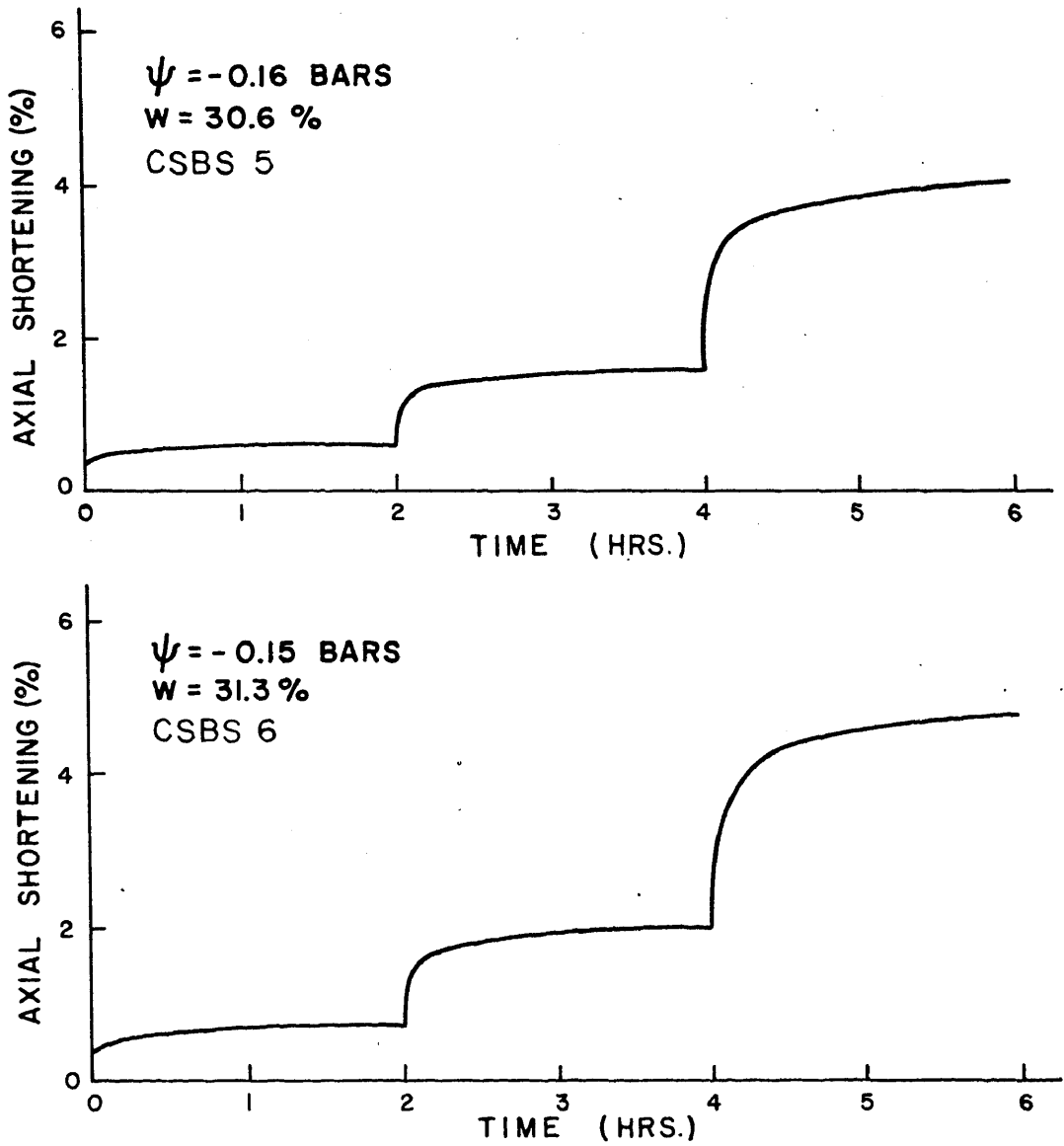


Figure 27. Creep curves for South Bosque shale, unconfined.

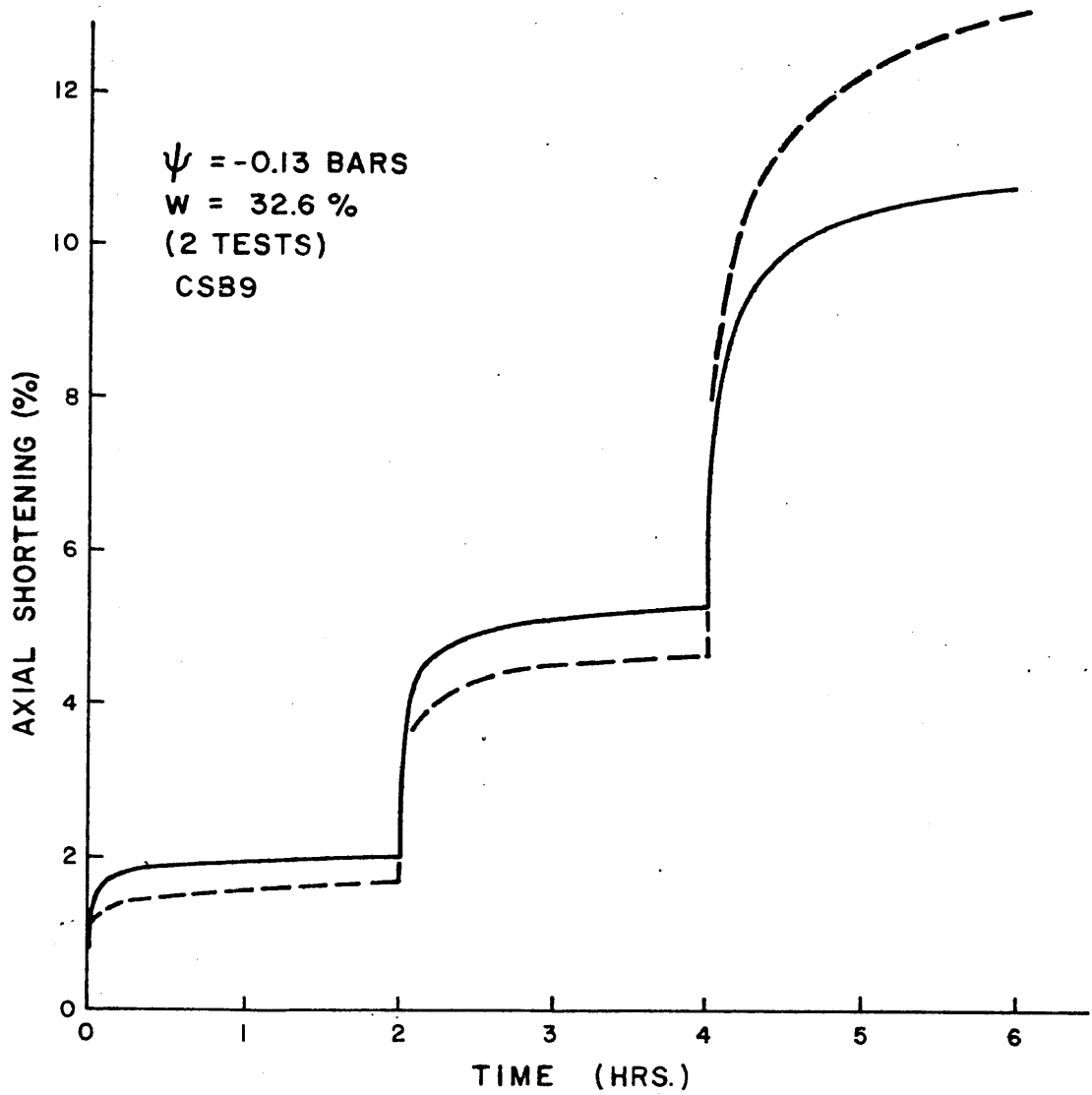


Figure 28. Creep curve for South Bosque shale, unconfined.

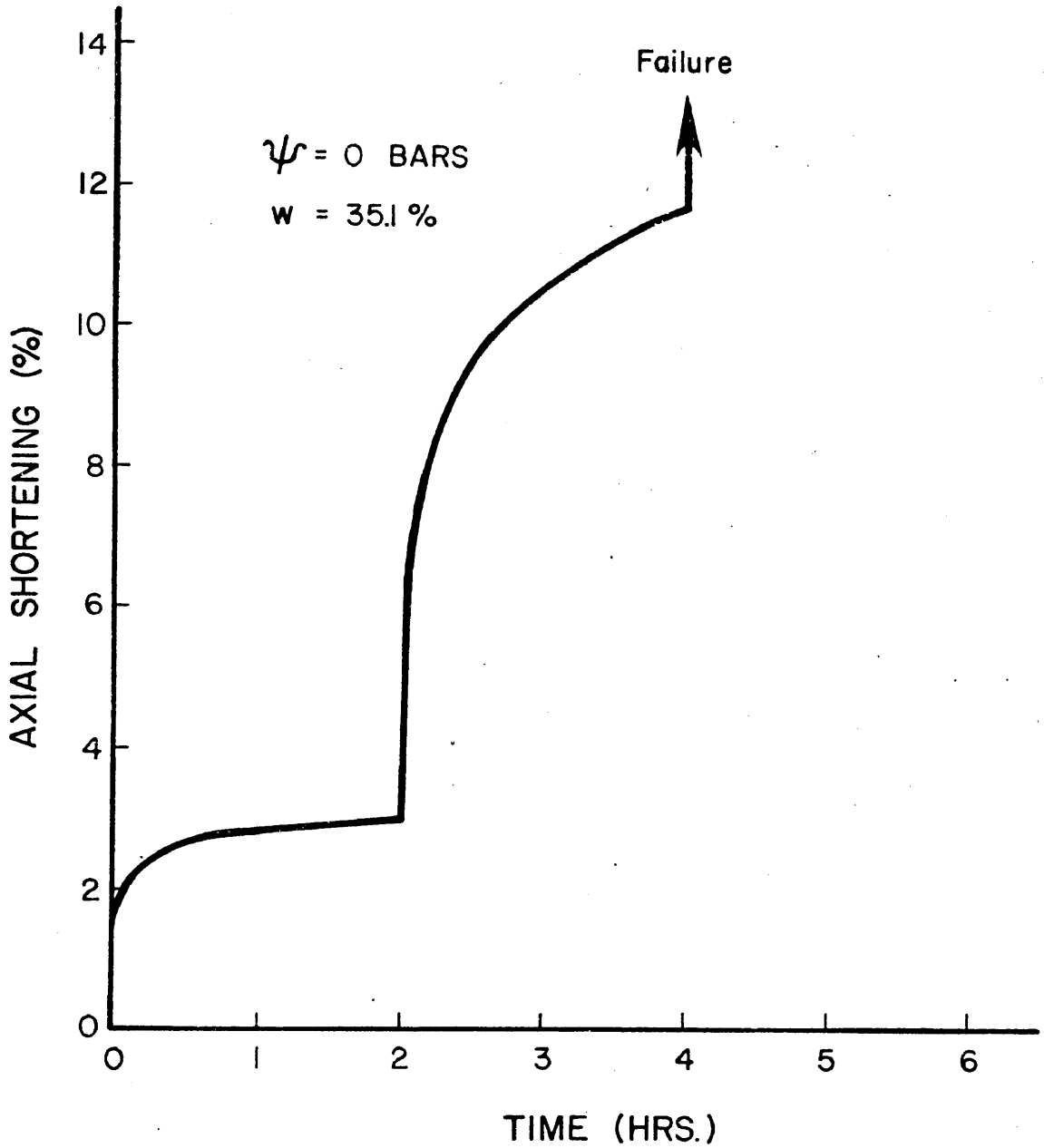


Figure 29. Creep curve for South Bosque shale, saturated, unconfined.

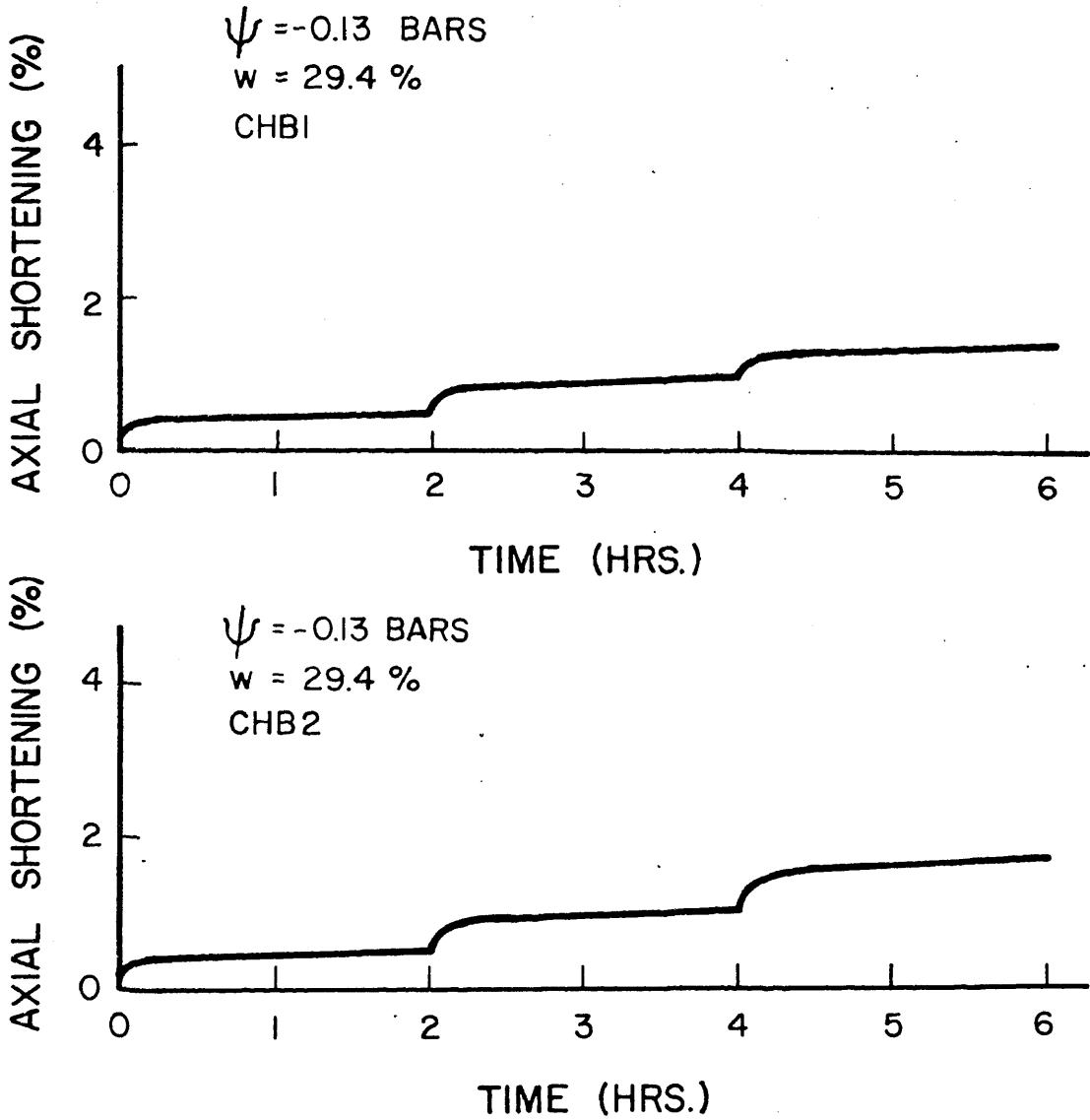


Figure 30. Creep curves for Houston Black clay, unconfined.

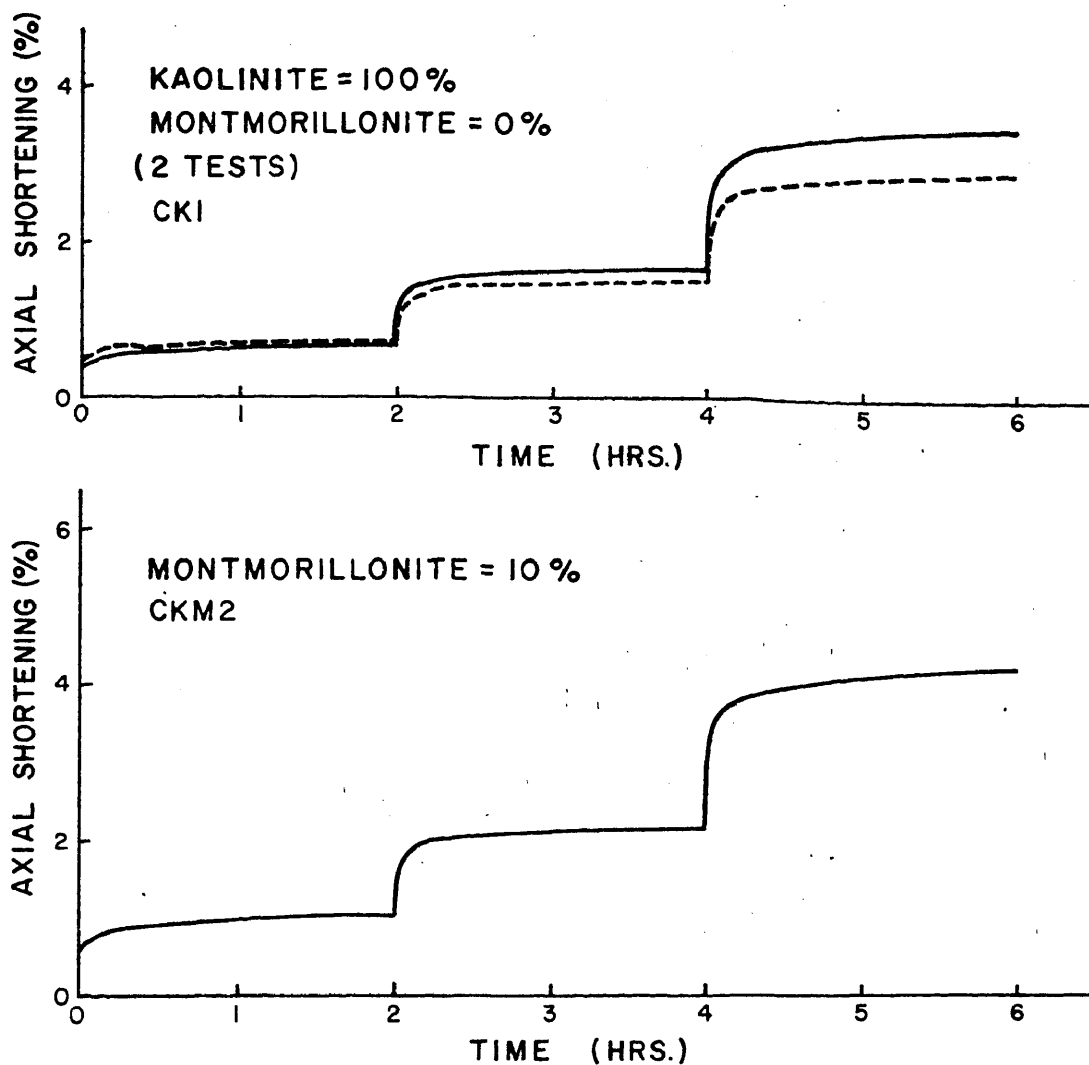


Figure 31. Creep curve for artificial soil, saturated, confined at 2 psi. For all creep plots:  
 deviator stress for 1st two hour segment = 2 psi,  
 deviator stress for 2nd two hour segment = 3.5 psi,  
 deviator stress for 3rd two hour segment = 5 psi.



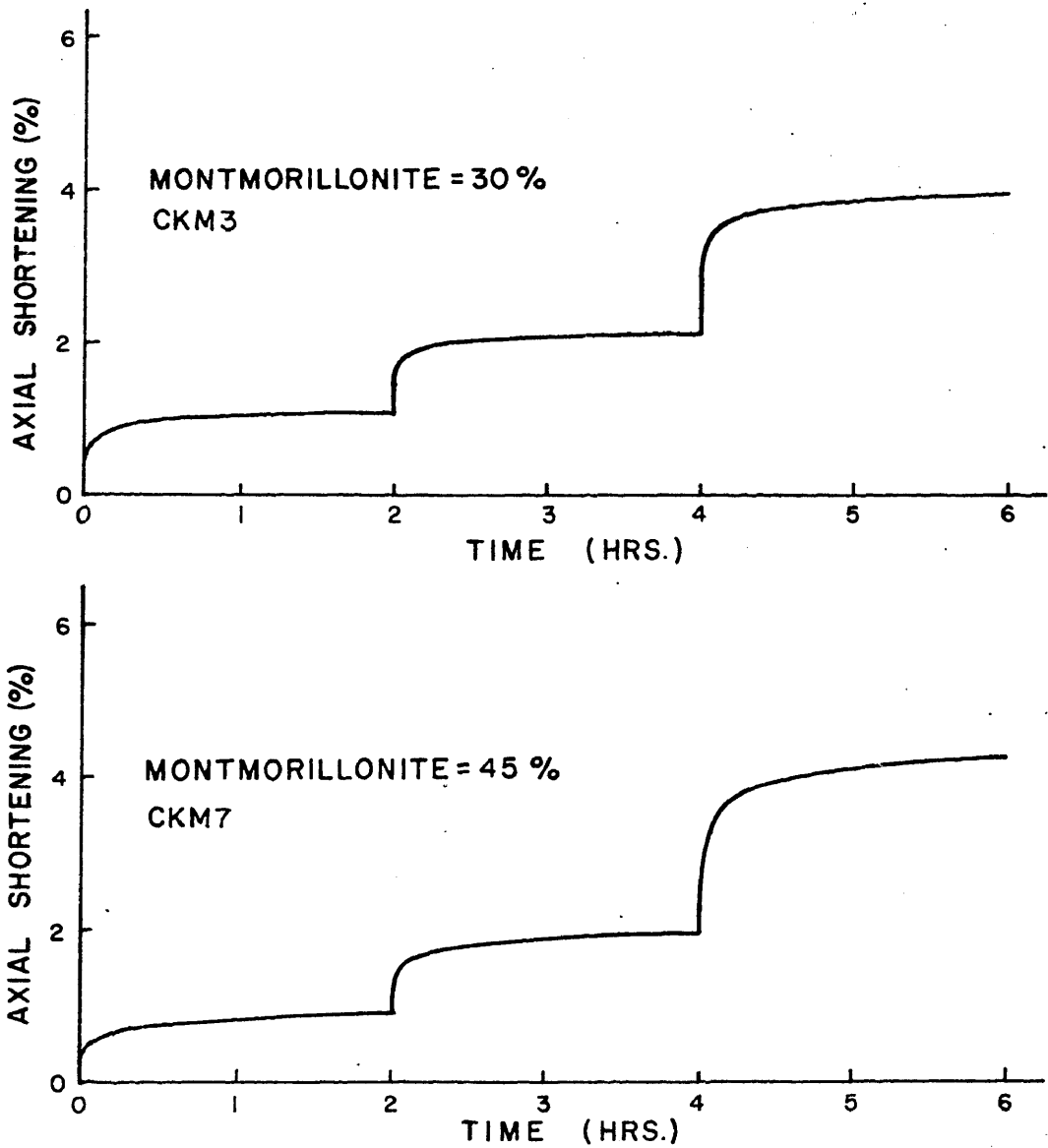


Figure 32. Creep curves for artificial soil, saturated, confined at 2 psi.

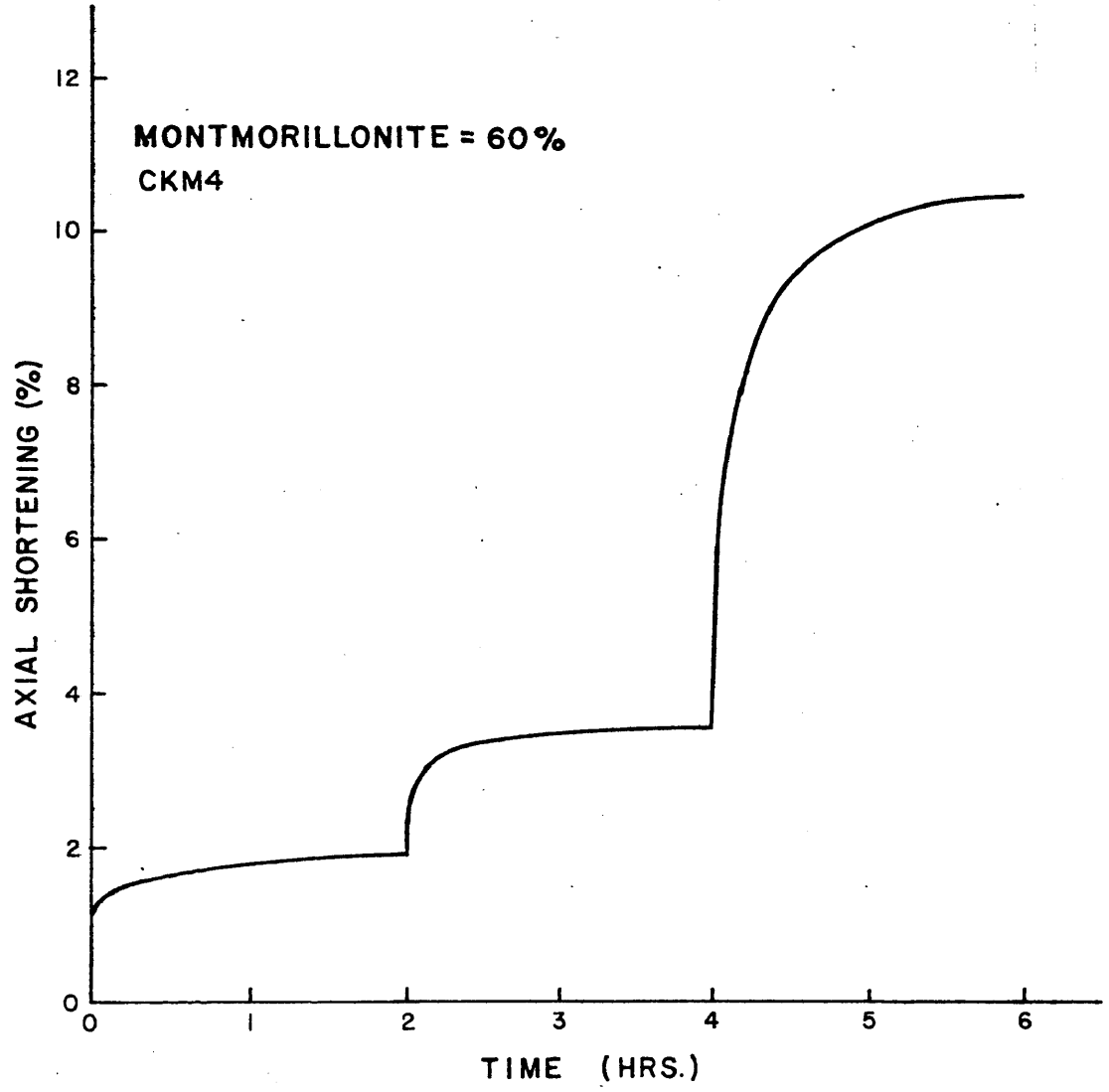


Figure 33. Creep curve for artificial soil, saturated, confined at 2 psi.

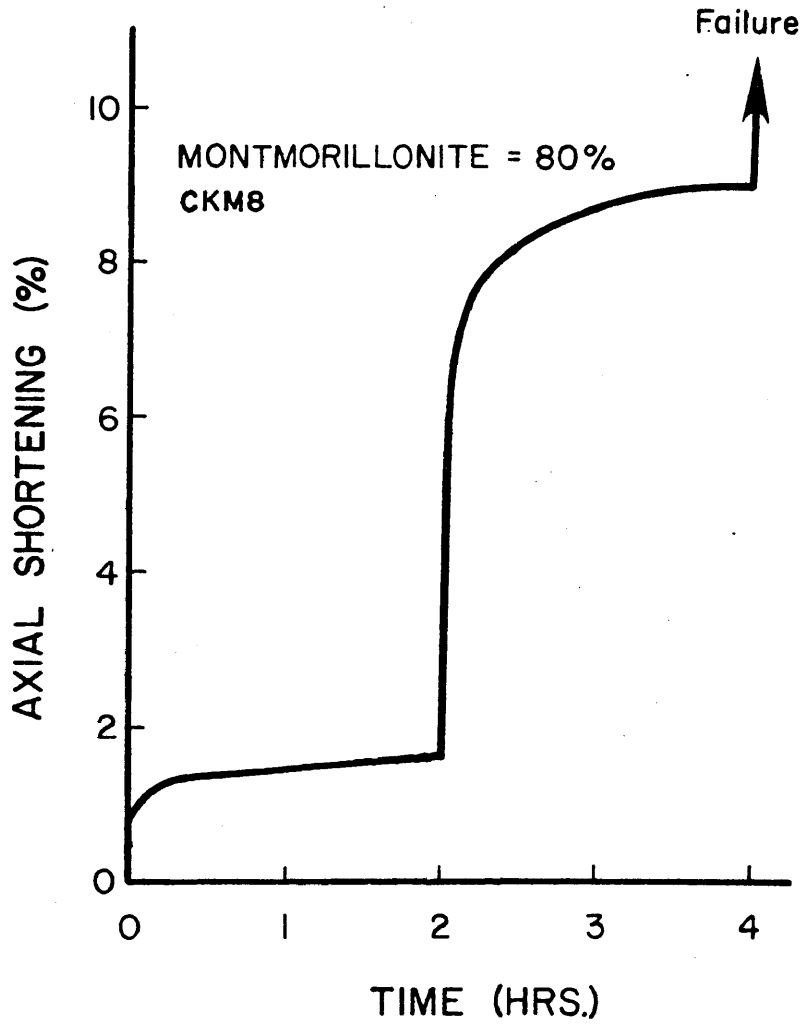


Figure 34. Creep curve for artificial soil, saturated, confined at 2 psi.

Table 5. Grain size analysis and Atterberg Limit data for artificial soils

	Grain Size Analysis				
	Clay <2 micron	Fine Silt 2 - 5	Med. Silt 5 - 20	Course Silt 20 - 60	Sand >60
Bentonite	57.2%	11.4	12.4	5.7	13.4
Kaolinite	87.3	6.4	5.6	0.7	-

Atterberg Limits for Artificial Soil Mixtures							
	0%	10	30	45	60	80	100
Bentonite							
Kaolinite	100	90	70	55	40	20	0
Liquid Limit	69	68	68	74	78	104	88
Plastic Limit	39	36	39	40	41	48	56

it was possible to achieve a wet bulk density within 10 percent of that of the saturated natural expansive soils. A confining pressure of 2 psi was used on all tests. Curves derived from plots of axial shortening versus time were shown for each artificial soil composition in Fig. 31-34. In the anticipation that the results of these tests could be correlated with a soil index property, the Atterberg limits of each artificial soil composition were determined. These results are also listed in Table 5. The atterberg limits do not appear to be highly sensitive to the observed change in creep properties. A liquid limit of 104 for the mixture containing 80% bentonite is suspect. It is possible that some samples of the bentonite had finer grain size distributions than that listed in Table 5. The relatively low values for the liquid limits of the bentonite are thought to be due to the presence of a considerable non-clay size fraction.

On each creep curve each of the three load segments show that a large proportion of the shortening for each stress is accomplished within a short period of time. Thus an approximate measure of this response is the total shortening at the end of each two hour interval. It may be considered that this response reflects a combination of elastic deformation and flow properties due to excess pore pressure developed with essentially instantaneous loading. On the other hand, the slope of each load segment at the end of each two hour load period gives a displacement rate that reflects the viscous properties of the soil. Where a saturated sample is involved, excess pore water pressure induced by the sudden loading has probably been released through a combination of dilatancy due to shear and drainage. What ever the effect of excess porewater pressure, the uniformity of test conditions allow the changes in mechanical behavior to be observed as soil water potential or soil composition is changed.

Results for creep tests conducted under pre-determined soil water potentials on natural soils

The total shortening of the South Bosque shale after each two hour period has been plotted against the soil water potential for each of the three stress increments in Fig. 35. It will be noticed that the

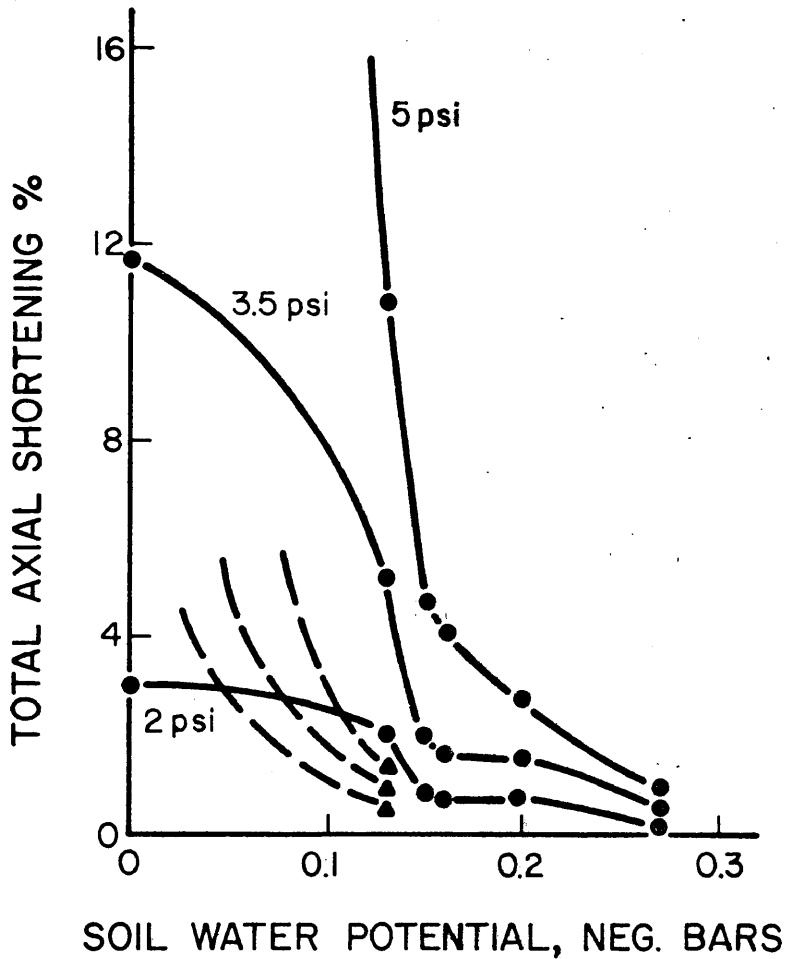


Figure 35. Synthesis of creep test data for South Bosque shale (solid lines) and Houston Black clay (dashed lines). Each curve shows the total axial shortening according to soil water potential at the end of each two hour stress increment (labelled).

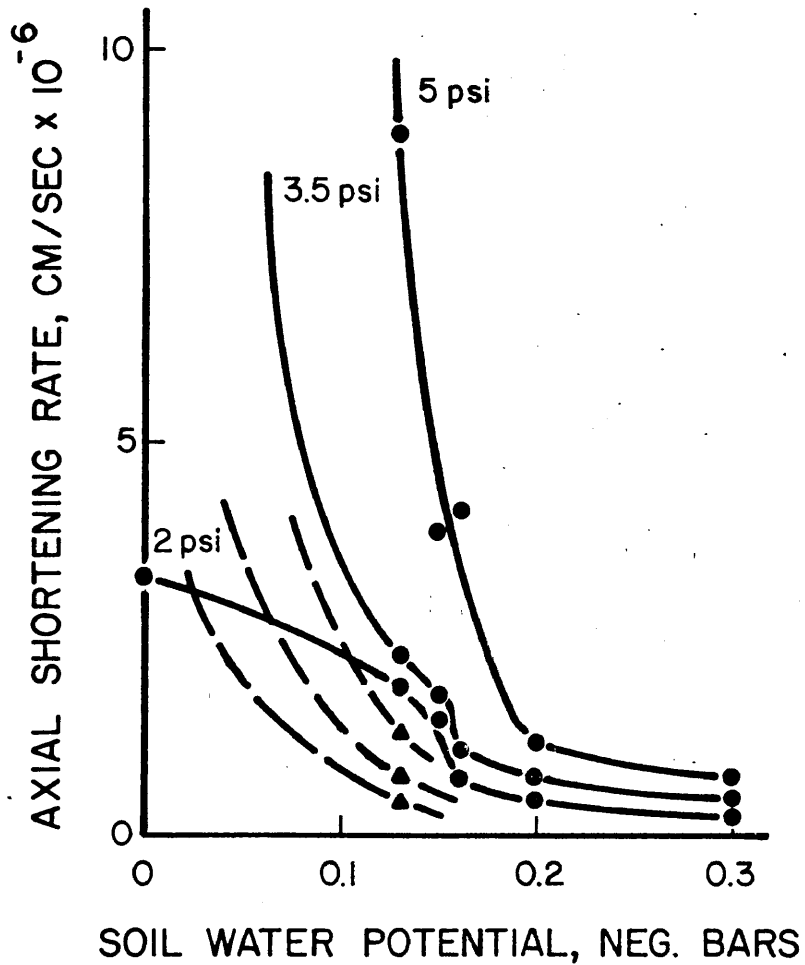


Figure 36. Synthesis of creep test data for South Bosque shale (solid lines) and Houston Black clay (dashed lines). Each curve shows the axial shortening rate according to soil water potential at the end of each two hour stress increment (labelled).

increase in shortening for all three curves is roughly proportional down to a potential of about  $-0.13$  bars. This suggests an almost elastic behavior for the specimens in that the deformation is proportional to stress. Below about  $-0.13$  bars some type of strain hardening must prevent a continued accelerating increase in total shortening for the two lower creep stresses. The highest creep stress is evidently enough to maintain an accelerating increase. Common to all three curves are sudden increases in the amount of shortening at about  $-0.25$  bars. These increases may reflect a fabric change related to the swelling of clay particles.

Figure 36, showing displacement rate at the end of each two hour creep stress increment, does not display a proportional relationship between the curves. The resistance to shear which has been mobilized by this time is perhaps an indication of what is available in nature, at least in terms of the relative increase in displacement rate with decrease in potential. The large acceleration in displacement rate shown by the highest creep stress curve is perhaps an indication of failure. For the two lower stresses the curves show a sudden upturn between  $-0.15$  and  $-0.20$  bars, roughly the same range of potentials that produced a similar response on the total shortening plot. The curves suggest that a significant change in the viscosity of the soil takes place in this range. The curve for the smallest creep stress again suggests work hardening but further increases in load override this tendency.

Very few specimens of Houston Black clay were tested but sufficient data were obtained to determine that this material remained relatively stiff down to a potential of  $-0.13$  bars. Results for the test at this potential are plotted on Fig. 35 and 36. Specimens of Houston Black clay tested at unconfined saturation display rapidly accelerating creep at the lowest creep stress.

Results for creep tests conducted on artificial soils

Curves plotted for identical axial shortening and displacement rate data for the artificial soils are shown in Fig. 37 and 38. For each composition up to a montmorillonite proportion of 45 percent the total shortening produced by each stress remains about the same and



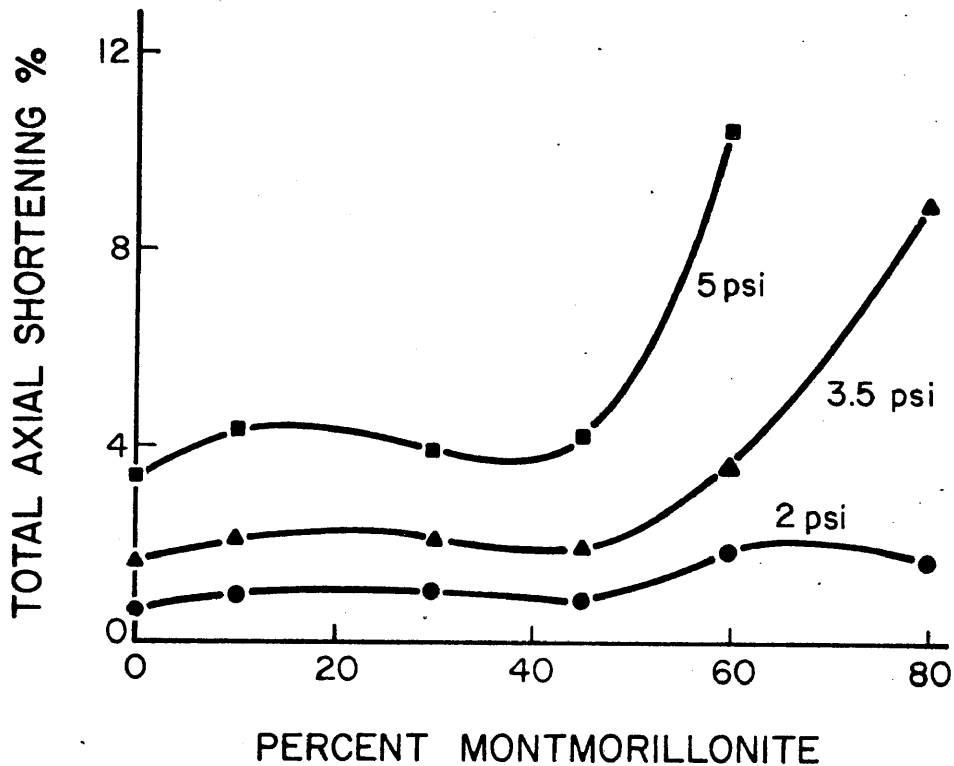


Figure 37. Synthesis of creep test data for artificial soils. Each curve shows the total axial shortening according to composition at the end of each 2 hour creep stress increment (labelled).

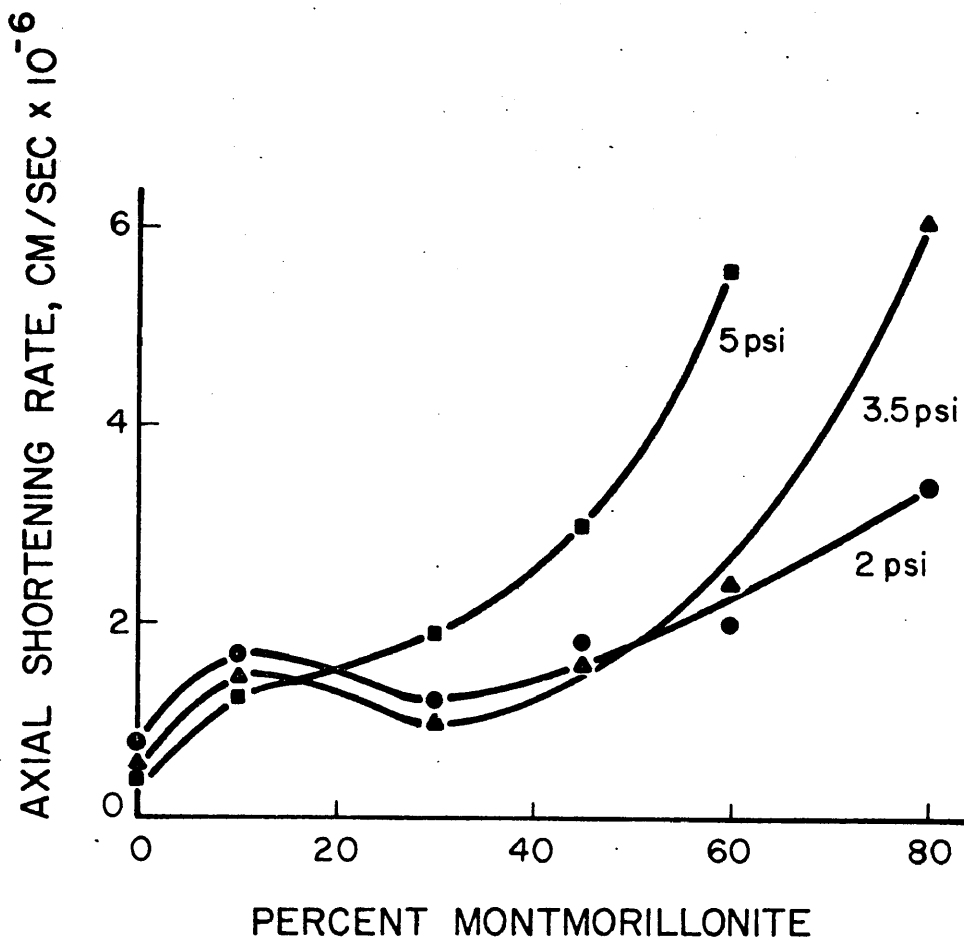


Figure 38. Synthesis of creep test data for artificial soils. Each curve shows the axial shortening rate according to composition at the end of each 2 hour creep stress increment (labelled).

increases for each soil roughly in proportion to the stress. For samples with more than 45% montmorillonite the strain hardening tendency continues for the lowest creep stress but the total displacements increase rapidly for the higher stress and the proportionality disappears.

For the displacement rate at the end of each stress increment period, the plots for the two smaller stresses are almost coincident up to a montmorillonite percentage of 60. This result can be seen in the total shortening behavior and suggests that the viscoelastic properties of such materials are stress dependent. For the two higher stresses the displacement rate does begin to increase rapidly beyond a montmorillonite content of 60 percent. The curves for the highest stress are particularly interesting in that while total shortening remains approximately constant up to about 45 percent montmorillonite content, the displacement rate is increasing rapidly. This indicates that as the montmorillonite content is increased the soil is behaving more and more in a viscous manner.

## ANALYSIS OF EXPERIMENTAL RESULTS

### Preliminary analysis

A review of the volume change tests and creep tests on both the undisturbed natural soils and the artificial soils suggests behavior that may be controlled by expansive clay minerals. There are significant departures from the kind of response that might be expected for soils composed of non-expansive minerals. While the experimental results for the two natural soils differ, there is an overall consistency that may be related to a common cause.

The South Bosque shale exhibits a sudden, very rapid increase in volume with decrease in soil water potential at a value that coincides with the beginning of a rapid decrease in the resistance to shear. The results for the Houston Black clay are not so clearly defined. The volume change characteristics of this soil lack the large degree of hysteresis exhibited by the South Bosque shale but there is still a relatively sudden, if subdued, volume increase. There is also much less creep test data but enough to reveal a similar rapid decrease in shearing resistance at a potential roughly coincident with the most rapid volume increase. The differences between the soils may be due to differences in soil fabric. The influence of montmorillonite as a fabric element may also explain the sudden decrease in shearing resistance that is seen with increasing montmorillonite content in the artificial soil experiments.

The character of the soil water potential versus volume change plots and the apparent dependence of shearing resistance on the volume change is unusual when compared with data available from other soils. Soil water characteristics determined for various soils (Topp, 1971; Staple, 1965) show most of the moisture content increase with wetting taking place at values of potential of less than 0.1 bar for clay-rich soils or the water content increase being relatively gradual for silt-rich soils. Little work has been done on relating shear strength to the soil water characteristic. Yong et al. (1971) have produced data on this relationship for kaolinite and a remolded natural clay. Their data are difficult to interpret because the soil water characteristics which

they determined for their materials do not form closed loops. The water content increases with wetting are small compared with the drying portions of the curves. They attribute this behavior to fabric collapse. While the changes in shear strength seem to be related to the changes in water content, there is no rapid change in resistance over a small range of potential as exhibited by the expansive soils.

The behavior of expansive clays as depicted by the experiments in this study suggests that the strength and volume change characteristics of such soils are closely related. These characteristics seem to be associated with the presence of montmorillonite but the actual behavior is modified by clay fabric. A closer look at shearing resistance studies of clays and clay fabric suggests that given the physico-chemical properties of montmorillonite, unique deformation properties for soils containing this mineral can be expected.

#### Mechanism of expansive soil hysteresis

It is claimed that expansive soils can have a characteristic volume change behavior as exemplified by the relatively wide hysteresis loop of the South Bosque shale and the sudden volume increase with wetting. However, fabric undoubtedly exerts its own influence. If a soil consisted of an assembly of discrete, non-touching montmorillonite particles, the volume during wetting and drying would probably be much the same for any given potential. It is conceivable that for a natural soil, particles touch and interlock in such a way that contraction with drying produces a cohesion that may suddenly be released on expansion of the montmorillonite component.

The theory of the diffuse double layer can be applied to describe the volume change process of a montmorillonite clay consisting of discrete, non-touching particles. The theory predicts the density of ions with distance away from a clay plate surface. In essence the density is an inverse exponential function of the distance from the plate. This density partially controls the osmotic potential between the ions collected between clay plates and the surrounding solution. The soil water potential is comprised in part of this osmotic potential and so can be related to the double layer theory.

Considering the idealized montmorillonite particle suspension again, it can be imagined that an increase in the soil water potential will act to draw water from between clay plates against the osmotic potential. The osmotic potential is an exponential function of the electric potential at the mid-plane between two clay plates. This is so because the electric potential and hence the cation concentration will increase exponentially as the plates collapse toward one another. The rate of volume shrinkage as the soil water potential increases will consequently fall off rapidly.

If a hypothetical curve for the idealized soil was superimposed on the hysteresis loop for the South Bosque shale it would probably fall somewhere between the two halves. The natural fabric of the South Bosque shale must resist volume decrease due to the energy required to compress the soil. Conversely, as the South Bosque shale is rewetted it does not respond by increasing in volume as quickly as the idealized soil would. The compressed fabric of the real soil has acquired a rigidity that resists osmotic pressure to a point. A rapid increase in volume takes place probably because the strength of some type of compression-included frictional bond has been exceeded and nothing remains to restrain the clay.

Warkentin et al. (1957) have subjected montmorillonite suspensions to successive compressions and relaxations at pressures of from 0.1 to 100 bars. After the first compression there is virtually no hysteresis. This observation supports the concept for the hypothesized non-bonded clay and the effects of induration can be added or subtracted to their results depending on whether compression or relaxation is taking place. Of course, while soil water potential cannot simply be substituted for applied pressure, it is probably a useful approximation for very low potentials.

#### Clay soil fabric

The resistance to shear offered by any material consisting of a collection of particles will in part be due to the interference these particles have with one another. The shape of the particles and their fabric will determine the exact contribution. Terzaghi (1925) was the

first to suggest that, in the case of very fine grained soils, more than frictional resistance might be offered where particles were so small that molecular forces became significant compared to the particle weight. Casagrande (1932) brought attention to the difference in strength between intact and remolded samples of soil and attributed this to the destruction, during remolding, of the bonds built between clay and silt particles. Better understanding of clay molecular structure allowed the concepts of flocculated and dispersed fabric to be developed but it was not until the advent of the electron microscope and most importantly the almost three-dimensional ability of the scanning electron microscope that the true nature of clay fabrics could be observed.

Alymore and Quirk (1959) proposed a concept of clay fabric that helped to visualize a mechanism by which volume change in montmorillonite was transmitted to the clay body as a whole. The montmorillonite particle was treated as a "domain" which presumably referred to the smallest element of volume change behavior. The "domain" concept has been included in the nomenclature of clay fabric but the application has evolved partly through conclusions drawn by indirect means. The failure of the double layer theory to closely predict the excessive expansive behavior of montmorillonite resulted in Van Olphen (1962) proposing a fabric element consisting of a stack of oriented montmorillonite plates enclosed or cross-linked by a relatively small number of non-parallel plates. These cross-linking plates provided the additional bonding force needed to augment the inadequate Van Der Waals attractive force.

The fact that collections of oriented clay plates exist has been established by electron microscope observation. Sides and Borden (1971) have obtained scanning electron microscope photographs of dispersed and flocculated kaolinite and illite. The simple cardhouse fabric rarely appears to exist. Rather the basic unit of a flocculated fabric is probably a stack or "book" of clay plates. The flocculated fabric then becomes an edge to face arrangement of these books. As a dispersed arrangement is approached, the books themselves become oriented to form a turbostratic fabric (Barden, 1972). Collins and McGown (1974) have arrived at the conclusion that fabrics consisting of single clay plate arrangements are rare in undisturbed soils and Bennett et al. (1977) use

the term "domain" to describe a common fabric element consisting of stacks of clay plates in offshore Mississippi Delta muds.

The conclusion one can arrive at is that oriented groups of clay plates or domains are a major component of clay fabrics. This component should have a strong influence on the ability of the clay to resist shear. Although edge-to-face contacts will exist in a flocculated fabric the domains, in the case of montmorillonite, may incorporate only adsorbed water as part of the bond. The expansive potential of montmorillonite will allow the adsorbed water intervals to increase in width to such a degree that the shear strength of the bond is reduced to essentially that of free water. A montmorillonitic clay thus behaves increasingly as a viscous substance as its water content is increased.

#### Shearing resistance of montmorillonite

That the seat of shearing resistance in clays may be in the adsorbed water has been demonstrated by Foster (1970). Using remolded samples of kaolinite, he has subjected them to creep testing at stress levels considerably below the peak strength shear stress. This has presumably promoted a more viscous type of behavior, eliminating the necessity to overcome the breaking of particle-to-particle bonds. From his experiments Foster calculated activation energies for creep of considerably less than those found by Mitchell et al. (1969) (30-45 kcal/mole). His value of approximately 20 kcal/mole represents the maximum required for hydrogen bonding and suggests that the strength mobilized is that of a viscous adsorbed phase. With higher creep stresses this resistance would be rapidly overcome and resistance transferred to particle-to-particle contacts. Conceivably, montmorillonite, with its ability to acquire adsorbed water, should be capable of accommodating deformation in this adsorbed water.

Andersland and Douglas (1970) have determined an activation energy of that of free water for dilute soil suspensions but obtain a value of 28 kcal/mole on consolidated samples. They claim this value to represent breaking of direct mineral-to-mineral contacts but do not specify their creep stress as a percentage of peak strength. Presumably the variation in activation energy values could be due to variations in the



proportion of mineral-to-mineral contacts. A different approach to deducing the behavior of montmorillonite is offered by Mesri and Olson (1970). They have conducted triaxial compression tests on calcium and sodium-saturated montmorillonite and obtained Mohr failure envelopes for these consolidated clays. The envelopes generally have slopes of less than  $10^0$  and for sodium-saturated montmorillonite the envelopes become horizontal. This behavior suggests a deformation mechanism that is independent of normal stress. Deformation must be confined primarily to shear of the adsorbed water for these results to be obtained.

#### Expansive soil deformation mechanism

The ability of montmorillonite to adsorb excessive amounts of water is probably the cause of similarly notable property of resistance to shear. The study of clay fabric has suggested that a common component of fabric is a face-to-face collection of clay plates. If this condition is typical of montmorillonite then a fabric element exists which should have an influence on resistance to shear. Deformation will be preferentially accommodated throughout the montmorillonite stack by the process of simple shear (Fig. 39).

This fabric element composed of montmorillonite may come into play by one of two means. In a natural expansive soil the fabric of the non-expansive component may favor mineral to mineral contacts and so resistance to shear through interlocking. The resistance will be reduced as adsorption by montmorillonite takes place. The fabric of the soil itself may retard the expansion until a certain pressure is reached whereby the retardation is overcome. This may be represented by a failure of mineral to mineral contacts. The whole fabric is then disturbed and the montmorillonite element can offer its relatively low component of resistance. Alternatively, resistance may be reduced simply by increasing the montmorillonite component. This has been demonstrated with the artificial soil experiments. An increase in the amount of montmorillonite will supply a greater number of these fabric elements capable of sustaining simple shear. For a given soil water potential (ie. a relatively low one) and stress, increasing montmorillonite content will, in effect, represent a decreasing number of

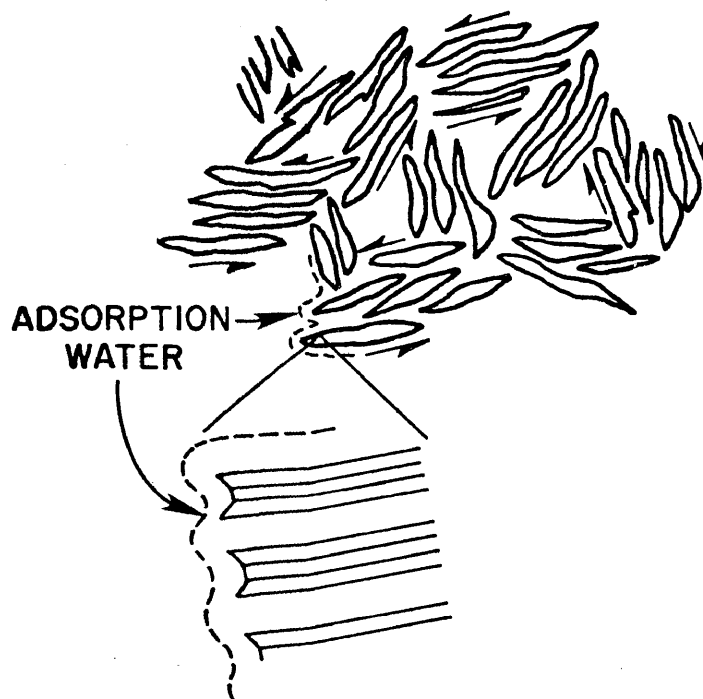


Figure 39. Two-dimensional inferred nature of clay fabric for a flocculated expansive soil. Shearing couples show hypothesized accommodation of shear by clay plate domains. Shear may also be accommodated between individual expanded layers of a montmorillonite particle (as shown by enlargement).

frictional mineral-to-mineral contacts. The relatively rapid acceleration in deformation is probably due to the loss of a minimum component of shearing resistance necessary to resist deformation.

The concept of expansive soil as a collection of clay particle domains implies a continuum approach. This may be satisfactory as long as no other larger fabric element is present. In fact, expansive soils are generally more complicated. The volume change behavior produces cracking which, if severe, can greatly modify the bulk permeability. Cracking also promotes drying because of the increased circulation afforded air (Johnson and Hill, 1941).

The largest cracks generally form a polygonal network with polygons several feet across. These will be the deepest and are thought to give rise to gilgai. Cracks also form at several smaller scales such that the upper layers of the soil become laced with a crack fabric. Heaving associated with gilgai formation produces shear zones which add to the overall fabric and downhill creep may produce a bulk strength anisotropy (Lytton, in press). To fully understand the bulk volume change behavior of expansive clays, Lytton considers that the cracking fabric must be taken into account. The added permeability that the crack fabric offers will, to begin with at least, afford a very high bulk permeability compared to that of a remolded laboratory specimen. Shear surfaces associated with gilgai formation may contribute to decreasing the shearing resistance.

Brackley (1975) has treated an expansive soil as a collection of "packets", soil units consisting of an aggradation of clay mineral particles. He feels this is appropriate because the volume change behavior of an unsaturated soil can be predicted by considering it to be macroscopically unsaturated but in reality to be an aggradation of saturated packets with interpacket voids filled with air. The behavior of the Houston Black clay may offer a verification for this concept in that the relatively small volume change (compared with the South Bosque shale) associated with the rapid change in water content. The expansion of soil packets in the Houston Black clay may be partly accommodated in interpacket voids. The highly overconsolidated origin of the South

Bosque shale has probably resulted in the elimination of large inter-packed voids such that the water content change is more closely reflected as a bulk volume change.

The shearing resistance of an expansive clay will also be influenced by large scale fabrics. Pre-existing fractures or slip surfaces in soils have been shown to significantly reduce the resistance from that of intact material (Skempton and Petley, 1967; Font, 1977). Slope failures along discrete surfaces have been observed in the South Bosque shale at the Waco site on the steepest slopes but it is considered that this process is not contributing to the damage observed in the homes. A slope failure under a house would probably result in wall cracking showing vertical displacement and being widest at the bottom. Such a style has not been observed. Cracks and slip surfaces in the soil are probably dense enough in spacing such that interlocking transfers most of the deformation penetratively, ie. as shear throughout the surface soil mass. In any event, shearing resistance of intact soil or along discontinuities in the soil will have a frictional component that may be controlled by the montmorillonite component.

#### Behavior of expansive soils on natural slopes

The results of the creep tests on natural expansive soils show that these soils have rapidly changing creep behavior at low values of soil water potential. Also the tests are characterized by a viscoelastic behavior whereby deceleration in creep rate takes place with increasing shortening. It is more than likely that both of these aspects of the tests occur in nature. However, the natural conditions differ from those of the tests.

Considering an element of soil at some depth in an expansive soil profile, the element will be subjected to a confining pressure and a shear stress dependent of the slope angle. The element is effectively being subjected to a continuous creep test. In this case the element may only begin to deform as the soil water potential is reduced by infiltration of water (ie. from rainfall, etc.). The minimum potential to which that element can be brought will depend on the confining pressure (ie. the confining pressure does substitute for the soil water

potential as suggested by the relation of the swell meter tests to the volume change hysteresis loop). By the results of the creep tests then, it should be possible to estimate the relative amount of creep deformation that a given depth will undergo, knowing the soil water potential to which that depth will be brought.

If the mathematical description of laminar flow in a sheet of viscous material is recalled from the chapter on insitu creep, (p. 4), it may be modified to predict a downhill velocity profile in an expansive soil. To do this the viscosity term must be changed to incorporate all the factors which control this property. Thus

$$\eta = f(\psi, \gamma)$$

for any given cycle of wetting. The term  $\psi$  refers to the total soil water potential which is a combination of the overburden potential, osmotic potential, and matric potential;  $\gamma$  refers to the downhill shear strain and accompanying strain hardening.

Combinations of idealized mechanical elements (springs, dashpots and friction blocks) can be used to simulate the stress-strain behavior of substances. Considering the results of the creep tests, it is apparent that, for each load increment on each test, there is an exponential-like decrease in shortening rate as the test proceeds. While a legion of linked mechanical elements can be used to produce a close fit to the stress-strain behavior, an approximation is achieved by simply using a spring and dashpot in series, ie. the Kelvin body. This does not account for the near-instantaneous initial deformation for any interval having a constant rate of deformation or for failure. However, the behavior of the test samples, save for those few that showed accelerating creep, may be adequately duplicated by this model.

The purpose of a mechanical analogy is to draw attention to the elements of mechanical behavior that can be analysed in more detail. There is an elastic response in each test, the size of which depends upon the soil water potential and applied creep stress. It is probably due to the cumulative distortion of individual soil particles and is governed by how firm the particle to particle contacts are. The viscous portion of the behavior is attributed to the deformation of

soil water adsorbed between soil particles and to a "macroscopic viscosity" produced by slippage between individual particles.

This viscous portion may be more clearly understood by using the theory of rate processes (Glasstone et al., 1941). Mitchell (1964) has used this to develop a theory to predict the rate of soil creep. Mitchell's expression for creep rate centers around the concept that the probability of a bond between mineral particles being broken is given by the Maxwell-Boltzman equation:

$$p(\Delta E) = e^{-\frac{\Delta E}{\kappa T}}$$

where  $p(\Delta E)$  is the probability of the energy state being at or greater than  $\Delta E$

$\Delta E$  is the energy required to surpass some energy barrier (activation energy)

$\kappa T$  is the product of Boltzwan's constant and absolute temperature which is equal to the average thermal energy of the material.

The expression for the frequency of rapture of a single bond is completed by taking into account two controls. These are the frequency of thermal oscillations,  $\frac{\kappa T}{h}$ , where  $h$  = Planck's constant and the contribution to the attainment of the activation energy that a shearing force makes,

$$e^{-\frac{f\lambda}{\kappa T}}$$

where  $f$  = the shearing force

$\lambda$  = the distance between successive equilibrium positions

The expression for strain rate ( $\dot{\epsilon}$ ) can then be written by multiplying the product of the components so far discussed (which gives the number of bonds broken per second) by the number of contacts per unit length(s) and the displacement due to a single bond rapture ( $\lambda$ )

$$\dot{\epsilon} = 2s \frac{\kappa T}{h} e^{-\frac{\Delta E}{\kappa T}} e^{-\frac{f\lambda}{\kappa T}}$$

This equation presents a phenomenological model of soil creep in that the process on the scale of individual molecules is described. Because this process is one of steady state or constant strain rate it may be likened to the viscous portion of the Kelvin body, ie. a Newtonian viscous substance,

$$\dot{\epsilon} = \frac{f}{\eta}$$

Here  $\eta$  is the coefficient of viscosity and the Mitchell equation contains a counterpart for this which would be

$$2s \frac{kT}{h} e^{-\frac{\Delta E}{T}}$$

This term is not dimensionally correct as an expression for viscosity. However, the analogy is permissible because the equation is a statistical description and the shear stress is represented only as a contribution to the probability of a bond being broken. If temperature is considered to be constant, then viscosity can be considered a function of  $e^{-\Delta E/kT}$  or  $e^{-\Delta E/RT}$  in terms of free energy of activation.

For soils that Mitchell has worked with, he feels that mineral to mineral contacts are common and that the activation energy for creep reflects such a contact. In soils containing montmorillonite, the concept of the montmorillonite particle domain would suggest that many contacts are by way of the adsorbed water between montmorillonite particles. The activation energy for creep would then be determined by this water.

Ravina and Low (1972) have investigated the relation between the free energy of water and water content of montmorillonite (Fig. 40). The slope of this curve is proportional to the change in free energy of each successive increment of water and hence will also be related to the soil water potential. From this plot it may be seen that after more than about 1 gram of water is added per gram of clay (ie. water content of 100%) little further change in free energy takes place. In the case of a clay plate domain, the activation energy for creep in the water midway between clay plates would be approaching that of free water at this water content. As drying takes place the activation energy for creep becomes that of ever more tenacious hydrogen bonds. The increase in this bonding strength will be of a form similar to that of the curve in Figure 40. The addition of 1 gram of water to 1 gram of the expansive soils treated in this study will result in relatively thicker adsorbed water layers because of the relatively larger particle size. A curve corresponding to that in Fig. 40 for a typical expansive soil would approach a flat slope even more quickly.

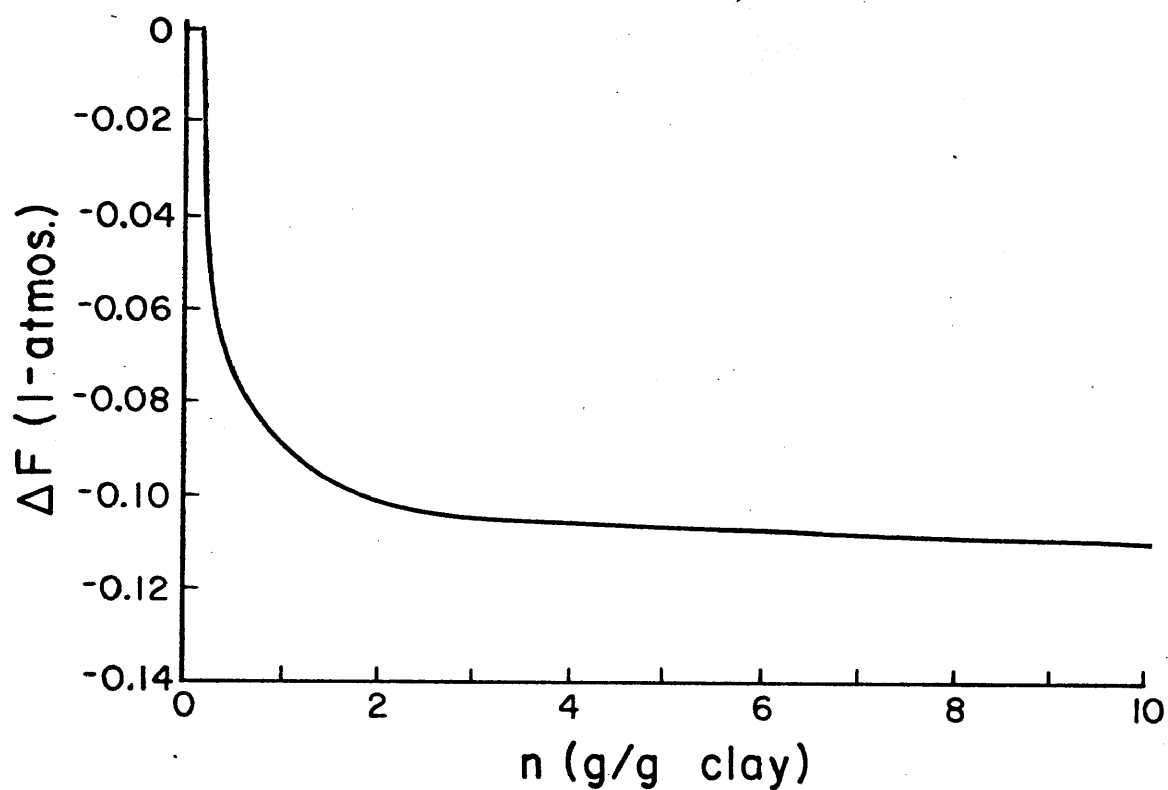


Figure 40. The relation between  $\Delta F$ , the change in free energy and  $n$ , the number of grams of water transferred from a source of free water to 1 gram of air-dried Na-montmorillonite (from Ravina and Low, 1972).



The creep tests reveal that the rapid increase in creep deformation for the expansive soils takes place at a water content of approximately 25%. At this stage of wetting much of the water is probably being utilized in the expansion of the montmorillonite and so the energy of activation for creep is rapidly decreasing if the montmorillonite content is high. It seems reasonable to anticipate that the behavior of the expansive soils as depicted in Figures 37 and 38 is closely related to the stage to which the interlayer water has been allowed to develop and hence to the activation energy for creep of the water midway between clay plates.

The soil water potential is most rigorously defined as a free energy and is related to the difference between the vapour pressure of free water ( $\rho_0$ ) and the water in the soil ( $\rho$ ),

$$\Delta F = RT \ln \frac{\rho}{\rho_0}$$

The derivation of this expression is given in Aitchison (1965). This free energy can be interpreted in terms of the pressure represented by a head of water,  $h$ , required to move the water to a body of free water

$$h = \frac{RT}{gM} \ln \frac{\rho}{\rho_0}$$

where  $g$  = acceleration due to gravity

$M$  = molecular weight of water

Therefore  $\Delta F = hgM$ .

The term in Mitchell's equation which is analogous to viscosity can now be evaluated in terms of soil water potential.

A large proportion of mineral to mineral contacts are undoubtedly present in expansive soils, especially between particles of coarse clay and larger size. Mitchell includes a component that takes into account frictional interference, proportional to normal stress. It takes the form of an equivalent bond energy whose magnitude is dependent on normal force. The total free energy of activation can now be thought of as the sum of the energy required to break hydrogen bonds in interlayer water and the energy to overcome friction at particle contacts,

$$\Delta F = hgM + \rho\phi$$

where  $\rho$  = normal force

$\phi$  = normal force-dependent bond energy

As a refinement, the two terms can be taken in proportion to the amount of each type of contact and then returned to the exponential form to give an expression proportional to viscosity

$$e^{-\left[\frac{n_1 (hgM)}{RT} + \frac{n_2 (p\phi)}{\kappa T}\right]},$$

where  $n_1$  is the proportion of adsorbed water bonds and

$n_2$  is the proportion of normal force-dependent bonds.

The normal force term  $p$  will be a function of the mean stress.

While the actual calculation of a strain rate requires that particle spacings be known, the above term can simply be evaluated to obtain relative changes in strain rate with changing soil water potential and composition. This has been done in Fig. 41 for three values of the proportion of normal stress-dependent bonds. Thus the curve  $n_2 = 1.0$  might represent a pore kaolinite,  $n_2 = 0.3$  might represent an expansive soil having 30-50% montmorillonite and  $n_2 = 0.1$  would indicate the behavior of a bentonite. These curves show a response in relative viscosity of the different soil compositions to a change in soil water potential. For  $n_2 = 0.3$ , a rapid change in viscosity is predicted over the same range of potential as observed for the natural soils. Soil water characteristics recorded in the literature for non-expansive clay and silt soils typically exhibit their greatest adsorption increases for a soil water potential of less than -0.1 bars. If it is reasonable to expect a corresponding increase in deformability, then the curve  $n_2$  equals about 0.3. This is in agreement with the data from the artificial soils. In summary these curves are intended to show that the observed behavior of the natural and artificial soils can be approximated by an adaption of rate process theory. The suggestion is afforded that the part played by interlayer water and mineral to mineral contacts in the theoretical approach may exist in nature.

While the average viscosity could be calculated knowing the downhill rate of movement, it is in effect already available from the analysis of the creep test results. The objective of predicting a creep profile is achieved by adapting the form of curves from creep response versus soil water potential to the observations on deformation in homes. If it is

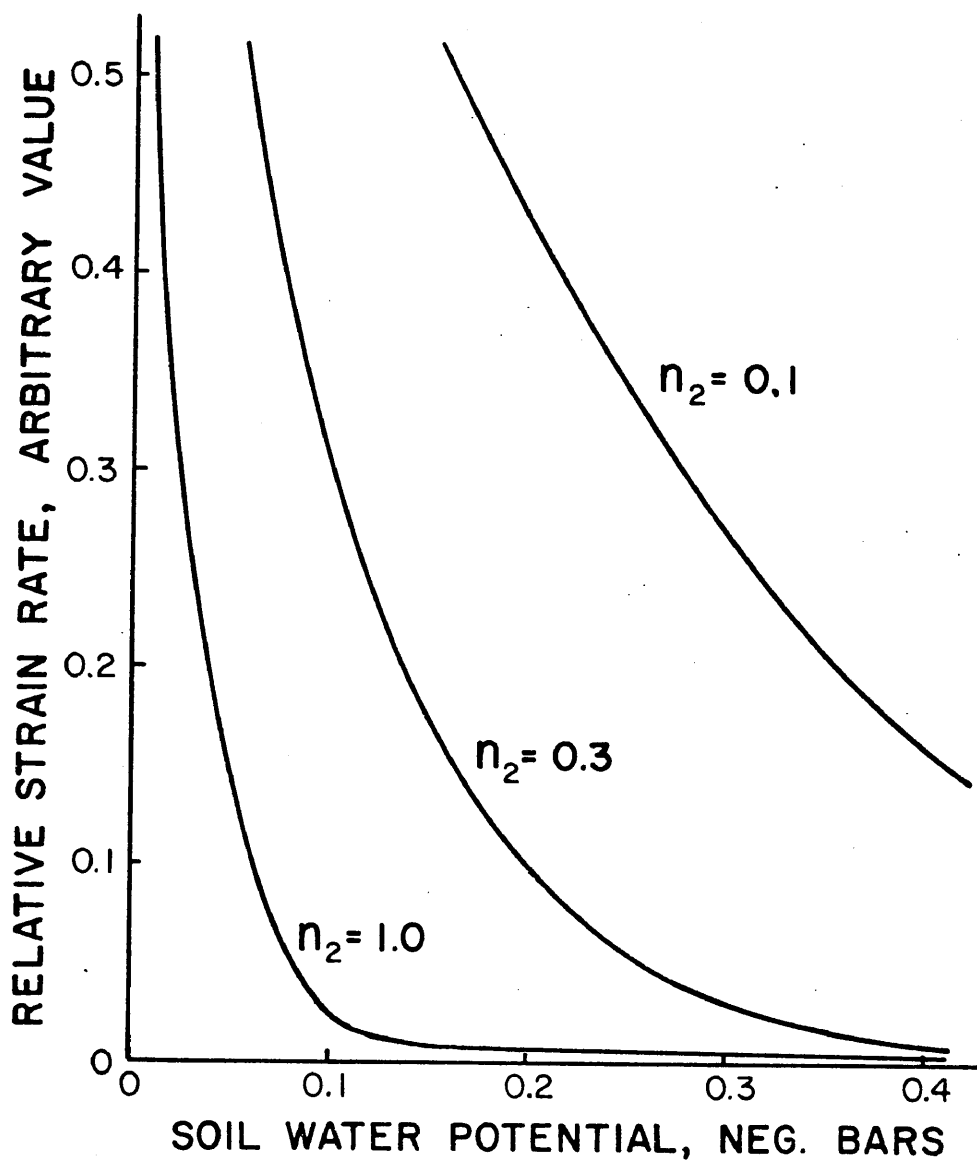


Figure 41. Prediction of relative strain rate based on rate process theory according to soil water potential and proportion ( $n_2$ ) of mineral to mineral bonding.

assumed that displacements recorded by cracks in walls reflect the maximum downhill movement for the life of the structure, then this displacement can be used as the calibration for the creep curves. If it is further assumed that overburden potential is a fully effective component of the total soil water potential, then the relative amount of creep for a given potential gives the actual amount of creep to expect in any depth below the homesite. The in situ creep mechanism will be a cyclic one, each cycle initiated by a wetting. Presumably the surface must reach a state of zero potential at each wetting with lower levels reaching their maximum potential by infiltration. The shear stress operating at these shallow depths is probably roughly the same or somewhat less than the smallest imposed in the creep tests. Downhill movement will accelerate during wetting but deceleration associated with drying and viscoelastic behavior is probably taking place most of the time.

The overburden potential should limit the maximum moisture content to which soil at a given depth can come. In fact, the almost constant moisture contents shown by the adsorption curves for the South Bosque shale and Houston Black clay below about -0.5 bars is reflected in the moisture content profiles in Figures 2, 4, and 10. It is typically observed that below 5-6 feet the moisture contents become relatively constant compared to the fluctuations seen above this depth. The apparent explanation is that the overburden pressure below this depth is great enough to prevent any significant increase in water content of the expansive soil beyond that suggested by the adsorption curves. The curves predict the depth to which significant changes may occur.

The actual expansion due to wetting probably constitutes a major part of the motion for each wetting cycle. Shear strain induced by downhill creep may increase the number or tenacity of grain contacts, so reducing the shear strain rate. However, a new expansion, because its motion is large compared to the shear strain motions, may alter each new grain contact configuration enough to promote another increment of shear strain. With this mechanism it is ensured that viscoelastic behavior cannot become cumulative. Downhill displacement then becomes proportional to the number of wetting events.

## CONCLUSIONS

Downhill creep in expansive soils has been studied using field measurements and laboratory tests. The field observations suggest that the expansive soils can promote downhill creep and will present a definite foundation problem for light structures on slopes as well as level ground. The laboratory swell and creep tests are simple enough that they may be conducted as part of a site investigation to determine the volume change and creep properties of a given soil. Site preparations may then be based on this information.

### Home Survey

1. Downhill creep tends to impart a distinctive style to wall cracking in brick, slab-on-grade homes situated on slopes. Typically, cracks occur on those sides paralleling the slope and facing downhill. The cracks tend to be widest at the top.

2. The homes constructed on slopes appear to be responding to downhill creep as encountered at varying depths in a foundation excavation. The downhill portion rests on the shallowest and therefore most rapidly moving horizon of the soil. The downward component of this motion results in a widest-at-the-top crack style in the walls paralleling the slope. Walls facing downhill may be free to move with a lateral component, promoting top tension cracking there.

3. Statistical analysis of the home survey data reveals that topography in terms of the relief on a lot, and expansive potential of the soil in terms of the average plasticity index, can influence the degree of cracking, depending on the mechanical properties of the expansive soil. Waco gave the most positive and confident correlations. While plasticity indices for both cities are similar, slope angles in Waco have a much greater range than in San Antonio. A strong interaction exists between plasticity index and topography, especially for those cracks that would most aptly record creep. The correlation of plasticity index with the size of the cracks indicates that expansive potential is an important factor as well as slope. Homes in San Antonio also record an influence of topography but it is obscured by relatively

shallow slopes, correspondence of shallow expansive soil horizons with the steepest slopes, and lower rainfall than in Waco. However the cracking at the San Antonio site is not time-dependent, indicating that downhill creep is not occurring there.

#### Volume change tests

1. Expansive soils display marked hysteresis with respect to changes in water content as the soil is dried then wetted through a given range of soil water potential. However a soil rich in montmorillonite will not necessarily be highly expansive.

2. Volume change behavior appears to be dependent on fabric and on stress history of the expansive soil. The South Bosque shale at Waco, a heavily overconsolidated material, displays marked hysteresis with respect to volume change. The Houston Black clay at San Antonio shows only weak hysteresis with respect to volume change. A natural soil differs from an artificial suspension by the departure from the identical volume change behavior that a suspension would exhibit during wetting and drying. In an overconsolidated soil, pore spaces are probably relatively small and so volume changes on the scale of the individual clay particle are readily transmitted to the bulk soil. In a normally consolidated or residual expansive soil the volume change behavior is likely to be closer to that of the suspension. A larger pore space distribution and less tenacious particle contacts allow greater freedom of individual particle movement. The large change in water content for a relatively small change in volume observed for the Houston Black clay suggests the presence of relatively large pores.

3. A consolidometer can be used as a swell meter for the purpose of determining the influence of overburden pressure on swell characteristics. For shallow depths (a few feet) a change in overburden pressure is equivalent to a change in the soil water potential. This comparison is valid because the soil very likely remains almost saturated over the range of potentials that is associated with the greatest amount of volume increase. The consolidometer adapted as a swell meter may be suitable by itself as a tool for predicting swell capability. Two initial water contents could be tried as determined for shallow depths during dry

and wet season conditions. Samples at both moisture contents would then be loaded under pressures of say, 1, 2, and 5 psi. The results would suggest the range of overburden pressures and moisture contents to be maintained to restrict volume change.

#### Creep tests

1. The resistance of expansive soils to shear, as recorded by the rate of deformation, is highly dependent on the volume state as the soil is wetted and dried. The greatest decrease in the resistance appears to coincide with the large increase in volume that takes place at a relatively low soil water potential.

2. As with volume change, there appears to be an association of the character of shearing resistance with soil fabric. While the data for the Houston Black clay is meager it depicts a very sudden decrease in resistance at a soil water potential somewhat less than that associated with the greatest change in resistance for the South Bosque shale. The retention of strength to a very low potential may be related to a rigidity offered by a three dimensional isotropic fabric (on a macroscopic scale) associated with the formation of a residual expansive soil and also the presence of a relatively coarse particle fraction. The shearing resistance behavior of the South Bosque shale is most closely related to its volume change behavior probably because of the more intimate association of montmorillonite particles with the fabric.

3. The effect of a change in soil water potential on resistance to shear appears to be equivalent to an increase in montmorillonite content at a constant potential.

#### General conclusions

Soils containing expansible clay minerals are especially capable of downhill movement depending on the clay fabric and history of formation. Montmorillonite, among the other clay minerals, can form fabric domains consisting of a stack of parallel mineral plates. The particular ability of montmorillonite to expand by the adsorption of water between the plates produces a weak link in the overall fabric. It is possible that individual montmorillonite mineral layers may also

accommodate shear. This fabric element can then deform internally by simple shear. The influence of this fabric element is dependent on the amount of volume increase that has taken place but will be modified by particular soil formation histories and compositions.

The degree to which an expansive soil at any given depth will creep downhill is dependent on soil water potential. Overburden pressure determines the minimum soil water potential to which a soil can come. Thus a combination of depth and soil water potential will determine the amount of creep at a given depth. The actual creep mechanism is cyclic in nature, each cycle being started by an infiltration event. Strain hardening will probably take place until drying and rewetting can return the soil to a state conducive to another increment of creep.

Volume change in the soil and hence creep can be reduced by applying an overburden pressure sufficient to prevent most of the expansive available in an unconfined state. At least 50 percent of the expansion for the soils studied takes place at a potential of less than the field capacity (approx. -0.3 bars). The soil water potential can be prevented from exceeding this value by applying the pressure of approximately 5 feet of overburden. Using a combination of an inert fill (say sand) to a sizeable fraction of this depth (say 3 feet) and drainage, the soil water potential beneath the fill could probably be kept from rising above the critical value. Damage to homes on level ground resulting from differential volume change and damage due to creep for homes on slopes may be significantly reduced by the recognition that much of the hysteresis in both volume change and shearing resistance can be eliminated by preventing the soil water potential from decreasing to the value associated with a rapid volume increase.



## REFERENCES

- Aitchison, G.D., Ed., 1965, Moisture equilibria and moisture changes in soils beneath covered areas: Symposium in Print, Butterworths, Sydney, Australia, p. 7.
- Aitchison, G.D. and Richards, B.G., 1965, A broad scale study of moisture conditions in pavement subgrade throughout Australia: Moisture Equilibria and Moisture Changes Beneath Covered Areas, Butterworths, Sydney, Australia, p. 184.
- Andersland, O.B. and Douglas, A.G., 1970, Soil deformation rates and activation energies: *Geotechnique*, v. 20, p. 1.
- Anderson, J.G., 1906, Solifluction, a component of sub-aerial denudation: *Jr. of Geology*, v. 14, p. 91.
- Aylmore, L.A.G. and Quirk, J.P., 1959, Swelling of clay-water systems: *Nature*, v. 183, p. 1752.
- Barden, L., 1972, The influence of structure on deformation and failure in clay soil: *Geotechnique*, v. 22, p. 159.
- Barshad, I., 1960, Thermodynamics of water adsorption and desorption on montmorillonite: *Clays and Clay Minerals*, v. 8, p. 84.
- Bartelli, L., 1976, Environmental effects on expansive soil deformation, abstract: *Abstracts with Programs, Geological Soc. of Am.*, v. 8, n. 6, p. 769.
- Bennett, R.H., Bryant, W.R. and Keller, G.H., 1977, Clay fabric and geotechnical properties of selected submarine sediment cores from the Mississippi Delta: National Oceanic and Atmospheric Administration Prof. Paper 9, U.S. Dept. of Commerce.
- Bjerrum, L., 1967, Mechanism of progressive failure in slopes of over-consolidated plastic clays and clay shales: *Jr. of the Soil Mechanics and Foundation Div., Am. Soc. of Civil Engineers*, v. 93, n. SM5, p. 1.
- Bolt, G.H., 1965, Physico-chemical analysis of the compressibility of pure clays: *Geotechnique*, v. 6, p. 86.
- Brackley, I.J.A., 1975, A model of unsaturated clay structure and its application to swell behavior: Sixth Regional Conf. for Africa on Soil Mechanics and Foundation Engineering, Darban, South Africa, p. 71.
- Burket, J.M., 1965, Geology of Waco in Urban geology of greater Waco, Part 1: Geology, Baylor Geological Studies, Bull. 8.
- Carson, M.A. and Kirkby, M.J., 1972: Hillslope Form and Process, Cambridge University Press, London.
- Casagrande, A., 1932, The structure of clay and its importance in foundation engineering: *Contributions to Soil Mechanics, Boston Society of Civil Engineers, 1925-1940*, p. 72.

- Castleberry, J.P., 1974, An engineering geology analysis of home foundations: unpublished Master's Thesis, Texas A&M University, College Station, Texas, 158 p.
- Chapman, D.L., 1913, A contribution to the theory of electro capilarity: *Philisophical Magazine*, v. 25, p. 475.
- Chattopadhyay, P.K., 1972, Residual shear strength of some pure clay minerals: unpublished Ph.D Thesis, The University of Alberta, Edmonton, Alberta, Canada.
- Collins, K. and McGown, A., 1974, The form and function of micro-fabric features in a variety of natural soils: *Geotechnique*, v. 24, p. 223.
- Croney, D. and Coleman, J.D., 1960, Pore pressure and suction in soil: in *Pore Pressure and Suction in Soils*, Butterworths, London, p. 26.
- Davis, W.M., 1892, The convex profile of badland divides: *Science*, v. 20, p. 245.
- Davison, C., 1889, On the creeping of the soil-cap through the action of frost: *Geological Magazine*, v. 6, p. 255.
- Davitz, J.C. and Low, P.F., 1970, Relation between crystal-lattice configuration and swelling of montmorillonites: *Clays and Clay Minerals*, v. 18, p. 325.
- Derjaguin, B., 1936, Range of action of surface forces: *Nature*, v. 138, p. 330.
- Dobson, M.B., 1978, The influence of stratigraphy on the behavior of expansive soils: unpublished Master's Thesis, Texas A&M University, College Station, Texas.
- Eisenberg, D. and Kauzwon, W., 1969, *The Structure and Properties of Water*: Oxford Univ. Press, New York.
- El Swaify, S.A. and Henderson, D.W., 1967, Water retention by osmotic swelling of certain colloidal clays with varying ionic composition: *Jr. of Soil Science*, v. 18, p. 223.
- Embleton, C. and King, C.A.M., 1975, *Periglacial Geomorphology*: John Wiley and Sons, New York, 203 p.
- Fleming, R.W. and Johnson, A.M., 1975, Rates of seasonal creep of silty clay soil: *Quarterly Jr. of Engineering Geology*, v. 8, p. 1.
- Font, R.G., 1973, Engineering geology study of the instability of the South Bosque shale and the Del Rio clay in the Waco area: unpublished Ph.D. Dissertation, Texas A&M University, College Station, Texas.
- Font, R.G., 1977, Influence of Anisotropies on the shear strength and field behavior of heavily over consolidated, plastic and expansive clay-shales: *Texas Jr. of Science*, v. 29, p. 21.
- Font, R.G. and Williamson, E.F., 1970, Urban geology of greater Waco, Part IV: *Engineering, Baylor Geological Studies, Bull.* 12.

- Foster, M.D., 1955, The relation between composition and swelling in clays: *Clays and Clay Minerals*, v. 3, p. 205.
- Foster, R.H., 1970, Behavior of kaolin fabric under shear loading at low stress, *Stress-Strain Behavior of Soils: Roscoe Memorial Symposium*, Cambridge, England, p. 81.
- Franzmeier, D.P. and Ross, S.J., 1968, Soil swelling: laboratory measurement and relation to other soil properties, *Soil Science Society of America Proceedings*, v. 32, p. 573.
- Gilbert, G.K., 1909, The convexity of hilltops: *Jr. of Geology*, v. 17, p. 344.
- Goldschmidt, V.M., 1926, Undersokelser ved Levsedimenter, *Nordisk forbrugsforskning, Kongress 3*, Kobenhaun, p. 434.
- Gouy, G., 1910, Sur la constitution de la charge électrique à la surface d'un électrolyte: *Ann. Phys., Serie 4*, v. 9, p. 457.
- Gromko, G.J., 1974, Review of expansive soils: *Journal of the Geotechnical Division, American Society of Civil Engineers*, v. 6, p. 667-687.
- Gustavson, T.C., 1975, Microrelief (gilgai) structures on expansive clays of the Texas coastal plain - their recognition and significance in engineering construction: *Geological Circular 75-7*, Bureau of Economic Geology, Univ. of Texas at Austin.
- Haefeli, R., 1950, Investigation and measurements of the shear strengths of saturated cohesive soils: *Geotechnique*, v. 2, p. 186.
- Hendricks, S.B., 1942, Lattice structure of clay minerals and some properties of clays: *Jr. of Geology*, v. 50, p. 276.
- Hendricks, S.B., Nelson, R.A. and Alexander, L.T., 1940, Hydration mechanism of the clay mineral montmorillonite saturated with various cations: *Jr. of the American Chemical Soc.*, v. 62, p. 1457.
- Hofman, R., Eudell, K. and Wilm, D., 1933, Kristallstruktur und Quellung von Montmorillonit: *Zeit schrift fur Kristallographie*, v. 86, p. 340.
- Hvorslev, M.J., 1960, Physical components of the shear strength of saturated clays: *Research Conf. on Shear Strength of Cohesive Soils*, Am. Soc. Civil Engineers, Boulder, Colo.
- Ingles, O.G., 1968, Soil chemistry relevant to the engineering behavior of soils in *Soil Mechanics, Selected topics*, I.K. Lee, Ed., p. 1.
- Jennings, J.E., 1953, The heave of buildings on desiccated clay, *Third International Conf. on Soil Mechanics and Foundation Engineering*, v. 1, p. 390.
- Johnston, J.R. and Hill, H.O., 1944, A study of the shrinking and swelling properties of Rendzina soils: *Soil Science Soc. of Am. Proc.*, v. 9, p. 24.
- Jones, D.E. and Holtz, W.G., 1973, Expansive soils - the hidden disaster: *Civil Engineering*, v. 43, p. 49-51.

- Kenney, T.C., 1967, The influence of mineral composition on the residual strength of natural soils; Proceedings, Geotechnical Conf. on the shear strength properties of natural soils and rocks, v. 1, p. 123, Oslo Norway.
- Kirkby, M.J., 1967, Measurement and theory of soil creep: Jr. of Geology, v. 75, p. 359-378.
- Kunze, G.W. and Templin, E.H., 1956, Houston Black clay, the type grum-usol: II. mineralogical and chemical characterization: Soil Science Soc. of Am. Proc., v. 20, p. 91.
- Lambe, T.W., 1951, Soil testing for engineers, John Wiley and Sons, Inc., New York, 165 p.
- Lambe, T.W., 1960, The character and identification of expansive soils, Federal Housing Administration, Technical Publication 701.
- Lambe, T.W. and Whitman, R.V., 1969, Soil Mechanics, John Wiley and Sons, New York, 553 p.
- Low, P.F., 1960, Viscosity of water in clay systems: Clays and Clay Minerals, v. 8, p. 170.
- Low P.F., 1961, Physical chemistry of clay-water interaction: Advances in Agronomy, v. 13, p. 269.
- Low, P.F. and White, J.L., 1970, Hydrogen bonding and polywater in clay-water systems: Clays and Clay Minerals, v. 18, p. 63.
- Lytton, R.L. and Woodburn, I.A., 1973, "Design and Performance of Mat Foundations on Expansive Clays", Proceedings 3rd International Conference on Expansive Clay Soils, v. 1, Haifa, Israel, p. 301.
- McDowell, C., 1974, Method for determining the potential vertical rise, PVR, Texas Highway Department, Test Method Tex-124-E.
- Martin, R.T., 1962, Adsorbed water on clay: a review, Clays and Clay Minerals, v. 9, p. 28.
- Mathewson, C.C., Castleberry, J.P. and Lytton, R.L., 1975, Analysis and modelling of the performance of home foundations on expansive soils in central Texas: Bull. Assoc. of Engineering Geologists, v. 12, p. 275-302.
- Mesri, G. and Olson, R.E., 1970, Shear Strength of Montmorillonite, Geotechnique, v. 20, p. 261.
- Mitchell, J.K., 1964, Shearing resistance of soils as a rate process: Jr. of the Soil Mechanics and Foundation Div., Am. Soc. Civil Engineers, v. 90, p. 29.
- Mitchell, J.K. and McConnell, J.R., 1965, Some characteristics of the elastic and plastic deformation of clay on loading: Sixth Int. Conf. on Soil Mechanics and Foundation Engineering, v. 1, p. 313-17.
- Mitchell, J.K., Camponella, R.G. and Singh, A., 1968, Soil Creep as a rate process: Jr. of the Soil Mechanics and Foundation Division, Proc. of the Am. Assoc. of Civil Engineers, v. 94, SMI, p. 231.

- Mitchell, J.K., Singh, A. and Camponella, R.G., 1969, Bonding, effective stress and strength of soils: Jr. of the Soil Mechanics and Foundation Division, Am. Society of Civil Engineers, v. 99, no. SM10.
- Morgenstern, N.R. and Tchalenko, J.S., 1967, Microscopic structures in kaolin subject to direct shear: *Geotechnique*, v. 17, p. 309-328.
- Mott, N.F., 1956, "Dislocations in Crystallized Solids", in *Surveys in Mechanics*, Cambridge University Press, p. 32.
- Neville, A.M., 1970, *Creep of Concrete: Plain, Reinforced and Prestressed*; American Elsevier, New York.
- Norrish, K., 1954, The swelling of montmorillonite: *Faraday Soc., London, Discussions*, n. 18, p. 120.
- Posner, A.M. and Quirk, J.P., 1964, Adsorption of water from concentrated electrolyte solutions by montmorillonite and illite: *Proc. Royal Soc. of London*, v. 278, p. 35.
- Ravina, I. and Low, P.F., 1972, Relation between swelling, water properties and b-dimension in montmorillonite-water systems: *Clays and Clay Minerals*, v. 20, p. 109.
- Ritchie, J.T., Kissel, D.E. and Burnett, E., 1972, Water movement in undisturbed swelling clay soil: *Soil Sc. Soc. of Am. Proc.*, v. 36, p. 874.
- Rosenquist, I.T., 1955, Investigations in the clay electrolyte water system: *Norwegian Geotechnical Inst. Pub.* 9, p. 9.
- Ross, C.S. and Hendricks, S.B., 1945, Minerals of the montmorillonite group: *U.S. Geological Survey Prof. Paper* 205B, p. 23.
- Russam, L. and Coleman, J.D., 1961, The effect of climatic factors on subgrade conditions: *Geotechnique*, v. 11, p. 22.
- Schmertman, J.H. and Hall, J.R., 1961, Cohesion after non-hydrostatic consolidation: *Jr. of the Soil Mechanics and Foundation Div., Am. Soc. Civil Engineers*, v. 87, n. SM4, Proc. Paper 2881.
- Sellards, E.H., 1919, The geological and mineral resources of Bexar County: *Univ. of Texas Bull.*, v. 1932.
- Sides, G. and Borden, L., 1971, The microstructure of dispersed and flocculated samples of kaolinite, illite and montmorillonite: *Canadian Geotechnical Jr.*, v. 8, p. 391.
- Skempton, A.W., 1964, Long-term stability of clay slopes: *Geotechnique*, v. 14, p. 77.
- Skempton, A.W. and Petley, D.J., 1967, The strength along structural discontinuities in stiff clays: *Proc. of the Geotechnical Conf., Oslo*, v. 2, p. 29.
- Smith, F.E., 1962, Tertiary and uppermost Cretaceous of the Brazos River valley, southeastern Texas, *Geology of the Gulf Coast and Central Texas*, Houston Geological Soc., p. 132.

- Staple, W.J., 1965, Moisture=tension, diffusivity and conductivity of a loam soil during wetting and drying: Canadian Jr. of Soil Science, v. 45, p. 78.
- Stern, O., 1924, Zur theorie der elektrolytischen doppelschicht, Zietschrift Electrochem, v. 30, p. 508.
- Sullivan, R.A. and McClelland, B., 1969, Predicting heave on unsaturated clays, 2nd International Research and Engineering Conference on Expansive Clay Soils, Texas A&M University, College Station, Texas.
- Swanson, D.N. and Swanson, F.J., 1976, Timber harvesting, mass erosion and steep land forest geomorphology in the Pacific Northwest in Geomorphology and Engineering, D.R. Coates, Ed., Dowden, Hutchinson and Ross, Stroudsburg, Penn.
- Terzaghi, K., 1925, Modern concept concerning foundation engineering: Jr. of the Boston Society of Civil Engineers, v. 12, p. 1.
- Terzaghi, K., 1928, The physical properties of clays: Mass. Inst. of Technology Technical Engineering News, v. 9, p. 10.
- Terzaghi, K., 1950, Mechanism of landslides, in Berkeley Volume, Geological Soc. of America, p. 83.
- Topp, G.C., 1971, Soil water hysteresis in silt loam and clay loam soils: Water Resources Research, v. 7, p. 914.
- United States Dept of Agriculture, 1958, Soil Survey, Brazos County, Texas.
- United States Department of Agriculture, 1966, Soil survey of Bexar County, Texas: U.S. Govt. Printing Office, Washington D.C., 126 p.
- Van Olphen, H., 1962, Unit layer interaction in hydrous montmorillonite systems: Jr. of Colloid Science, v. 17, p. 660.
- Van Olphen, H., 1977, An Introduction to Clay Colloid Chemistry, Second ed., John Wiley and Sons, New York.
- Wahrhaftig, C. and Cox, A., 1959, Rock glaciers in the Alaska Range: Geological Soc. of Am. Bull., v. 70, p. 383-436.
- Ward, W.H., 1953, Soil movement and weather: Third Int. Conf. on Soil Mechanics and Foundation Engineering, v. 4, p. 477.
- Warkentin, B.P., Bolt, G.H. and Miller, R.D., 1957, Swelling pressure of montmorillonite: Soil Science Soc. of Am. Proc., v. 21.
- Washburn, A.L., 1967, Instrumental observations of mass wasting in the Mesters Vig district, northeast Greenland: Meddeleser om Gronland, v. 166, p. 296.
- Williams, J. and Shaykewich, 1970, The significance of soil water matric potential on the strength properties of unsaturated soil: Soil Science Soc. of Am. Proc., v. 34, p. 835.
- Yaalon, D.H. and Kalmor, D., 1972, Vertical movement in an undisturbed soil: continuous measurement of swelling and shrinkage with a sensitive apparatus: Geoderma, v. 8, p. 231.

Yong, R.N., Japp, R.D. and How, G., 1971, Shear strength of partially saturated clays: Proc. of the Fourth Asian Regional Conf. on Soil Mechanics and Foundation Engineering, v. 1, p. 183.

**APPENDIX****Mechanism of Volume Change in Expansive Soils****Home Survey Data: San Antonio, Waco****Creep Test Data**



## MECHANISM OF VOLUME CHANGE IN EXPANSIVE SOILS

With a change in water content, most soils exhibit a change in volume. The basic cause for this is the electrical attraction that exists between water and soil particles. Water does not simply fill up pore space, rather it is adsorbed onto particle surfaces, first forming thin films which join when particles are close or touching. As the adsorption proceeds, the tension formed by the attraction between particles and water decreases, resulting in separation. At this stage the soil fabric may determine which way the bulk volume change goes. If the fabric is very open, decreased interparticle friction may result in collapse. However, for soils that are overconsolidated, the initially compact spacing of particles will only permit separation.

The amount of water that is adsorbed depends most notably on both the surface area available for adsorption and the presence of an electrical charge on the surface. In clays these quantities are both large, resulting in the relatively great attraction that clay minerals show for water. When adsorption starts from some arbitrary dry state, the interstitial water will be in a state of tension. Hydrogen bonding is thought to exist in free water between water molecules (Eisenberg and Kauzman, 1969) enabling water to support a small tensional force. Adsorption on particles probably imparts an ordered structure to water, which in turn promotes the bonding. When a soil is unsaturated the directions in which bonding may take place are limited, enabling the most energy to be used in keeping particles together. As the soil approaches saturation there is less directional control on bonding and the tension decreases.

The process of volume change in an expansive soil requires that work, in the form of dilation of the soil mass, be done. While the change in volume it undergoes is accomplished by a change in water content, this physical condition is not a precise indicator of the expansive state. Rather, a measure must be used that shows how much potential energy is available for producing movements. This is because the attraction between soil particles is not only dependent on the

water content but more explicitly on other physical and chemical aspects that influence the attraction between water and soil particles.

#### Clay as a charged particle and clay-water interaction

While those involved in the use of clays for making ceramics have known of the excessive water-adsorbing characteristics of certain clays for centuries, it was not until the 1930's that the basic mechanism accounting for this phenomenon began to be understood. X-ray diffraction studies have documented the layered structure of clays and it has been determined that the clay mineral montmorillonite exhibits an increasing separation of the layers as water content is increased (Hofman et al., 1933). It had already been suggested that water is attracted to clay particles due to the dipolar nature of water (Terzaghi, 1928) but the source of the attraction in the clay was not determined until numerous chemical analyses were examined (Hendricks, 1942; Ross and Hendricks, 1945). This revealed the presence of cations of lower valence substituting for those ideally suited to electrically balance the structure. The result was interpreted as a net negative charge manifesting itself on the surface of a clay particle.

The mineral montmorillonite is one of that class of silicates commonly known as clays in the mineralogical sense of the term. Clays are layer silicates having as their ideal structure a plane of aluminum atoms octahedrally coordinated by oxygen atoms and hydroxyl radicals (aluminum octahedra), to one or both sides of which are joined a plane of silicon atoms tetrahedrally coordinated by oxygens (silica tetrahedra). The silica tetrahedra are arranged such that they point inwards with respect to a clay layer, the apical oxygens being shared to form corners of the aluminum octahedra. A single tetrahedral sheet joined to an octahedral sheet forms the 1:1 clay layer known as kaolinite (Fig. 42). In this case, the outer sides of the octahedra consist of hydroxyls which permit hydrogen bonding with the basal tetrahedral oxygens of another hydrogen bonding with the basal tetrahedral oxygens of another 1:1 layer. A 2:1 layer is formed when an octahedral sheet is enclosed by two tetrahedral sheets. Montmorillonite, mica and vermiculite are members of this group. With this arrangement, basal oxygens are

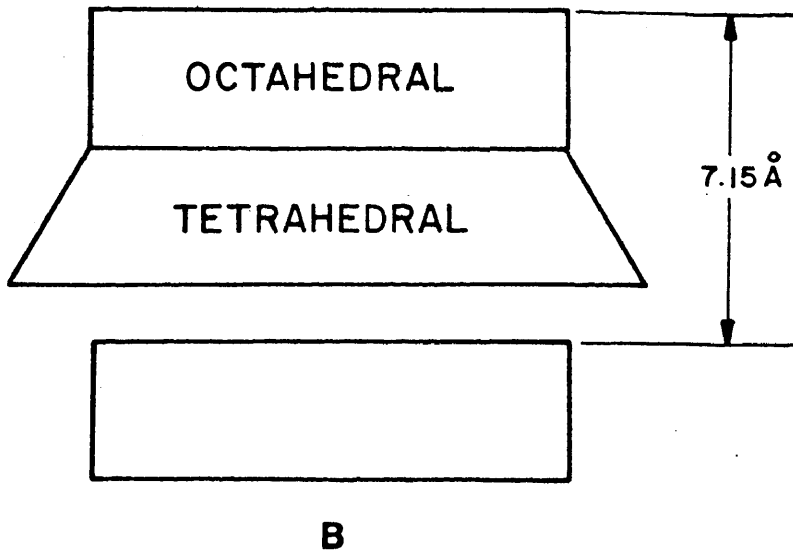
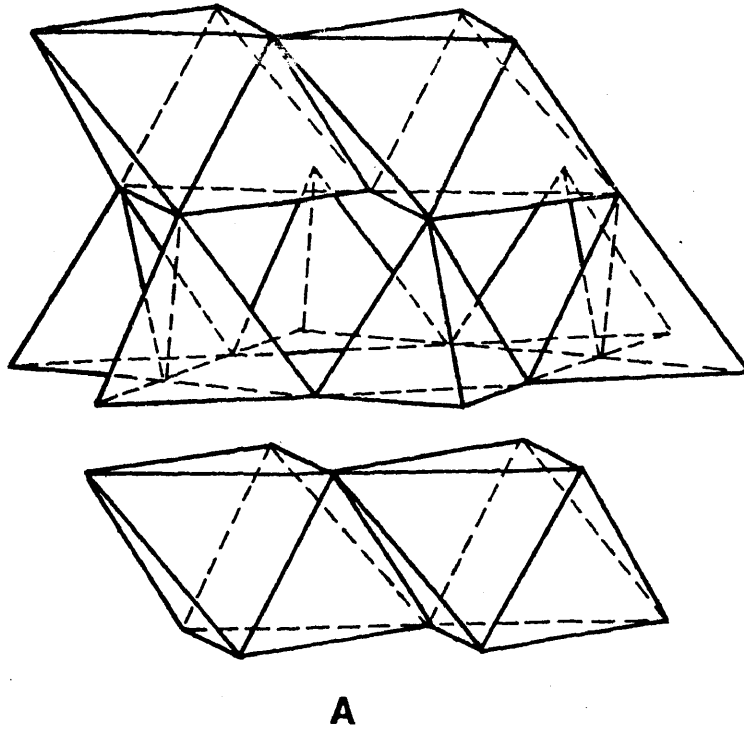


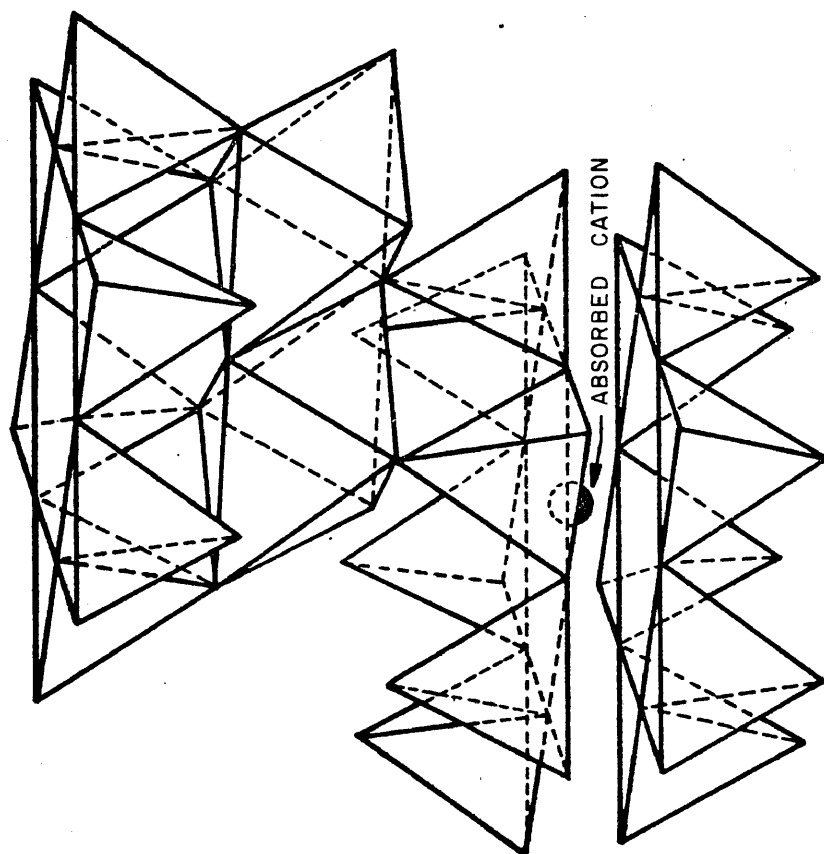
Figure 42. A 1:1 clay mineral, kaolinite. a. Diagrammatic sketch. Octahedrons represent Al-octahedra, tetrahedrons represent Si-tetrahedra. b. Schematic view showing repeat distance of layers.

presented to both sides of a layer, denying the electrical polarization seen in kaolinite. Bonding between layers in this case is accomplished by the presence of interlayer cations.

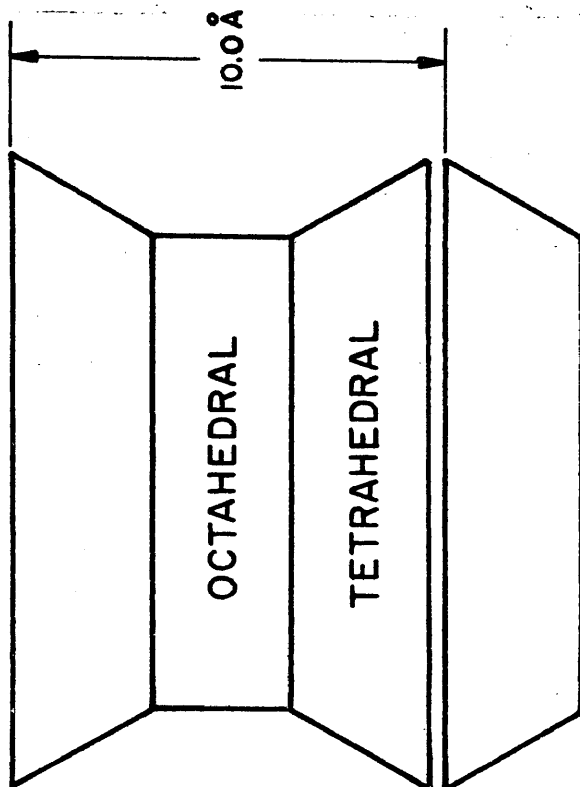
All clays deviate from their idealized structure due to cation substitutions within the octahedral and tetrahedral sheets. Cations of lower valence take the place of the ideal silicon or aluminum. In mica (Fig. 43) about one quarter of the silicons are replaced by aluminum and a charge deficiency results within the layer because of the lower valence of  $Al^{3+}$ . It is made up for by the presence of potassium ions between the layers. The proximity of the seat of charge imbalance to the outside of a layer and the snugness of the fit for potassium ions in the hexagonal openings between the bases of the silica tetrahedra result in a relatively strong interlayer bond.

In the case of montmorillonite (Fig. 44), the substitution is usually in the octahedral sheet, with the replacement of about one sixth of the aluminums by magnesiums. Of course, other cations of appropriate size (e.g., iron) may reside in these sites in any proportion and such randomness is a characteristic of clays. However, magnesium is commonly present in montmorillonite in the proportion stated. The charge deficiency in montmorillonite is compensated for by exchangeable cations, so called because they can be replaced by other cations in solution. Of all the 2:1 type clays exhibiting cation substitution, montmorillonite shows the smallest charge imbalance. This, together with the screening effect of the interlayer cation is not as strong as in mica. It is this condition of weak interlayer bonding that allows the layers to separate relatively easily.

As cations are attracted to surface and interlayer sites, so are dipolar molecules, most notably water. The source of this attraction lies with the direct and indirect response of the water dipoles to the net negative charge of the clay particles. The Gouy-Chapman theory was developed to predict the distribution of ions adjacent to charged surfaces (Gouy, 1911; Chapman, 1913). The negatively charged clay surface together with the atmosphere of ions in the adjacent solution constitute the so-called electric or diffuse double layer (van Olphen, 1977). The



A



B

Figure 43. A 2:1 clay mineral, muscovite. A. Diagrammatic sketch. The adsorbed cation in muscovite is  $K^{+1}$ . Ionic substitution occurs in the tetrahedral layers where 1 out of every 4  $Si^{+4}$  atoms is replaced by  $Al^{+3}$ . B. Schematic showing repeat distance of layers.

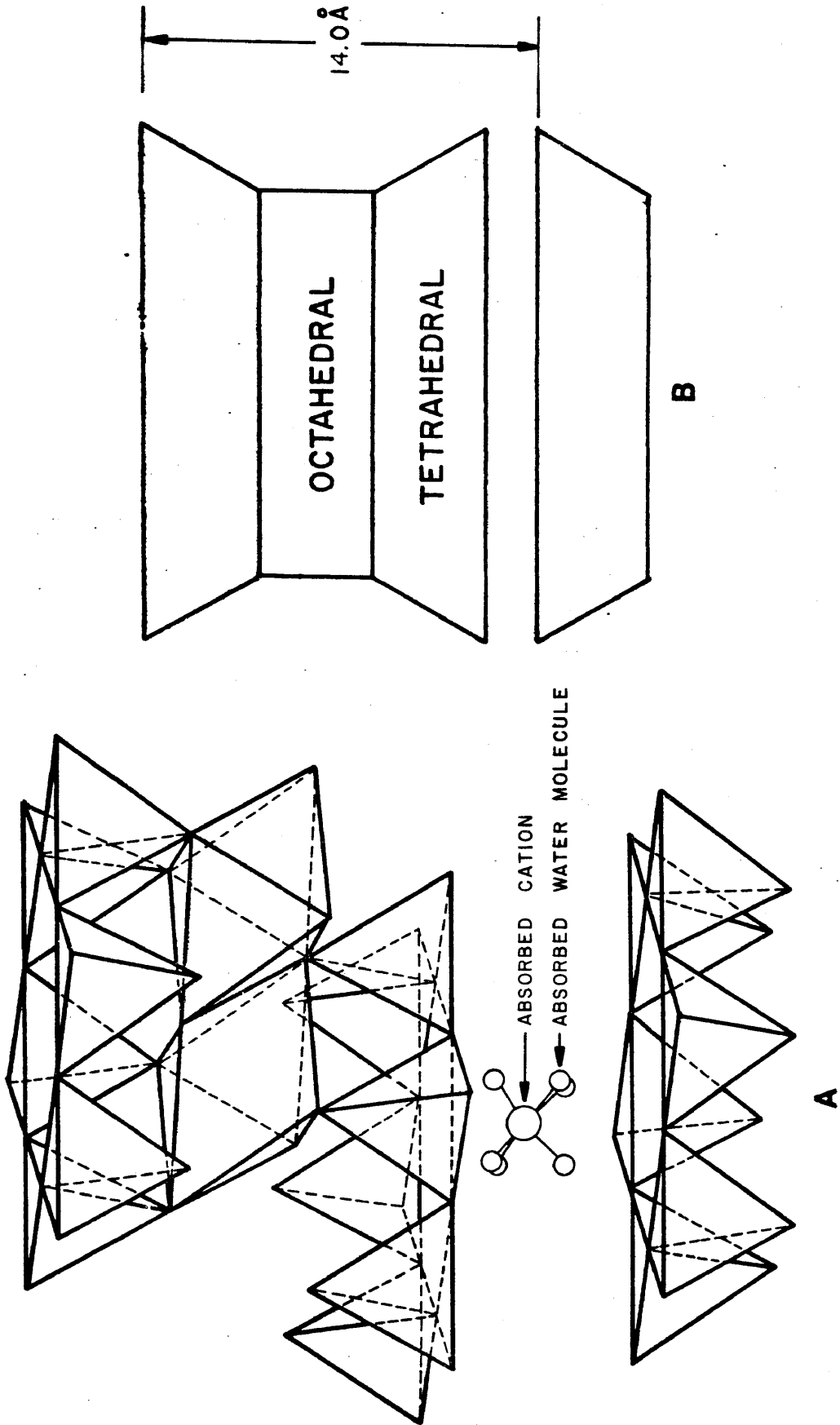


Figure 44. Montmorillonite, one of the smectite groups of clay minerals. A variety of cations can be adsorbed by smectite including,  $K^{+1}$ ,  $Na^{+1}$ ,  $Ca^{+2}$ ,  $Fe^{+2}$ . Ionic substitution occurs primarily in the octahedral sheet. B. Schematic showing the repeat distance of layers.

theory predicts the distribution of ions using the Boltzman equation for the concentration of ions in an electric force field with the Poisson equation expressing the strength of the electric force field.

While the double layer theory strictly applies to the distribution of ions, it must also apply to water molecules because of ion hydration. In fact water molecules are thought to be preferentially attracted to the clay surface because of their positioning about ions (Posner and Quirk, 1964). With increasing concentration of a given cation, Posner and Quirk have shown that water is probably displaced from the clay surface above cation concentrations of about 1N.

Hydrogen bonding with surface oxygens also serves to preferentially attract water (Low, 1961). This tendency is strong enough that water is thought to propagate itself from an oxygen surface in a semi-structured form (Ravina and Low, 1972). It is evident that with solutions of the type likely to be found in natural soils (ie. relatively low concentrations of ions) water is a major component of the double layer. The ability of the clay particle to develop this adsorbed layer gives clay soils their range of consistancies over a wide range of water content, ie. the "elasticity" of engineering soil classification.

#### Mechanisms of volume change

The negative charge that exists on the surface of clay particles also exists between layers, serving to attract cations and their associated water of hydration. This accomodation of hydrated cations leads to the separation of the montmorillonite layers and is the first stage of volume increase in an expansive clay. Hendricks et al. (1940) demonstrated that the initial water uptake is orderly and attributed its control to hydration of the adsorbed cations. In all likelihood the inter-layer cations remain in place during water uptake or loss during this first stage because they are relatively tightly held. At very low water contents the first adsorption of water has been shown to be associated with a high heat of wetting (Barshad, 1960) and this adds weight to the conclusion of Norrish (1954) that this water is in a highly organized or crystalline state. The attainment of the crystalline state is probably aided by the tendency of water to bond with surface oxygens and,

if tetrahedral substitution by aluminum is present, the tendency to associate by hydration with this ion of very high hydration energy (Ingels, 1968). Ingles suggests that in this case the exchangeable cations may even be partitioned to the central position of the interlayer water-cation zone.

The bonding of water to surface oxygens bordering the interlayer sites is a mechanism of swelling proposed by Davidtz and Low (1970). They verified the findings of Foster (1955) that swelling potential shows no apparent correlation with cation exchange capacity (CEC) for a given clay mineral. Rather the CEC decreases with increasing octahedral substitution. As well as being a function of charge deficiency, the CEC is related to the surface area of clay mineral present. The charge deficiency and surface area can vary independently and so independently control the CEC. Instead, another effect of cation substitution, namely to cause a change in the lattice dimensions to accommodate different sized cations, has been considered. Specifically Davidtz and Low proposed that the b-lattice dimension is related to free swell. Water forms a pseudomorph after the tetrahedral component of the montmorillonite structure and as this happens both structures become strained. The basal oxygens of the montmorillonite adjust to conform to the water structure which itself undergoes a readjustment. However, a loss of free energy accompanies the rearrangement of the basal oxygens, enabling the adsorption of the water to occur spontaneously. The theory accounts for a change in the b-dimension of the montmorillonite unit cell and offers an alternate explanation to osmosis for montmorillonite swelling.

The initial swelling of a montmorillonite is likely controlled by the presence of interlayer cations. It has been noted that the 2:1 layer silicates not having a charge deficiency, i.e. talc and pyrophyllite, are not separated by water (Norrish, 1954). Initial swelling seems to occur in four discrete states, each stage representing a layer of water that enters to satisfy both the hydrating tendency of the interlayer cations and the bonding tendency with surface oxygens. The exterior of clay particles are also involved in this process, i.e. the



development of the adsorbed water layer.

Beyond the initial stage of swelling, a process often referred to as osmotic swelling is thought to take over. Here the theory of the diffuse double layer becomes important because the tendency toward hydrogen bonding with layer surface oxygens has been met by the initially adsorbed water. The presence of the excess of negative charge continues to be effective in attracting cations and enables expansion to take place.

The excess of charge maintains an electric potential at the clay layer surface which will have some maximum value depending on the amount of cation substitution. This potential then decays exponentially with distance as described by the Boltzman-Poisson equation. According to this description both the concentration of cations and their valence affect the magnitude of the electric potential with distance from the charged surface. It is this potential that generates the repulsive force between clay layers and particles, the repulsion being most highly developed when the mineral surfaces are parallel. Of course, parallel alignment is assured between layers of a clay particle. Between particles the fabric will determine the amount of parallelism.

The Guoy-Chapman theory deals with the interaction between the double layers of parallel plates. It is assumed that the same mathematical description of potential distribution will apply to both separated clay layers and parallel clay particles. The only difference between the two cases might be the surface density of charge, ie. surface potential. This difference would depend on the extent to which the charge differences within each layer were additive.

For an increasing concentration of a given cation in the solution in which clay particles exist, the double layer is suppressed in the sense that the distance out to which there is a concentration higher than that of the solution decreases. The concentration in the double layer is, of course, increased for a given distance from the layer surface. A corresponding effect is seen for the potential distribution, as the concentration increases the potential at any given distance from the particle surface decreases. The cation component of the double

layer becomes tightly drawn up against the clay surface thereby neutralizing the excess of charge at a relatively close distance to the surface. This phenomenon also permits flocculation to take place as the suppression of the double layer permits particles to approach closely enough for the Van der Waals attraction to become effective. If the cation concentration is decreased, the double layer will expand and the potential will increase at any given distance from the clay surface. This increase in potential results in increased repulsion between clay particles and so they separate. If the amount of clay versus water is great enough, a volume increase of the mixture will take place.

Osmosis is a process by which solutions of differing concentration attempt to equilibrate themselves (ie. equilibrate their free energies as determined by the amount of water occupied in hydrating ions) by transfer of the solvent through some kind of boundary impermeable to the solute. Such a process can result in a pressure being exerted if the solution into which the solvent is flowing is confined. A pressure sufficient to resist further osmosis will be developed. The interlayer area of a clay particle can act as the confining area for one of the solutions, usually that of higher concentration. The counterpart of the impermeable boundary exists as the attraction of the clay surface potential for the interlayer cations. Osmosis then takes place as water from the outside solution is drawn into the clay interlayers. The actual expansion is then accomplished by the progradation of the electric potential as the interlayer concentration of cations is reduced. The expansive pressure that is developed will decrease as the clay particle system is allowed to increase in volume and thereby reduce the interaction of the repulsive surface potentials.

TABLE 6

## HOME SURVEY DATA: San Antonio

House	Approx. % Slope	Age	Depth of Act. Zone	Total Width of Cracking		
				Uphill	Sides	Downhill
				mm	mm	mm
25/21 SA	2	13 yr.	6 ft.			
6/22	3	12	6	5T	3B	3T
16/23	3	9	5	1B	1B	
18/23	2	5	4			
19/23	5	7	4	1T	2B	1B
21/23	5	5	4	2T	1T	1T
22/23	5	5	4	2T	2C	1T
23/23	3	5	5	2T	1C	1C
34/23	5	9	2	2B		
39/23	4	11	2			
35/23	6	9	2	3T	4T	2T
36/23	7	9	2	1B	2B	1B
37/23	5	10	2		1B	
40/23	4	12	2	1C	2C	
41/23	4	10	2	1T	1T	1T
42/23	5	10	4	1C	5C	
44/23	5	12	4		2T	1B
45/23	4	11	4	1C	3T	1C
46/23	6	11	4			
47/23	5	12	5	2C	2C	6C
48/23	5	8	5	2T	1T	
54/23	3	12	6		2C	3T
55/23	3	12	5		2C	
56/23	3	12	5	2T	7T	5C
57/23	2	6	5		2T	2C
9/29	2	10	5	1C	3T	
10/29	3	11	4	1C	1C	
11/29	4	11	4	1T	2T	
12/29	4	11	5	2B	2C	2C
13/29	3	12	5	3T	4T	5T
9/75	9	4	5	3C	2C	1C
10/75	6	4	5	1C		
11/75	6	4	5	1C	4C	3C
12/75	8	4	4			
14/75	6	4	5	2C	4T	
15/75	6	4	5	2T		1T
16/75	4	4	5	1T	1C	2T
3/76	6	4	5	5C	3C	3T
8/76	4	4	5	2C		
12/76	6	4	5	5C	7T	5T
9/78	4	4	5	1T	6T	
7/79	6	3	4	1T	6T	4T
8/79	6	4	4	1	2T	2T

T = top tension, C = center tension, B = bottom tension

TABLE 6 (continued)

## HOME SURVEY DATA: San Antonio

House	Approx. % Slope	Age	Depth of Act. Zone	Total Width of Cracking		
				Uphill	Sides	Downhill
				mm	mm	mm
9/79	6	2	5	1C		
11/76	4	4	5	6B	2C	9T
10/78	7	2	5	3T	8T	2B
11/78	8	4	5	2B	1T	1T
10/79	4	4	3	1T	10T	2C
12/78	7	3	5	5T	4T	2C
6/79	6	4	4	4C	5T	2C
9/79	4	4	4	1B	2B	4T
11/79	4	4	3	2B	2T	
12/79	5	3	3	3T	3C	1C
13/79	4	3	3			
14/79	7	2	4	1C	1B	1T
15/79	8	2	4	4C	8T	
16/79	7	4	4	3C	3C	1C
1/66	4	5	4	2C		
2/66	7	3	3		1C	1C
3/66	8	4	2	1C		
4/66	8	4	3	1T		
7/66	6	4	3	2T		
9/66	2	5	4			
11/66	7	4	4			2B
12/66	6	4	3	2T	2C	3T
13/66	6	4	3	2T		4T
14/66	6	4	3	2T	1T	1B
1/67	9	3	3		3C	1C
3/67	10	3	3		2C	3T
5/67	10	3	3		3T	2C
6/67	6	3	3	1C	4B	
7/67	6	3	3	1T	2T	1C
8/67	3	3	3			
9/67	2	4	3			
13/67	6	3	3	1T	3T	
15/67	10	4	3			
16/67	7	5	3	6C	3T	1B
17/67	10	4	4	1B	1B	3B
1/68	11	4	3			
2/68	12	3	0	1C	3C	
3/68	12	3	0			
5/74	4	4	5	5T	1T	5B
6/74	4	4	5	6T	2C	1C
7/74	3	4	4		2C	2T
8/75	8	4	6			

TABLE 7

## HOME SURVEY DATA: Waco

House	Approx. % Slope	Age	Avg. PI	Total Width of Cracking		
				Uphill	Sides	Downhill
				mm	mm	mm
1 WA	2	2 yr.	45			
2	5	2	43			
3	4	2	45			
4	7	3	37	15T	1T	2B
5	6	4	47	1T	2T	
6	5	4	47			2C
7	10	3	25	2T		2B
8	7	4	47		1C	
9	12	4	33	2C	2C	
10	8	3	26		4T	
11	7	4	32	1C		
12	6	3	33		3T	
13	5	4	30	2C	2T	5T
14	2	3	26	2C	1C	
15	5	4	26		1C	
16	5	4	41	1T		4T
17	9	4	25		1T	
18	8	4	40		2T	1C
19	9	4	45		2T	
20	9	4	26		3T	1T
21	6	4	46		5T	3T
22	5	3	26	1T		1T
23	7	4	24			1T
24	12	3	24			
25	2	2	26		2C	
26	3	2	25			1T
27	5	3	25			
28	7	4	45	4T	4T	2T
29	13	10	36			9T
30	11	2	33			
31	3	2	40		1T	
32	6	5	48	5T	5B	1B
33	14	5	38		7T	4T
34	6	2	19			1T
35	16	9	38	20T	6B	6T
36	7	5	16			
37	14	2	48	1C	3C	
38	14	6	48	1B	2B	5T
39	9	5	38		7T	12T
40	7	4	46	2C		1C
41	8	3	41	1T	3T	
42	6	3	46		3B	1T
43	17	3	43	2C		

T = top tension, C = center tension, B = bottom tension

TABLE 7 (continued)

HOME SURVEY DATA: Waco

House	Approx. % Slope	Age	Avg. PI	Total Width of Cracking		
				Uphill	Sides	Downhill
				mm	mm	mm
44	25	9	19	3T	1B	1T
45	4	11	19			
46	16	9	19			1C
47	25	10	19	10T	2T	8C
48	24	1	16		2T	3T
49	15	12	16	1C		1C
50	5	4	29			
51	8	13	16	4T	4B	2T
52	2	5	26	2T	2T	2T
53	6	12	48	4B	4B	7T
54	18	2	19			
55	10	2	19	7C		2T
56	15	3	48	3T	1T	2T
57	3	2	48	1	5T	3T
58	5	2	48	1C	1T	2T
59	5	2	19			
60	17	5	36		12T	
61	8	4	36		4B	3B
62	6	3	37		1T	
63	6	5	45	1C	2B	5T
64	10	9	47	1T	20C	10T
65	15	9	44	5C	18T	
66	8	11	40	5T	3C	7T
67	3	9	19	2T		
68	25	12	38		3T	10T
69	10	5	19	10C		
70	12	8	43	4T	3C	6B
71	14	6	43		5T	6C
72	13	6	38	2T	2T	
73	12	5	35		10T	20T
74	11	4	43	8T		5T
75	10	5	39		3T	1T
76	25	6	40	24T	8C	2T
77	13	10	19		1C	
78	10	9	19			
79	12	11	43	7T	4T	13T
80	17	12	43	12T	12T	8T
81	10	11	38	13T	20T	25T
82	10	10	38	9T	10C	
83	14	4	48	13T	1B	2T
84	11	5	48	7T	5T	2T
85	15	5	48	11T	50T	9T
86	8	5	23	2T	1T	

TABLE 7 (continued)

HOME SURVEY DATA: Waco

House	Approx. % Slope	Age	Avg. PI	Total Width of Cracking		
				Uphill	Sides	Downhill
				mm	mm	mm
87	9	5	23		1T	
88	5	12	28			
89	10	5	48	2T	3C	4T
90	10	5	17	4T		
91	10	5	24	1C		
92	16	6	16	1C		
93	5	5	18			
94	4	8	18	1B		
95	11	6	16		1T	
96	11	6	16	1	2T	
97	5	12	16	3T	2T	2C
98	10	12	16	1T	7T	3T
99	10	10	17	12T	20C	10T
100	9	6	16		2T	

TABLE 8  
CREEP TEST DATA

South Bosque shale CSBS3 $\psi = -0.27$ bars $\omega = 24.5\%$ Init. Length = 4.10"		South Bosque shale CSBS4 $\psi = -0.20$ bars $\omega = 28\%$ Init. Length = 4.02"		South Bosque shale CSBS5 $\psi = -0.16$ bars $\omega = 30.6\%$ Init. Length = 4.00"	
Time	Dial Rdg.	Time	Dial Rdg.	Time	Dial Rdg.
$\sigma_1 = 2$ psi		$\sigma_1 = 2$ psi		$\sigma_1 = 2$ psi	
5 sec.	$3 \times 10^{-3}$ "	5 sec.	$15.1 \times 10^{-3}$ "	5 sec.	$8.7 \times 10^{-3}$ "
10	4.1	10	17.2	10	10.4
15	4.8	15	18.1	15	11.9
30	5.8	30	19.2	30	12.9
1 min.	6.2	1 min.	21.0	1 min.	15.1
2	7.1	2	22.8	2	16.5
13	9.0	6	25.2	6	18.7
27	9.8	12	26.9	12	20.2
1 hr. 06 min	10.9	41	29.1	43	22.9
1:28	11.2	1 hr. 30 min.	30.9	1 hr. 20 min.	23.9
2:01	11.7	2:16	31.5	2:18	24.8
$\sigma_1 = 3.5$ psi		$\sigma_1 = 3.5$ psi		$\sigma_1 = 3.5$ psi	
5 sec.	2.0	5 sec.	6.5	5 sec.	9.0
10	2.2	10	8.8	10	11.8
15	2.8	15	9.5	15	13.3
30	3.1	30	11.3	30	16.0
1 min.	3.8	1 min.	13.3	1 min.	18.2
2	4.2	3	17.0	2	21.0
6	5.1	6	18.9	6	25.9
40	7.1	13	22.1	12	29.0
47	7.3	33	25.0	29	32.8
2 hr. 59 min.	9.1	1 hr. 01 min.	26.9	1 hr. 03 min.	35.9
		1:37	28.9	1:37	38.0
		2:02	29.8	2:23	39.2
$\sigma_1 = 5$ psi		$\sigma_1 = 5$ psi		$\sigma_1 = 5$ psi	
5 sec.	1.8	5 sec.	8.5	5 sec.	13.5
10	2.1	10	11.1	10	18.0
15	2.8	15	12.8	15	21.5
30	3.2	30	15.8	30	27.8
1 min.	4.1	1 min.	19.8	1 min.	35.5
2	5.0	2	24.0	2	44.4
8	7.1	8	34.1	6	60.0
37	9.6	12	44.8	12	70.0
2 hr. 09 min.	12.1	1 hr. 11 min.	48.1	24	79.2
		1:45	50.6	52	89.9
		2:13	51.9	1 hr. 23 min.	94.8
				1:37	96.2
				2:00	98.6



TABLE 8 (continued)

## CREEP TEST DATA

South Bosque shale CSBS6 $\psi = -0.15$ bars $\omega = 31.3\%$ Init. Length = 4.02"		South Bosque shale CSB9 $\psi = -0.13$ bars $\omega = 32.6\%$ Init. Length = 4.10"		South Bosque shale CSB10 $\psi = 0.00$ bars $\omega = 35.1\%$ Init. Length = 4.00"	
Time	Dial Rdg.	Time	Dial Rdg.	Time	Dial Rdg.
$\sigma_1 = 2$ psi		$\sigma_1 = 2$ psi		$\sigma_1 = 2$ psi	
5 sec.	$10.4 \times 10^{-3}$ "	5 sec.	$41.0 \times 10^{-3}$ "	5 sec.	$43.0 \times 10^{-3}$ "
10	11.7	10	46.0	15	51.8
15	12.3	15	48.3	30	57.5
30	13.6	30	53.8	1 min.	64.6
1 min.	14.9	1 min.	57.0	2	72.1
2	16.8	2	62.0	6	85.0
6	19.6	6	69.6	12	93.8
12	21.8	12	74.0	32	105.9
31	24.8	34	78.7	1 hr. 01 min.	113.7
57	27.0	1 hr. 03 min.	81.1	1:16	116.4
1 hr. 31 min.	28.8	1:44	83.1	4:28	131.5
2:32	31.0	2:02	83.9		
$\sigma_1 = 3.5$ psi		$\sigma_1 = 3.5$ psi		$\sigma_1 = 3.5$ psi	
5 sec.	10.0	5 sec.	32.0	5 sec.	60.0
10	12.8	10	39.5	10	72.0
15	14.5	15	44.5	15	80.0
30	17.1	30	53.8	30	96.0
1 min.	20.7	1 min.	64.	1 min.	115.0
2	25.0	2	76.6	2	136.0
6	32.0	6	96.0	6	184.0
12	36.4	12	106.9	12	219.0
39	43.1	31	120.2	54	298.0
1 hr. 05 min.	46.4	1 hr. 09 min.	128.9	1 hr. 41 min.	337.0
1:44	49.0	1:35	131.1	2:00	348.0
2:10	50.1	1:58	132.8		
$\sigma_1 = 5$ psi		$\sigma_1 = 5$ psi		$\sigma_1 = 5$ psi	
5 sec.	14.0	5 sec.	26.0	5 sec.	60.0
10	19.5	10	37.5	10	95.0
15	23.0	15	46.0	15	130.0
30	29.6	30	59.3	Accelerating rate of creep.	
1 min.	38.0	1 min.	81.0		
2	47.6	2	101.0		
6	65.8	6	139.6		
12	77.6	12	163.5		
36	97.3	25	185.4		
1 hr. 14 min.	105.9	1 hr. 00 min.	212.2		
1:34	108.5	1:31	223.0		
2:01	111.0	2:08	230.8		

TABLE 8 (continued)

## CREEP TEST DATA

Houston Black clay CHB1 $\psi=0.13$ bars $\omega=29.3\%$ Init. Length = 4.12"		Houston Black clay CHB2 $\psi=-0.13$ bars $\omega=29.4\%$ Init. Length = 4.03"			
Time	Dial Rdg.	Time	Dial Rdg.	Time	Dial Rdg.
$\sigma_1 = 2$ psi		$\sigma_1 = 2$ psi			
5 sec.	$7.5 \times 10^{-3}$ "	5 sec	$7.0 \times 10^{-3}$ "		
10	8.9	10	7.5		
15	9.1	15	8.1		
30	9.8	30	9.0		
1 min.	11.0	1 min.	10.0		
2	12.4	2	11.8		
6	14.2	6	13.9		
14	15.9	12	15.2		
35	17.1	26	16.3		
1 hr. 04 min.	18.2	1 hr. 35 min.	19.0		
1:30	18.8	2:14	19.9		
2:10	19.3				
$\sigma_1 = 3.5$ psi		$\sigma_1 = 3.5$ psi			
5 sec.	5.0	5 sec.	4.8		
10	5.9	10	5.5		
17	6.2	15	6.0		
35	7.1	30	6.9		
1 min.	7.9	1 min.	8.0		
2	8.9	2	9.2		
6	11.1	15	14.5		
12	12.3	34	16.6		
33	14.6	1 hr. 06 min.	18.2		
1 hr. 38 min.	16.9	1:40	19.2		
2:04	17.2	2:10	20.3		
$\sigma_1 = 5$ psi		$\sigma_1 = 5$ psi			
5 sec.	4.6	5 sec.	4.8		
10	5.2	10	5.5		
15	5.8	15	6.0		
30	6.8	30	7.2		
1 min.	7.9	1 min.	8.9		
2	9.5	3	11.7		
13	14.8	13	16.9		
23	16.4	1 hr. 32 min.	24.6		
40	18.3	2:32	26.9		
1 hr. 05 min.	19.8				
1:41	21.3				
2:04	21.8				

TABLE 8 (continued)

## CREEP TEST DATA

Artificial Soil CK2 Kaol. = 100% Init. Length = 4.06"		Artificial Soil CKM1 Kaol.=90%, Mont.=10% Init. Length = 4.17"		Artificial Soil CKM3 Kaol.=70%, Mont.=30% Init. Length = 4.24"	
Time	Dial Rdg.	Time	Dial Rdg.	Time	Dial Rdg.
$\sigma_1 = 2 \text{ psi}$		$\sigma_1 = 2 \text{ psi}$		$\sigma_1 = 2 \text{ psi}$	
5 sec.	$10.8 \times 10^{-3}$ "	5 sec.	$17.0 \times 10^{-3}$ "	5 sec.	$18.0 \times 10^{-3}$ "
10	12.1	10	20.3	10	20.5
15	12.8	15	21.6	15	22.0
30	14.5	30	24.0	30	24.2
1 min.	16.0	1 min.	26.2	1 min.	26.8
2	17.5	2	28.5	2	29.1
6	20.1	6	32.2	6	32.9
12	21.9	12	35.0	12	35.3
24	24.9	37	39.3	27	38.4
1 hr. 00 min.	26.9	1 hr. 14 min.	41.8	1 hr. 00 min.	41.0
1:44	27.9	1:57	43.3	1:25	42.0
2:14	28.3	2:16	44.1	1:51	42.7
$\sigma_1 = 3.5 \text{ psi}$		$\sigma_1 = 3.5 \text{ psi}$		$\sigma_1 = 3.5 \text{ psi}$	
5 sec.	6.1	5 sec.	10.0	5 sec.	8.0
10	10.0	10	15.0	10	11.5
15	12.5	15	17.8	15	14.1
30	16.1	30	22.2	30	18.0
1 min.	20.1	1 min.	26.6	1 min.	22.1
2	24.0	2	30.8	2	26.1
9	31.0	6	36.2	6	31.7
12	31.9	12	39.1	12	34.7
34	35.7	36	43.1	12	34.7
55	37.1	1 hr. 10 min.	45.2	27	37.2
1 hr. 22 min.	38.1	1:38	46.3	37	38.2
1:55	39.1	2:10	47.4	1 hr. 02 min.	39.8
2:09	39.3	$\sigma_1 = 5 \text{ psi}$		1:22	40.2
$\sigma_1 = 5 \text{ psi}$		5 sec.	13.0	1:50	41.1
5 sec.	5.0	10	20.0	2:14	41.6
10	8.5	15	25.0	$\sigma_1 = 5 \text{ psi}$	
15	12.4	30	32.6	5 sec.	9.0
30	21.1	1 min.	40.8	10	15.2
1 min.	30.4	2	48.8	15	19.0
2	39.8	6	60.6	30	26.8
6	52.7	13	68.1	1 min.	34.8
12	59.3	31	76.5	2	42.5
42	68.9	1 hr. 10 min.	82.5	6	53.1
1 hr. 18 min.	72.9	1:48	86.0	12	58.4

TABLE 8 (continued)

## CREEP TEST DATA

Artificial Soil CK2 Kaol. = 100% Init. Length = 4.06"		Artificial Soil CKM1 Kaol.=90%, Mont.=10% Init. Length = 4.17"		Artificial Soil CKM3 Kaol.=70%, Mont.=30% Init. Length = 4.24"	
Time	Dial Rdg.	Time	Dial Rdg.	Time	Dial Rdg.
$\sigma_1 = 5$ psi		$\sigma_1 = 5$ psi		$\sigma_1 = 5$ psi	
1 hr. 48 min.	75.8	2 hrs. 14 min.	87.8	30 min.	64.8
2:15	76.1			1 hr. 14 min.	69.7
				1:42	71.2
				2.08	72.8

TABLE 8 (continued)

## CREEP TEST DATA

Artificial Soil CKM7 Kaol.=55%, Mont.=45% Init. Length = 3.98"		Artificial Soil CKM4 Kaol.=40%, Mont.=60% Init. Length = 3.98"		Artificial Soil CKM8 Kaol.=20%, Mont.=80% Init. Length = 4.02"	
Time	Dial Rdg.	Time	Dial Rdg.	Time	Dial Rdg.
$\sigma_1 = 2$ psi		$\sigma_1 = 2$ psi		$\sigma_1 = 2$ psi	
5 sec.	$10.0 \times 10^{-3}$	5 sec.	$35.0 \times 10^{-3}$	5 sec.	$23.0 \times 10^{-3}$
10	12.5	10	38.0	10	25.5
15	13.6	15	39.2	15	27.5
30	15.2	30	42.1	30	30.8
1 min.	17.5	1 min.	45.6	1 min.	34.9
2	19.6	2	49.8	2	39.3
7	23.4	6	55.6	6	47.7
17	26.9	12	60.0	12	52.9
24	28.3	34	66.9	24	57.5
1 hr. 05 min.	33.0	60	71.1	1 hr. 31 min.	66.1
1:21	33.9	1 hr. 26 min.	73.1	2:03	68.7
2:13	36.1	1:58	75.9		
		2:25	77.2		
$\sigma_1 = 3.5$ psi		$\sigma_1 = 3.5$ psi		$\sigma_1 = 3.5$ psi	
5 sec.	5.0	5 sec.	9.5	5 sec.	42.0
15	9.6	10	13.5	10	57.0
30	12.8	15	16.0	15	68.0
1 min.	16.7	30	21.2	30	92.0
2	20.8	1 min.	27.5	1 min.	127.0
6	26.8	2	33.8	2	165.0
12	30.7	6	44.6	6	224.0
25	34.2	12	50.9	12	254.0
1 hr. 13 min.	38.9	18	54.0	51	294.0
1:34	39.9	27	57.2	1 hr. 50 min.	310.0
2:17	41.6	51	61.8	2:15	314.0
$\sigma_1 = 5$ psi		$\sigma_1 = 5$ psi		$\sigma_1 = 5$ psi	
5 sec.	6.2	1 hr. 28 min.	65.2	Accelerating rate of creep.	
15	13.5	1:55	66.5		
30	20.9	2:11	67.4		
1 min.	30.3				
2	40.6	$\sigma_1 = 5$ psi			
6	58.3	5 sec.	14.0		
13	69.9	10	18.5		
30	80.0	15	31.0		
1 hr. 00 min.	86.4	30	45.5		
1:30	89.8	1 min.	65.5		
2:06	91.9	2	93.0		
		6	149.0		
		12	187.0		

TABLE 8 (continued)

## CREEP TEST DATA

		Artificial Soil CKM4 Kaol.=40%, Mont.=60% Init. Length. = 3.98"			
Time	Dial Rdg.	Time	Dial Rdg.	Time	Dial Rdg.
		$\sigma_1 = 5 \text{ psi}$			
		18	209.0x10 <sup>-3</sup> "		
		38	246.0		
		58	261.0		
		1 hr. 19 min.	268.0		
		1:46	273.0		
		2:00	275.0		